# Mechanistic insights into Gram-negative envelope remodeling for protection against severe outer membrane defects

by

KATIE N. KANG

---

DISSERTATION

Submitted in partial fulfillment of the requirements
for the degree of Doctor of Philosophy

The University of Texas at Arlington
Arlington, Texas

May 2022

---

Supervising Committee:

Dr. Joseph M. Boll, Supervising Professor and Committee Chair
Dr. Cara C. Boutte, Committee Member
Dr. Todd A. Castoe, Committee Member
Dr. Laura D. Mydlarz, Committee Member
Dr. Michael R. Roner, Committee Member

COPYRIGHT



# Dedication

This dissertation is dedicated to my father, Larry Wayne Williams, whose "leave everything better than you found it" philosophy has shaped my approach to life and work for the better. Additionally, he set a lifelong example that overcoming challenges requires hard work and grit. Thank you for inspiring me to be the best human that I can be.

# ACKNOWLEDGEMENTS

Firstly, I am grateful to my research advisor, Joseph Boll, who was willing to take a chance on me. This dissertation would not have become a reality without your support. You dedicated tremendous time and effort to help me grow as a scientist. Regardless of the situation, you have remained supportive and encouraging. I am truly thankful for such an awesome mentor, and I will miss our whiteboard brain storming sessions. The Boll Laboratory fostered an environment for curiosity and critical thinking. I thank the past and present members of our laboratory, who have all played a role in this work. I need to thank my dissertation committee, Cara Boutte, Todd Castoe, Laura Mydlarz and Michael Roner, for their suggestions and advice over the years. The insights offered regarding both science and career mentoring have been instrumental. Additionally, a huge thank you to Cara Boutte who taught me the microscopy and image analysis skills critical for this dissertation. I am grateful for the friends I have made within the biology department. They were, and continue to be, a valuable source of thoughtful advice and support. I have greatly enjoyed the scientific discussions (and laughs) we have shared together over the years. Thank you to those of you who have helped me wrangle data in FIJI and deal with the inexplicable things that bacteria do when you are not looking. Thank you for pulling me aside to share with me your new figures, posters, and other elements of your work that you were so excited about. Being a part of those moments were wonderful. Finally, I would like to acknowledge the support of my family. Words are not enough to express my love and gratitude for you, but I will try. To my spouse Chanwool, who is a rock and an ever-present source of pragmatic wisdom. To my in-laws who welcomed me into their family and have since sent love and warmth across language barriers. To my dad, who actually read my entire first paper, thank you for always being a supportive and uplifting presence. Without all of you, this dissertation would not be possible.

# ABSTRACT

Gram-negative bacteria account for the majority of antibiotic resistant infections. Regulated modifications within the cell envelope can promote resistance to clinically important antibiotics. The increased prevalence of antibiotic treatment failure highlights the importance of investigating the underlying resistance mechanisms. Of particular concern is resistance to last-line antimicrobials, such as polymyxin E (colistin). Colistin is a cationic antimicrobial lipopeptide that binds the negatively charged lipid A domain of lipopolysaccharide, a glycolipid enriched in the Gram-negative outer membrane, to perturb the envelope and lyse the cell. However, several Gram-negative pathogens have evolved intrinsic colistin resistance mechanisms. For example, many Enterobacteriaceae modify their LPS with amine-containing moieties to prevent colistin binding. *Enterobacter cloacae* (*Ecl*) exhibits colistin heteroresistance, where a subpopulation is resistant to the antibiotic. Here, we demonstrate that colistin heteroresistance in *E. cloacae* is facilitated by 4-amino-4-deoxy-L-arabinose (L-Ara4N) addition to lipid A via regulation by the PhoPQ two-component system. Prior to this study, there was not detailed understanding of heteroresistance mechanisms in *Ecl*. While several pathogens modify lipid A to prevent colistin binding, only *Acinetobacter baumannii* (*Ab*) is known to mutationally inactivate lipid A biosynthesis to develop colistin resistance. Notably, LOS was considered essential for viability in Gram-negatives; however, the mechanism that enables *Ab* to survive without LOS ($LOS^-$) is unknown. We found that two LD-transpeptidases, LdtJ and LdtK, were essential for $LOS^-$ survival in *Ab*. Furthermore, we characterized their biochemical activities and showed they are important for mechanical stability during cell envelope stress. Lastly, we found that the PG synthase PBP1A in *Ab* is necessary for productive division in *Ab*. PBP1A and is required for rapid growth, which may be detrimental for $LOS^-$ cells to assemble an outer membrane.

# Table of Contents

# LIST OF TABLES

# LIST OF FIGURES

# LIST OF ABBREVIATIONS

1. **aPBP** - class A penicillin-binding protein
2. **AST** - antimicrobial susceptibility testing
3. **CAMP** – cationic antimicrobial peptide
4. **CL** - cardiolipin
5. **CFU** - colony-forming unit
6. **CRAB** - carbapenem-resistant *Acinetobacter baumannii*
7. **CRE** - carbapenem-resistant Enterobacteriaceae
8. **DAP** - meso-2,6-diaminopimelic acid
9. **DAB** - 2,4-diaminobutyric acid
10. **DD-TPase** - DD-transpeptidase
11. **ECC** - *Enterobacter cloacae* complex
12. **EMSA** - Electrophoretic mobility shift assay
13. **Glc*N*Ac** - *N*-acetylglucosamine
14. **GTase** - glycosyltransferase
15. **HAI** - Healthcare associated infection
16. **HPLC** - high-performance liquid chromatography
17. **IS** - insertion sequence
18. **Kdo** - 3-deoxy-α-D-manno-octulosonic acid
19. **Ldt** - LD-transpeptidase
20. **LOS** - lipooligosaccharide
21. **LOS$^-$** - lipooligosaccharide-deficient
22. **LPS** - lipopolysaccharide
23. **MDR** - multi-drug resistant
24. **MIC** - minimum inhibitory concentrations
25. **Mur*N*Ac** - *N*-acetylmuramic acid
26. **NADA** - 4-chloro-7-nitrobenzofurazan D-alanine
27. **NADH** - nicotinamide adenine dinucleotide hydrogen
28. **OM** - outer membrane
29. **OMV** - outer membrane vesicles
30. **PAP** - population analysis profile
31. **PBP** - penicillin-binding protein
32. **PE** - phosphatidylethanolamine
33. **PG** - peptidoglycan
34. **PG** - phosphatidylglycerol
35. **SEDS** - shape, elongation, division and sporulation
36. **TCS** - two-components system
37. **TLC** - thin layer chromatography
38. **TLR4** - Toll-like receptor 4
39. **TPase** - transpeptidase
40. **XDR** - extensively-drug resistant

# PUBLICATIONS

1. **Kang KN** and Boll JM. PBP1A is required for proper division in *A. baumannii*. *J Bacteriol*. *In preparation*. Estimated submission May 2022.

2. Islam N, Kazi MI, **Kang KN**, Biboy J, Gray J, Ahmed F, Schargel RD, Boutte CC, Dörr T, Vollmer W, Boll JM. Peptidoglycan recycling promotes outer membrane integrity and carbapenem tolerance in *Acinetobacter baumannii*. *mBio. In press*. doi:10.1101/2021.11.23.469614

3. **Kang KN**, Kazi MI, Biboy J, Gray J, Bovermann H, Ausman J, Boutte C, Vollmer W, Boll JM. Septal class A penicillin-binding protein activity and LD-transpeptidases mediate selection of colistin-resistant lipooligosaccharide-deficient *Acinetobacter baumannii*. *mBio*. 2021;12(1). doi:10.1128/mBio.02185-20

4. Kazi MI, Perry B, Card DC, Schargel RD, Ali HB, Obuekwe VC, Sapkota M, **Kang KN**, Pellegrino MW, Greenberg DE, Castoe TA, Boll JM. Discovery and characterization of New Delhi metallo-β-lactamase-1 inhibitor peptides that potentiate meropenem-dependent killing of carbapenemase-producing Enterobacteriaceae. *J Antimicrob Chemother*. 2020;75(10):2843-2851. doi:10.1093/jac/dkaa242

5. **Kang KN***, Kelin DR*, Kazi MI, Guerin F, Cattoir V, Broadbelt JS, Boll JM. Colistin heteroresistance in *Enterobacter cloacae* is regulated by PhoPQ-dependent 4-amino-4-deoxy- L -arabinose addition to lipid A. *Mol Microbiol*. 2019;111(6):1604-1616. doi:10.1111/mmi.14240
   *Authors contributed equally

6. Mohammed AD, Khan WM, Chatzistamou I, Chamseddine D, **Kang KN**, Enos R, Angela M, Gomez G, Aladhami A, Oskeritzian CA, Jolly A, Chang Y, He S, Pan Z, Kubinak JL. Gut antibody deficiency in a mouse model of CVID results in development of a spontaneous gluten-sensitive enteropathy. *Front. Immunol*. 2019;338(10):1664-3224 doi:10.3389/fimmu.2019.02484

# CHAPTER 1: INTRODUCTION

Despite infection control efforts, antibiotic-resistant nosocomial pathogens permeate healthcare facilities globally. Healthcare-associated infections (HAIs) are thought to be the leading cause of adverse safety events for patients and result in undue mortality and morbidity[1–6]. HAIs are frequently caused by drug-resistant Gram-negative pathogens, where failure of front-line therapeutics are increasingly commonplace[7]. When standard of care options become ineffective, clinicians turn to "last-resort" antimicrobials, like colistin sulfate (Polymyxin E)[8] which targets the ubiquitous outer membrane glycolipid, lipid A[9–11], which was thought to be essential for Gram-negative bacterial viability. Alarmingly, colistin-resistant HAIs are also increasing.

Further complicating efforts to address antibiotic-resistant HAIs, colistin-heteroresistance was identified in some Enterobacter cloacae complex (ECC) clusters, including the nosocomial pathogen, *Enterobacter cloacae*[12,13]. Evidence is accumulating that heteroresistance is an underappreciated cause of antibiotic treatment failure[13–15] and colistin resistant subpopulations go undetected in clinical antibiotic susceptibility panels. The first study herein, defined the regulatory mechanisms required for colistin heteroresistance in *E. cloacae*. My work found that only one two-component system (TCS), PhoPQ, regulates colistin heteroresistance in *Enterobacter cloacae* Colony-forming unit (CFU) survival assay identified only PhoPQ as essential for survival in the presence of colistin at concentrations above the clinical breakpoint. Next, we confirmed the heteroresistance phenotype in wild type E. cloacae in Δ*phoPQ* using the gold standard for antimicrobial susceptibility testing (AST), population analysis profiles (PAP). We further tested for heteroresistance using routine clinical ASTs, microdilution and E-strip assays. The ASTs demonstrated PhoPQ activity was not only necessary but also sufficient for colistin-heteroresistance. These studies are significant because other well-studied models of colistin

resistant Enterobacterales rely on a second TCS, PmrAB, which contributes to colistin resistance but not heteroresistance. Therefore, the unique PhoPQ signaling pathway in *E. cloacae* likely contributes to colistin heteroresistance.

In other Enteroabcterales, PhoPQ and PmrAB regulate chemical modification of the lipid A domain of lipopolysaccharide[16]. To determine the structure of lipid A in colistin heteroresistant *E. cloacae*, we extracted lipid A from cells grown with and without colistin selective pressure. Additionally, lipid A was isolated from Δ*phoPQ* grown without colistin. Samples were analyzed using direct infusion nano-ESI-MS/MS, revealing three distinct lipid A modifications. Two modifications, palmitoylation and hydroxylation, were conserved between wild type and Δ*phoPQ*, suggesting *E. cloacae* produces hepta-acylated and hydroxylated lipid A independently of colistin selection. Importantly, the MS spectra also revealed addition of 4-amino-4-deoxy-l-arabinose (L-Ara4N) to lipid A in wild type and colistin treated cells, but not Δ*phoPQ*. Taken together, MS/MS spectra and PAP data suggest colistin heteroresistance in *E. cloacae* is dependent upon PhoPQ-regulated L-Ara4N lipid A modification.

We next investigated how PhoPQ regulates the *arn* operon, which encodes genes that synthesize and transfer L-Ara4N to lipid A. RNA-sequencing libraries were constructed in wild type, Δ*phoPQ* and Δ*pmrAB E. cloacae* to compare regulatory products. Previous work in other Enterobacteriaceae have shown that both TCSs, PhoPQ and PmrAB, engage in crosstalk through a linker protein called PmrD, which is required for transcriptional activation of *arn*. Surprisingly, our transcriptomics revealed *arnBCADTEF* genes were downregulated in Δ*phoPQ* compared to wild type, but not in Δ*pmrAB*. Reduced expression of *arnBCADTEF* in Δ*phoPQ* further supported a model where PhoPQ is the sole factor that regulates the *arn* operon in *E. cloacae*.

Next, we asked if PhoP directly regulates transcription of *arn*B, the first gene in the *arn* operon. Here, we performed an electrophoretic mobility shift assay (EMSA) and found that PhoP directly bound *arnB* DNA, which is included a predicted PhoP-box. Importantly, the synthetic DNA polymer (poly(dI-dC)) did not compete with *E. cloacae ParnB* for PhoP binding, highlighting the substrate specificity of the PhoP *ParnB* interaction.

Finally, we sought to determine if PhoPQ-dependent L-Ara4N lipid A modifications reduced innate immune reactivity. We tested the antagonistic properties of native and L-Ara4N-modified lipid A to human Toll-like receptor 4 (TLR4). TLR4 responds robustly to hexa-acylated, bis-phosphorylated lipid A through pro-inflammatory signaling cascades to clear the pathogen. While both *E. cloacae* wild type lipid A and *E. cloacae* L-Ara4N-lipid A stimulated TLR4 to a lesser degree than the canonical lipid A structure from wild type *E. coli*, the presence of L-Ara4N did not further reduce TLR4 response. These findings show PhoPQ-dependent modifications yield resistance to colistin but do not contribute to diminished innate immune response compared to wild type *E. cloacae* lipid A.

Prior to this study, there was not detailed understanding of heteroresistance in *E. cloacae*. Our data shows *E. cloacae* lipid A Ara4N modifications are PhoPQ-dependent and PmrAB-independent, where PhoP directly activates the transcription of the *arn* operon. This pathway is unique in that it uncouples the PhoPQ and PmrAB TCSs that are known to work synergistically in some γ-Proteobacteria. This uncoupling is thought to allow colistin-resistant subpopulations to emerge due to loosened regulation of the *arn* operon. Our study provides insights into the origins of colistin heteroresistant subpopulations in *E. cloacae*, which is information necessary for informed therapeutic regimes.

While our previous study on colistin heteroresistance in *E. cloacae* focused on lipid A modifications, the next collection of studies describes fitness requirements for colistin resistance as mediated by complete loss of lipooligosaccharide ($LOS^-$) in the outer membrane (OM) of the nosocomial pathogen A*cinetobacter baumannii*. To date, *A. baumannii* is one of only three Gram-negative bacteria known to survive depletion of LOS[17]. Despite the importance of the LOS-enriched OM in cell viability, intrinsic and adaptive resistance to antibiotics, protective responses to LOS depletion are poorly understood. Our studies offer mechanistic insights into the physiological requirements for $LOS^-$ Gram-negative viability. Moreover, they provide a better understanding of how Gram-negative cells withstand severe envelope defects, which is broadly relevant for cellular response to several classes of envelope-targeting antibiotics, including the polymyxin colistin.

Here we asked the question, what are the physiological requirements of $LOS^-$ viability, which leads to colistin resistance. We performed a transposon mutagenesis screen in *A. baumannii* Δ*pbp1A*, which contains the *pbp1A* compensatory mutation required for colistin selection of $LOS^-$ mutants, as described below. The screen identified two putative LD-transpeptidases (Ldts), LdtJ and LdtK, as synthetically lethal in Δ*pbp1A*. Accordingly, we were unable to recover Δ*ldtJ* and Δ*ldtK* $LOS^-$ populations following colistin selection.

Ldts are a class of envelope remodeling enzymes with three disparate activities[18]. To characterize LdtJ and LdtK activity, we analyzed peptidoglycan (PG) composition with high-performance liquid chromatography (HPLC) and MS/MS analysis of Δ*ldtJ* and Δ*ldtK* compared to wild type. Here, we identified attenuation of alternative, 3-3 crosslinking between PG peptide stems in Δ*ldtJ* PG. Moreover, there was significant loss of D-amino acid incorporation in Δ*ldtJ* PG. These findings were supported by our fluorescent microscopy data which revealed LdtJ

activity was required for PG incorporation of a D-alanine fluorophore conjugate (NADA). Lastly, osmotic stress assays found Δ*ldtJ* was hypersensitive to osmotic shock, consistent with data showing D-amino acid incorporation facilitates resistance to osmotic stress and increased turgor pressure. These data point to a role for LdtJ in PG remodeling and structural support through alternative crosslinking and D-amino acid incorporation and are consistent with Ldts characterized in other bacteria[19–21].

Our MS/MS analysis of Δ*ldtK* PG revealed increases in tetra peaks and alternative 3-3 crosslinks compared to wild type. However, tetrapeptide accumulation and increased abundance of 3-3 crosslinking was not characteristic of Ldt mutants. We next sought to identify LdtK activity via enzyme homology. Through homology prediction, we hypothesized LdtK might function to tether the OM to the PG via lipoprotein or β-barrel protein attachment. Consistent with this hypothesis, we observed hypervesiculation in Δ*ldtK* compared to wild type through quantification of the 3-deoxy-α-D-manno-octulosonic acid (Kdo) moiety in outer membrane vesicles (OMVs). Hypervesiculation is indicative of OM instability or stress, demonstrating LdtK is important for envelope stability.

While analyzing LdtK domain predictions, we observed LdtK does not contain a signal sequence or transmembrane helix, surprisingly suggesting LdtK is cytoplasmic. Thus, we next determined LdtK cellular compartmental localization. Localization assays using wild type cell fractions were analyzed with western blotting and protein-specific anti-sera. We found LdtK exclusively localized in the cytoplasmic compartment, positioning it as the first known cytoplasmic member of the Ldt enzymatic family.

Having established LdtK as cytoplasmic, we hypothesized it was important for modifying peptide stems within the PG recycling pathway. PG fragments imported into the cytoplasm enter

recycling as *N*-Acetylmuramic acid (Mur*N*Ac) tetrapeptides. We suspected LdtK would cleave tetrapeptides, providing the tripeptide substrate for which early recycling enzymes have high specificity. As such, we purified recombinant wild type and catalytically inactive LdtK and incubated each with purified Mur*N*Ac tetrapeptide stems. MS/MS analysis revealed LdtK amidase activity on tetrapeptides, thereby fulfilling a necessary role in PG recycling.

The next study builds on previous findings from our laboratory showing activity of the bifunctional class A penicillin-binding-protein (aPBP) cell wall synthase, PBP1A, is deleterious in *A. baumannii* LOS$^-$. Literature precedent from studies in *E. coli* consider PBP1A primarily involved in elongation; however, we show it is important for division in *A. baumannii*. Conversely, we found PBP1B, a semi-redundant class A PBP thought to be involved in division in *E. coli*, did not affect LOS$^-$ viability or wild type fitness under standard laboratory conditions. CFU growth curves showed *pbp1A* alone impaired growth rate compared to wild type. Over expression of PBP1B did not change wild type morphology, whereas over expression of PBP1A produced shortened cells with blunted septal sites indicative of increased activity in the divisome complex. Moreover, we found protein levels of each aPBP were not increased when the other was deleted. Taken together, these data suggest PBP1A and 1B are not semi-redundant in *A. baumannii* as expected based on studies in other bacteria[22]. The independent nature of these aPBPs lead us to hypothesize Δ*pbp1A* and Δ*pbp1B* would have disparate β-lactam minimum inhibitory concentrations (MICs). Indeed, Δ*pbp1A* demonstrated significantly higher resistances to clinically important penicillin and cephalosporin derivatives compared to Δ*pbp1B* and wild type.

Interestingly, PBP1A is not transcribed in all *A. baumannii* clinical isolates[17]. In such PBP1A-deficient isolates, we recovered LOS$^-$ subpopulations at frequencies between 1.47E-7 and 8.09E-8 following colistin selection. Additionally, we identified native and induced expression of

PBP1A prevented recovery of LOS$^-$ subpopulations. Further colistin selection experiments showed a point mutation in the glycosyltransferase (GTase) but not the transpeptidase domain (TPase) was sufficient to attenuate PBP1A toxicity. Our findings support previous evidence for *pbp1A* as a necessary, compensatory mutation in LOS$^-$ viability.

To better understand cell wall biogenesis in PBP1A-deficient wild type strains, fluorescent PG precursor stains were adapted for use in six clinical isolates. PBP1A-expressing isolates had the characteristic cocco-bacilli morphology of *A. baumannii*. In contrast, PBP1A-deficient isolates formed multi-septal phenotypes. We next sought to establish PBP1A colocalization to sites of septal-PG biogenesis. PBP1A was fused to the red fluorescent protein, mCherry, and expressed under a native promoter in *A. baumannii*. Furthermore, pPBP1A$_{\Delta GTase}$-mCherry and pPBP1A$_{\Delta TPase}$-mCherry constructs were also made. Here, we found wild type PBP1A and pPBP1A$_{\Delta TPase}$ diffuse throughout the cell but importantly, also concentrated at the septa. However, pPBP1A$_{\Delta GTase}$ remained diffuse and did not readily localize to the site of septal synthesis. Importantly, only pPBP1A$_{\Delta GTase}$ and not pPBP1A$_{\Delta TPase}$ demonstrated a division defect. Further examination identified similar septation defects leading to cell chaining in LOS$^-$ strains, suggesting slowed division rate was a factor in LOS$^-$ fitness.

Given the strong correlation between full abrogation of PBP1A toxicity by Δ*pbp1A* and pPBP1A$_{\Delta GTase}$ and the conserved septation defects in Δ*pbp1A*, pPBP1A$_{\Delta GTase}$ and LOS$^-$ cells, we hypothesized that division perturbation was sufficient for LOS$^-$ viability. To test this hypothesis, we incubated wild type *A. baumannii* expressing native PBP1A with half MIC of individual β-lactam antibiotics known to induce filamentation and prevent division. Filamentation phenotype was confirmed with microscopy and treated cells were plated onto colistin agar plates. Contrary to expectations, we were unable to recover LOS$^-$ cells despite disruption to division. These data

suggest division defects alone are not sufficient to prime cells for survival without LOS and PBP1A-toxicity is more complex than just its role in proper septation.

To further investigate PBP1A interaction with the divisome and elongasome, we used a co-immunoprecipitation assay. Whole cells expressing Flag-tagged PBP1A were fixed with Lomant's reagent, a primary amine crosslinker. The cells were lysed and PBP1A-Flag was immunoprecipitated with anti-Flag affinity resin. Proteins constituting the crosslinked PBP1A-Flag complex were interrogated with anti-sera raised against PBP3, PBP2, and PBP1A. Here, we found PBP1A formed a complex with PBP3, a PBP synthase restricted to the divisome, but not PBP2, an elongasome homolog. This is notable as PBP1A is not known to interact with PBP3 in other Gram-negative bacteria.

While PBP1A activity has been well characterized in *E. coli*, it is not well understood in *A. baumannii*. Moreover, there is a paucity of studies considering PBP1A activity in division. By adapting fluorescent microscopy techniques to several lineages of clinical isolates and creating fluorescent protein fusions for localization studies, we have shown wild type PBP1A is both diffuse within the cell and concentrated at the divisome where it is required for proper septal site formation. Additonally, our microscopy has shown an interesting correlation between defective division in LOS$^{-}$, Δ*pbp1A*, pPBP1A$_{\Delta GTase}$ strains. Further, biochemical evidence directly associates PBP1A with PBP3. Lastly, our data show PBP1A and 1B are not semi-redundant in *A. baumannii* where PBP1A is the primary driver of both lateral and septal PG biogenesis.

Collectively, these studies in two Gram-negative pathogens of concern will inform better anti-microbial stewardship practices for treating nosocomial infections with the valuable last line of defense antibiotic, colistin, and combat the growing threat of antibiotic resistance in healthcare facilities. First, we identified the previously unknown mechanism behind colistin heteroresistance

in *E. cloacae*. Next, we studied the requirements for viability during the extreme OM defect of LOS depletion. We identified and characterized two previously unknown *A. baumannii* Ldts, LdtJ and LdtK, that are required for $LOS^-$ viability. Importantly, our characterization of LdtK revealed a previously unknown role for Ldts in early-phase PG recycling. Lastly, this work found PBP1A plays a more prominent role in division than previously appreciated. We have established PBP1A as the primary aPBP PG synthase in *A. baumannii* where 1A and 1B are not semi-redundant. Loss of only PBP1A increased resistances to β-lactam antibiotics compared to wild type. As some clinical isolates do not express PBP1A, these findings have concerning implications for drug susceptibility in these strains. This dissertation is expected to be useful to advance three areas of knowledge: (1) Regulation of envelope remodeling that enables Gram-negative pathogens to develop clinically relevant antimicrobial resistances. (2) Informing better antimicrobial therapeutic strategies to combat increasing antimicrobial resistance. (3) The basic science of Gram-negative envelope assembly and minimal requirements for viability.

# CHAPTER 2: LITERATURE REVIEW

## The global burden of anti-microbial resistance

One of the most critical challenges to global public health is the emergence and rapid spread of antibiotic-resistance. Healthcare facilities are a concerning reservoir for pathogens primed to acquire drug resistance[1]. Despite stringent infection prevention and control measures, healthcare-associated infections (HAIs) remain the leading cause of adverse safety events for hospitalized patients internationally, with consequences including financial burden, delayed convalescence, morbidity and mortality[1–6]. The burden of drug-resistant HAIs in the United States alone is

substantial, with an estimated 2.8 million resistant infections yearly[5] - an estimate that has increased 140% from a report published 6 years prior[4].

The increased infection estimates reflect rapid expansion of multi and extensively-drug resistant (MDR and XDR, respectively) HAIs. MDR is characterized in the medical literature as resistance to more than one class of antibiotic whereas XDR is considered as resistant to all but two empirical treatment classes[23]. The first line of defense against MDR infections is the β-lactam derivative, carbapenem[24]. However, carbapenem efficacy is declining[7] with the emergence of carbapenem-resistant pathogens. There are no established, effective practices to address XDR currently. Of particular concern for MDR and XDR are Gram-negative bacteria, as their robust cellular envelopes provide intrinsic resistance to many antimicrobials[25]. As a graduate student, I have uncovered many factors involved in Gram-negative cell envelope assembly and remodeling that contribute to antibiotic treatment failure, which are detailed below.

The Centers for Disease Control designated Gram-negative, carbapenem-resistant Enterobacteriaceae (CRE) and *Acinetobacter baumannii* (CRAB) among the most urgent threats to public health in the United States[5]. Furthermore, the World Health Organization identified treatment failure in CRE and CRAB as concerning with the potential for extensive spread[26,27]. The increased threat posed by failing carbapenem efficacy due to CRE and CRAB are driving demand for novel antimicrobial development to replace failed treatment options. Concerningly, the rapid spread of antimicrobial resistance is outpacing new drug development[28]. A detailed understanding of how bacteria acquire resistance to current therapeutics will inform new antimicrobial drug development and inform appropriate empirical treatment choices to keep our current antibiotic arsenal potent for as long as possible.

## Biogenesis and structural function of the Gram-negative envelope

Gram-negative (diderm) bacteria are defined by their multi-layered cell envelope, which includes three distinct layers: an inner membrane (IM) lipid bilayer, the periplasmic space containing peptidoglycan (PG) and an asymmetric outer membrane (OM), enriched with surface-exposed lipopolysaccharide (LPS) or lipooligosaccharide (LOS). The tripartite structure defines cellular shape[91,92], supports internal and external mechanical loads[91,93,94] and defends against environmental insults[95], including antibiotics[96,97]. Gram-negative bacteria must tightly coordinate the assembly of each cell envelope layer during growth to maintain cellular integrity[98–101].

## The inner membrane bilayer

The IM is a symmetrical phospholipid bilayer, typical of biological membranes. Here, the major glycerophospholipid species are phosphatidylethanolamine (PE), phosphatidylglycerol (PG) and cardiolipin (CL)[102]. The IM is a semi-permeable barrier that delimits the cytoplasmic and periplasmic space. Additionally, this barrier is the site of electrochemical gradients that provide potential cellular energy. It also serves as scaffolding for critical, multiprotein machines that work to protect the cell. These include integral IM sensors which detect envelope disturbances via their periplasmic domains[35] and the synthases responsible for polymerizing PG which shields the IM from immense cytoplasmic turgor[105–107] and external stress.

## The peptidoglycan layer

PG is an elastic yet rigid mesh[103] that is assembled by multiprotein complexes and is ubiquitous in nearly all bacteria[98,103,104]. PG consists of alternating *N*-acetylglucosamine (Glc*N*Ac) and *N*-acetylmuramic acid (Mur*N*Ac) glycan chains. In nascent PG, each Mur*N*Ac residue is

conjugated to a pentapeptide stem. The peptide stem amino acids are largely conserved between species with some variation at the third amino acid. The amino acids, proximal to distal, include: L-ala, D-glu, meso-2,6-diaminopimelic acid (DAP) or L-lys, D-ala and D-ala[109]. Peptide stems are crosslinked between opposite, parallel glycan chains. The majority (90-98%) of crosslinks in *E. coli* are catalyzed by penicillin binding proteins (PBPs) and occur between the fourth D-ala and DAP (4-3 crosslink)[98]. The rigid glycan chains and elastic peptide stems contribute to the anisotropic nature of PG[94,98] and allow the PG to expand to 300% above resting size without rupture[110]. The porous, flexible architecture permits large trans-envelope complexes[111–113] to span the wall without weakening the structural support needed to resist considerable turgor stress. Cytoplasmic turgor is thought to be between 3-6 atm in Gram-negative bacteria and 20-25 atm in Gram-positive species[105–107]. Intriguingly, only one PG layer is sufficient to withstand turgor in a Gram-negative cell[98,108]. The PG sacculus is thought to be one continuous macromolecule with synthesis beginning in the cytoplasm and remodeling continuing in the periplasm[114].

## The key enzymes of *de novo* peptidoglycan biogenesis

The Glc*N*Ac and Mur*N*Ac glycan subunits and the pentapeptide stem are synthesized in the cytoplasm. Glc*N*Ac is synthesized from fructose-6-phosphate by GlmSMU in four enzymatic steps[115]. Following GlcNAc synthesis, GlmU catalyzes uridylyltransfer of uridine diphosphate (UDP), a nucleotide carrier, to Glc*N*Ac[116]. UDP-Glc*N*Ac is a precursor in UDP-Mur*N*Ac synthesis by MurAB. In parallel, the pentapeptide stem is assembled from the essential ligases, MurCDEF[115]. Nascent PG pentapeptide contains two noncanonical D-amino acid species: D-glu and D-ala. D-glu is synthesized by MurI[117] and the terminal D-ala peptides are synthesized by D-ala racemases encoded by *alr* and *dadX*[118,119]. At the inner leaflet of the IM, UDP-Glc*N*Ac and UDP-Mur*N*Ac-

pentapeptide are conjugated to the C55 undecaprenyl phosphate lipid carrier, creating the PG precursor termed "lipid II"[29]. Early models suggested FtsW and RodA, glycosyltransferase (GTase) enzymes of the divisome and elongasome, respectively, were lipid II flippases[30,31]. Furthermore, *in vitro* data suggested the bifunctional cell wall synthase PBP1A may also have flippase activity[32]. However, recent work has established MurJ as the sole lipid II flippase[30]. Once in the periplasm, lipid II is integrated into the PG by DD-transpeptidases (DD-TPases) and GTases of the divisome and elongasome[33,34].

## Elongation and division

Coordination of growth and division involves all layers of the tripartite envelope and is required to maintain cellular integrity[35]. A constellation of proteins regulate elongation and division, including several functionally homologous proteins that retain specificity for either the elongasome or the divisome[33]. Complex feedback networks underlie protein recruitment and activation and the tradeoff between elongation and division[37].

Based on studies largely in *E. coli*, it is generally accepted there are three main synthase categories within Gram-negative bacteria: monofunctional TPases (PBP2 in elongation and its division paralog PBP3/FtsI), monofunctional GTases (RodA in elongation and its division paralog FtsW) and bifunctional GTase-TPases (PBP1A, PBP1B and PBP1C)[38]. *In vitro* data of bifunctional PBPs (aPBPs) showed transpeptidation depends on functional GTase activity[32,39]. Conversely, the opposite may be true for the monofunctional PBPs, PBP2 and RodA[40]. Each of are integral membrane proteins[34], and with the exception of aPBPs, are restricted to their respective elongation or division complexes[41].

The biological implications of aPBP activity are not fully understood. Though they catalyze the same molecular reactions, the aPBPs likely serve independent roles. PBP1C is thought to be important for virulence. In *E. coli*, PBP1A and PBP1B are thought to be primarily involved in elongation[34,42] and division[34,35,43,44], respectively. PBP1A and PBP2 may interact at the elongasome[42], while PBP1B and PBP3 are enriched at divisome[44]. Intriguingly, neither aPBP is required for elongation[41] or division[45]. PBP1A and PBP1B are considered semi-redundant as only one is essential for growth[22]. For example, the overlapping activity of PBP1A and PBP1B allows *E. coli* to grow at different ends of the pH scale. In this instance, PBP1A is important for growth in alkaline conditions and PBP1B activity tolerates acidic pH[46].

Interestingly, PBP1B has unique activities outside of division in PG repair, including along the lateral wall[20,47]. Recent work revealed PBP1B forms a repair complex with a monofunctional, 3-3 crosslinking LD-transpeptidase to repair PG holes left behind after the disassembly of a large transenvelope complex[20]. The repair complex prevents lysis during incubation with otherwise lethal ampicillin concentrations[48]. Additionally, PBP1B is important for extending cellular viability in DAP auxotrophs[47] and when lipid II is limited[49]. PBP1B, but not PBP1A, is required for PG reassembly after β-lactam stress-induced spheroplast formation[45]. PBP1B as repair machinery is supported by earlier work showing cells without PBP1B have reduced cylindrical wall stiffness and greater plasticity[50].

To date, PBP1A remains enigmatic. Studies in *E. coli* showed that PBP1A localizes along the lateral cell wall in distinct foci[42], but it is not required for elongation[41]. PBP1A is not thought to interact with the divisome complex and PBP3 does not have an affinity for immobilized PBP1A in *E. coli*[42]. However, because either PBP1A or PBP1B are required viability[22], it may contribute to division if PBP1B is defective. However, previous work from our laboratory demonstrated

PBP1A and PBP1B are not semi-redundant in all bacteria. In *A. baumannii,* PBP1A but not PBP1B promotes cell lysis when lipid A biosynthesis is mutationally inactivated[17]. Other studies have tested PBP1A for PG repair activity[20,45,48], but reported it does not contribute to maintenance. A role unique for PBP1A outside of cell wall biogenesis remains unresolved.

## LD-transpeptidases are agents of peptidoglycan repair, remodeling and recycling

*LD-t*ranspeptidases (Ldts) are a family of monofunctional enzymes containing a YkuD PG-binding domain with a conserved active-site cysteine. The domain was named for the first characterized enzyme of this class, YkuD[51]. Several Ldt orthologs have since been identified[52–54]. Ldts are ubiquitous in Gram-negative and Gram-positive bacteria, with some species encoding up to twenty Ldts[18,55]. In general, Ldts increase cellular fitness and defend against lysis via envelope modification. Ldts catalyze four distinct chemical reactions: covalent attachment of lipoprotein[56] or β-barrel proteins[57,58] to PG, amidase cleavage of PG-attached proteins[54], LD-carboxypeptidase amidation of tetrapeptides stems in PG recycling[59–61] and 3-3 crosslink formation between adjacent stem peptides[52,53] or D-amino acid incorporation[62] into tetrapeptide stems.

The only known covalent attachment between PG and the OM is catalyzed by Ldts. Other PG-associated proteins like OmpA and Tol-Pal are noncovalently attached[63]. Several redundant Ldts in *E. coli* conjugate the lipoprotein, Lpp (Braun's lipoprotein), to the *m*-DAP residue of PG[56,64]. Recently, Ldts were demonstrated to attach β-barrel proteins in bacteria not encoding Lpp[57,58]. While lipoprotein and β-barrel linkages are not mutually exclusive, Ldts have substrate specificity for one protein species[58]. Presumably, strong OM-PG covalent linkage increases fitness during extreme environmental fluctuations between pH, osmolarity and temperature[65].

In *E. coli*, Lpp contributes robustly to OM stability and stiffness[56]; however, extensive Lpp crosslinking would presumably decrease cellular fitness in some environments. However, LdtF, cleaves Lpp-PG crosslinks, a reverse reaction that is also important for fitness adaptations[66,67]. Interestingly, LdtF also stimulates the 3-3 crosslinking activities of other Ldt paralogs in *E. coli*[20]. This suggests lipoprotein binding and alternative crosslinking provide disparate fitness benefits to the cell, despite both being linked to increased envelope stiffness.

Although *E. coli* Ldts are not essential in standard laboratory conditions, Ldts that catalyze 3-3 crosslinking become essential in bacteria with severe envelope defects[20,48], allowing for growth under otherwise lethal conditions. Alternative 3-3 crosslinking is resistant to lysozyme[19] and β-lactam disruption[52,53]. 3-3 crosslinked PG is thought to prevent envelope failure[68] and is increased in cells with severe OM defects[20]. Additionally, this category of Ldt mediates PG remodeling via noncanonical D-amino acid incorporation. D-amino acid incorporation is implicated in resistance to bacterial warfare agents where they obscure effector protein targets and prevent type six secretion (T6SS) dependent killing[69]. Moreover, D-amino acids increase resistance against lysis from osmotic stress[70,71]. In addition to passive fortification of PG, D-amino acids regulate cell wall biogenesis. A reconstituted mixture of D-amino acids excreted in stationary phase supernatant was demonstrated to plateau PG biosynthesis in logarithmically growing bacteria[71]. Likewise, D-amino acids broadly inhibit bacterial growth and are being investigated as antimicrobial agents[72].

Recently, a noncanonical cytoplasmic LD-carboxypeptidase Ldt, LdtK or ElsL, was characterized in *A. baumannaii*[59–61]. LdtK is thought to be involved in early steps of PG recycling due to its cytoplasmic subcellular localization and preferential specificity for tetra-muropeptides[60]. Transposon sequencing data revealing disruption to later steps of the recycling pathway decreased fitness in Δ*elsL* (Δ*ldtK)*[59], contributing to further evidence for LdtK in the PG recycling. LdtK is

required for viability in *A. baumannii* under severe envelope stress, including meropenem tolerance and loss of OM asymmetry[60,73].

## The detailed complexity of PG biogenesis gives rise to species specific differences

Our understanding PG biogenesis and synthase regulation in Gram-negative bacteria is largely built upon studies in the model organism *E. coli*. However, the established *E. coli* literature does not always translate to other, lesser studied organisms. Functional distinctions are becoming especially evident in the nosocomial pathogen *Acinetobacter baumannii*, a γ-Proteobacteria relative of *E. coli*. PBP1A and PBP1B in *A. baumannii* contain low (40%) homology to their aPBP orthologs in *E. coli*. Several lines of evidence, including Chapter 5 of this dissertation, suggest PBP1A and PBP1B activities are not functionally redundant in *A. baumannii* as they are thought to be in *E. coli*[17,73,74]. Our studies[73] and others found PBP1A but not PBP1B is important for cellular fitness in *A. baumannii*. Our findings further show PBP1A, unexpectedly, associates with the divisome and directly interacts with PBP3. To the author's knowledge, this has not been demonstrated before in other Gram-negative bacteria.

Regulation of aPBPs in *A. baumannii* differs from literature precedent. In γ-Proteobacteria like *E. coli,* PBP1A and PBP1B are regulated by specific OM lipoproteins[33,34,75]. While *A. baumannii* does encode for an ortholog of LpoP, the PBP1B regulator initially discovered in *Pseudomonas aeruginosa*[76], it is not known to encode for an orthologous PBP1A lipoprotein regulator. Interestingly, *A. baumannii* also does not encode for hydrolytic PG enzymes important for septation[77,78] including the PG hydrolase activator EnvC, the amidases AmiA, AmiB, AmiC and AmiD or their lipoprotein regulator NlpD. Moreover, *A. baumannii* does not encode for FtsEX[79] which are key division enzymes in several Gram-negative bacteria[80]. This suggests there

are significant knowledge gaps pertaining to PG biosynthesis and specifically division in *A. baumannii*.

There is clinical importance in delineating these differences between *E. coli* and other Gram-negative organisms. Bactericidal literature on PBP-targeting β-lactams is largely based on *E. coli*[81]; however, recent studies show this killing model does not directly apply to other Gram-negative pathogens that form spheroplasts and tolerate β-lactam exposure[82], including *A. baumannii*[60]. This highlights the necessity of detailing PG biogenesis and maintenance in pathogens other than the model organism *E. coli* to understand antibiotic resistance mechanisms.

## Biogenesis of an asymmetric outer membrane layer

The OM is a protective barrier that is highly conserved, yet dynamic. It is an asymmetric glycolipid bilayer wherein the dominate glycerophospholipid species of the inner leaflet is phosphatidylethanolamine, followed by phosphatidylglycerol then cardiolipin[83]. The outer leaflet is enriched with LPS or LOS, depending on species. LPS contains three domains: the membrane anchor lipid A, the core oligosaccharide, and the O-antigen[84,85]. In contrast, LOS contains only the former two[86] and is the primary glycolipid encoded by mucosal organisms[87]. The glycolipid-enriched OM of Gram-negative bacteria prevents envelope translocation of large, lipophilic macromolecules including potentially useful antibiotics.

The membrane anchor of LPS/LOS, $Kdo_2$-lipid A, is assembled at the IM via the highly conserved Raetz pathway[85,88]. The Raetz pathway consists of nine constitutively expressed, essential enzymes (LpxACDHBKLM and KdtA) and is one of the most fundamental pathways in Gram-negative bacteria[85,88,89]. $Kdo_2$-lipid A is essential for viability in Gram-negative bacteria, with few notable exceptions[90–92]. LPS/LOS-deficient ($LOS^-$) Gram-negative bacteria contain

mutations in one of the first three enzymatic steps of the Raetz pathway, LpxACD[90–93]. However, to date, these genes remain essential in all other Gram-negative species that encode them[94]. This rationale makes LpxC, the first committed step in lipid A biogenesis[85,95], an attractive potential target for antibiotics. LpxC inhibitors are currently in development and being patented[96].

Distal to $Kdo_2$ in mature LPS/LOS is the core oligosaccharide, which is synthesized in parallel in the cytoplasm[97]. The core oligosaccharide is conjugated to $Kdo_2$-lipid A, forming the LOS unit. Following assembly, LOS is flipped across the IM into the periplasm by MsbA flippase[98,99]. Here, LOS can be either be transported across the periplasm via the essential Lpt bridge (LptA-LptG)[100–102] for insertion into the outer leaflet of the OM[103], or it can be conjugated to the O-antigen moiety to form LPS prior to localization[85,101]. Transport occurs at a rate of $10^3$ molecules $s^{-1}$ to ensure coverage of the cell surface during growth[104,105].

## The outer membrane is a load-bearing structure

Previously, PG was considered sufficient for reinforcing cellular structure; however, pivotal research redefined the Gram-negative OM as an equal load-bearing element[106]. Bis-phosphorylated lipid A is negatively charged and will therefore repel adjacent lipid A moieties[107]. To overcome electrostatic repulsion, divalent cations intercalate between phosphate groups thus electrostatically linking lipid A across the surface of the cell[106,107]. It was recently hypothesized that these tight parallel associations between lipid A moieties contribute significantly to envelope stiffness[106]. The study further investigated OM stiffness through cellular envelope contraction during hyperosmotic shock and depletion of cellular turgor[106]. Importantly, when the OM was removed, the cell contracted the same distance in both width and length, suggesting the OM stabilizes PG and maintains it above its resting length[106]. Thus, PG and the OM contribute equally

as load-bearing structures that sustain turgor pressure and provide mechanical envelope stability. Accordingly, it is thought lipid A perturbations pose extreme biophysical stress for the cell.

## Defensive lipid A remodeling

While the canonical lipid A structure is conserved among Gram-negative bacteria, some organisms, including many associated with human disease can modify the lipid A structure to increase environment-specific fitness[16,85,108]. For example, deacylation of the canonical hexa-acylated lipid A structure allows evasion of host recognition[109]. Hexa-acylated lipid A is a potent agonist of toll-like receptor 4 (TLR4)[110,111]; hence, pathogens displaying penta- or tetra-acylated lipid A may increase avoidance of innate defenses and persist within the host[112,113]. Conversely, acylation of lipid A prevents desiccation and increases OM hydrophobicity which is thought to reduce translocation of harmful charged molecules into the cell, including cationic antibiotics[114]. Polymyxins are last-line antimicrobials prescribed when carbapenem treatment fails, oftentimes to combat CRE and CRAB[8]. Polymyxin resistance in Gram-negative bacteria involves IM sensor kinase signaling cascades that detect periplasmic perturbations and upregulate the synthesis and transport of protective, charge neutralizing moieties to prevent electrostatic interactions between lipid A and the cationic polymyxin antibiotic[9–11]. Intriguingly, polymyxin-resistance in *A. baumannii* can further manifest from mutational inactivation of the Raetz pathway, resulting in $LOS^-$ cells.[17]. These resistance mechanisms are detailed below.

## The resurgent interest in polymyxin antimicrobials provided short-lived hope for addressing CRE and CRAB infections

The failure of front-line therapeutics to prevent HAI following crucial, invasive procedures is an increasing problem. Consequently, antibiotic resistance sets back the progress of modern healthcare. The standard of care for MDR HAI, carbapenem, is becoming increasingly ineffective and clinicians are turning to "last-resort" antimicrobials, like polymyxins[115]. Polymyxins are antimicrobial peptides that were first discovered in *Bacillus polymyxa* in 1947. The polymyxin derivatives, polymyxins A-E, are effective antibiotics, but are not widely used as therapeutics in humans due to acute nephrotoxicity and neurotoxicity[116]. Currently, two polymyxins are commercially available, polymyxin B (Neosporin®) and polymyxin E (colistin). Polymyxin B is approved for use in humans as a topical antibiotic for dermal, ocular or ear infections. Colistin is approved for the treatment of bacteriemia. Colistin fell out of common use due to the availability of effective, comparably less toxic antibiotic options. Thus, the renewed interest in colistin is due to unfortunate necessity.

Colistin is a nonribosomal polypeptide consisting of a decapeptide ring and a terminal fatty acid moiety[117]. It includes the noncanonical amino acid, 2,4-diaminobutyric acid (DAB), which is cationic under physiological conditions[117]. Colistin is a cationic detergent that robustly disrupts both the OM and IM[118–120] of Gram-negative bacteria. It electrostatically binds to anionic phosphate groups of lipid A and perturbs the lipid bilayers[117,121]. After binding, colistin promotes transmembrane pore formation through its amphipathic, detergent properties and is thought to form micellular aggregates by insertion of the lipophilic acyl moiety into the lipid bilayer[121,122].

Compromising the load-bearing potential of OM was thought to be sufficient for cell death[117]; however, recent studies show additional mechanisms of action at the IM[118–120]. *E. coli* spheroplasts,

cells without the LPS-enriched OM, were used to demonstrate colistin interaction with LPS at the IM. The authors hypothesized that this interaction with LPS at the IM could lead to lysis[120]. Furthermore, secondary colistin mechanisms have been linked with the formation of hydroxy radicals[123] and NADH quinone reductase toxicity[124] leading to pH imbalance and proton motive force disruption. Despite recent dependence on colistin for addressing CRE and CRAB infections[8], colistin resistance quickly emerged[125–128].

## Mutational inactivation of lipid A biosynthesis contributes to colistin resistance and challenges our understanding of factors essential for Gram-negative viability

Lipid A is essential for viability in Gram-negative bacteria, with few notable exceptions[90–92]. LOS$^-$ *Neisseria*[90] and *Moraxella*[92] strains were successfully engineered *in vitro*, with limited CFU viability being reported for LOS$^-$ *Neisseria*[129]. Intriguingly, depletion of lipid A as a colistin resistance mechanism is unique to select strains of *A. baumannii* and represents the first known spontaneously occurring instance of lipid A loss[17].

LOS/LPS transport to the outer leaflet of the OM occurs via the seven essential Lpt proteins that constitute the Lpt translocation machinery, LptA[102,130], LptBFG[101,102,131], LptC[130,131] and LptDE[130,131], as detailed above. Disruption of the LOS/LPS transport apparatus is thought to lead to the toxic accumulation of LOS/LPS in the outer leaflet of the IM. Consistent with this hypothesis, *Neisseria*[90] and *Moraxella*[92] LOS$^-$ strains were engineered with kanamycin cassette disruptions in the first gene of the Raetz pathway, *lpxA*. Point mutations or varying insertion sequences (IS) in the first three genes of the Raetz pathway, *lpxA, lpxC* and *lpxD,* were documented in clinical isolates of LOS$^-$ *A. baumannii*[91]. Further studies attributed disruption of *lpxACD* to the IS element

IS*Aba11*, specifically, in the same clinical isolates[93]. These studies suggest that IS elements have a central role in lipid A biogenesis disruption and colistin resistance in *A. baumannii.*

In contrast to engineered LOS$^-$ *Neisseria*[90] and *Moraxella*[92], disruption of lipid A biosynthesis at early steps in the Raetz pathway is not typically sufficient to produce viable LOS$^-$ *A. baumannii*. Previously, our laboratory screened fifteen *A. baumannii* laboratory-adapted and clinical isolates under colistin selective pressure for lipid A depletion[17]. Here, we identified a conserved *pbp1A* compensatory mutation in viable LOS$^-$ isolates[17]. Our study further found the original LOS$^-$ isolate[91], ATCC 19606, did not transcribe PBP1A at levels detectible by western blot[132].

Two independent transcriptomic studies in LOS$^-$ isolates, from our laboratory[132] and others[133], demonstrated increased expression of proteins associated with Mla-retrograde phospholipid transport, lipoprotein synthesis and Lol-dependent transport compared to a colistin-sensitive isolate. These data suggest LOS$^-$ cells may densely pack lipoproteins into the OM to compensate for the loss of lipid A and LOS.

## Heteroresistance challenges clinical antimicrobial susceptibility testing methods

Further complicating efforts to address the global challenge of antibiotic resistance, heteroresistant clinical isolates have been identified[12,128,134]. Broadly, heteroresistance is defined as a drug-susceptible clonal population containing a drug-resistant subpopulation[135]. Enrichment of the resistant subpopulation under antibiotic selection through growth, defines heteroresistance relative to f persister cells, which do not grow. This definition of heteroresistance includes resistances that arise from spontaneous, stable mutations during treatment and from variation in gene expression. Stable heteroresistant populations will not readily revert to a drug-susceptible

phenotype. In contrast, heteroresistance manifesting from transcriptional regulation or mutations with fitness costs are unstable if the antibiotic selective pressure is removed[12,136].

In both instances, the resistant subpopulation can remain undetected during standard antimicrobial susceptibility testing (AST), leading to treatment failure[13–15]. Even with AST best practices, results are expected to lead to treatment failure in 10% of all clinical applications or 60% if the therapeutic is suboptimal[137]. These expected treatment failures are thought to be a result of undetected heteroresistance. Unstable heteroresistance is thought to contribute significantly to false-negative AST results due to drug-susceptible phenotype reversion[135].

The reliability of heteroresistance detection with clinical ASTs vary based on method. Gradient diffusion methods[138], including Etest and disk diffusion, may show colonies growing in the zone of inhibition; however, these methods frequently fail to detect resistant subpopulations[135]. In contrast, population analysis profiling (PAP) is the gold standard method for identifying heteroresistant cells[135,139]. In PAP, a standard dilution of a genetically homologous population is incubated with microdilutions of increasing antibiotic concentration, often in a 96-well plate. The individual wells are then collected and plated onto solid media to quantify colony forming units (CFUs). With this method, the lower limit for detection is near 1e-7[135]. Despite being the gold standard method, PAP assays are time and labor-intensive, making them subpar for clinical use[135].

Heteroresistance to several classes of clinically important antibiotics has been detected, including sulfonamides[140], aminoglycosides[141], tetracycline[142], penicillins and penicillin-derivatives[143–146] and polymyxins including colistin[13,128,147,148]. As a last-resort therapeutic, heteroresistance to colistin further complicates the struggle to treat carbapenem-resistant infections. Concerningly, a PAP screen of clinical CRE isolates uncovered severe colistin-sensitivity

misclassification where identification of colistin heteroresistance was higher than double the original detection rate[13].

## Two-Component Systems PhoPQ and PmrAB promote colistin heteroresistance in Enterobacteriaceae

Colistin heteroresistance readily manifests in Enterobacteriaceae, which includes the common CRE pathogens *Escherichia coli, Klebsiella pneumoniae, Salmonella enterica* serovar Typhimurium and *Enterobacter* spp., through varied alterations to the PhoPQ and PmrAB two-component regulatory systems (TCSs). PhoPQ and PmrAB are extensively studied phospho-relay transcriptional regulators of lipid A modifying enzymes[11,149,150]. PhoPQ and PmrAB are highly conserved in Enterobacteriaceae but are variable in respect to gene regulation between species[16].

PhoQ and PmrB are integral IM sensor kinases that detect envelope disturbances through their periplasmic domains. Following signal detection, the kinases autophosphorylate and phosphotransfer to the cognate cytosolic response regulators, PhoP and PmrA, respectively[149]. PhoQ is stimulated by low pH[151], depletion of divalent cations ($Mg^{2+}$ and $Ca^{2+}$) critical to OM stability[152] and cationic antimicrobial peptide OM perturbations [9,153]. Phospho-PhoP upregulates genes encoding virulence factors, acid resistance and structural lipid A modifications[154]. PmrAB detects and responds to iron ($Fe^{3+}$) stress[155] and other OM perturbations indirectly via cross-regulatory interaction with PhoPQ. PhoPQ and PmrAB systems are coupled in some Enterobacteriaceae where lipid A modification involves indirect activation of PmrAB through PhoPQ[9,150]. The PhoPQ signal-transduction cascade activates *pmrD* transcription which binds and stabilized phospho-PmrA[156]. PmrA induces the transcription of the *arn* operon (*arnBCADTEF)*[156]. These gene products are enzymes that synthesize and conjugate L-Ara4N (4-amino-4-deoxy-L-

arabinose) moieties to lipid A and reduce the electrostatic attraction to colistin. Moreover, the PmrAB regulon activates *pmrC* and *cptA*, which encode phosphoethanolamine (pEtN) transferases, for pEtN addition to lipid A[157]. However, L-Ara4N lipid A modifications are known to contribute more substantially to colistin resistance than pEtN[157], placing a greater importance on the *arnBCADTEF* operon over *pmrCAB*.

The tight cross-regulatory interactions of PhoPQ and PmrAB may reduce the response sensitivity for lipid A modifications necessary for survival. Mutations in the PhoPQ-PmrAB TCSs can cause constitutive expression of the *arnBCADTEF* and *pmrCAB* operons[10,158–162], priming a subpopulation for survival. Similarly, CRE *K. pneumoniae* inserts a stop codon into MgrB, a negative regulator of PhoPQ, to develop colistin heteroresistance[163]. Another adaptive mechanism, spontaneous gene duplication, leads to tandem gene amplifications that typically do not incur fitness cost for the cell[164]. Resistance via tandem gene amplification in clinical isolates is not uncommon. In a study of heteroresistant Enterobacteriaceae and *A. baumannii* clinical isolates, the authors attributed half of the resistance mechanisms to tandem amplification of known antibiotic resistant gene pathway[135]. In particular, colistin heteroresistance has been attributed to amplification of *pmrD* in *S. enterica*[165]. Lastly, our lab described a colistin heteroresistance mechanism in *E. cloacae* wherein crosstalk between PhoPQ and PmrAB is not necessary for L-Ara4N lipid A modification[166]. We found *E. cloacae* encodes a PhoP binding site upstream of *arnB*, allowing PhoPQ signal cascades to directly upregulate and conjugate L-Ara4N to lipid A[166].

# CHAPTER 3: Colistin heteroresistance in *Enterobacter cloacae* is regulated by PhoPQ-dependent 4-amino-4-deoxy-L-arabinose addition to lipid A

Katie N. Kang[a], Dustin R. Klein[b], Misha I. Kazi[a], François Guérin[c], Vincent Cattoir[d], Jennifer S. Brodbelt[b], and Joseph M. Boll[a,#]

Affiliations:

[a]Department of Biology, University of Texas at Arlington, Arlington, TX, USA

[b]Department of Chemistry, University of Texas at Austin, Austin, TX, USA

[c]Department of Clinical Microbiology, Caen University Hospital, Caen, France; EA4655, University of Caen Normandie, Caen, France

[d]Department of Clinical Microbiology and National Reference Center for Antimicrobial Resistance (Lab Enterococci), Rennes University Hospital, Rennes, France; Inserm Unit U1230, University of Rennes 1, Rennes, France

#Correspondence:

Joseph M. Boll

The University of Texas at Arlington

Arlington TX, 76010

Phone (817) 272-4045

Email: joseph.boll@uta.edu

K.N.K. and D.R.K contributed equally to this work.

** Published as: Kang KN, Klein DR, et al. Colistin heteroresistance in *Enterobacter cloacae* is regulated by PhoPQ-dependent 4-amino-4-deoxy-L-arabinose addition to lipid A. *Mol Microbiol.* 2019 Jun;111(6):1604-1616. doi:10.1111/mmi.14240

## ABSTRACT

The *Enterobacter cloacae* complex (ECC) consists of closely-related bacteria commonly associated with the human microbiota. ECC are increasingly isolated from healthcare-associated infections, demonstrating that these Enterobacteriaceae are emerging nosocomial pathogens. ECC can rapidly acquire multidrug resistance to conventional antibiotics. Cationic antimicrobial peptides (CAMPs) have served as therapeutic alternatives because they target the highly conserved lipid A component of the Gram-negative outer membrane. Many Enterobacteriaceae fortify their outer membrane with cationic amine-containing moieties to prevent CAMP binding, which can lead to cell lysis. The PmrAB two-component system (TCS) directly activates 4-amino-4-deoxy-L-arabinose (L-Ara4N) biosynthesis to result in cationic amine moiety addition to lipid A in many Enterobacteriaceae such as *E. coli* and *Salmonella*. In contrast, PmrAB is dispensable for CAMP resistance in *E. cloacae*. Interestingly, some ECC clusters exhibit colistin heteroresistance, where a subpopulation of cells exhibit clinically significant resistance levels compared to the majority population. We demonstrate that *E. cloacae* lipid A is modified with L-Ara4N to induce CAMP heteroresistance and the regulatory mechanism is independent of the $PmrAB_{Ecl}$ TCS. Instead, $PhoP_{Ecl}$ binds to the $arnB_{Ecl}$ promoter to induce L-Ara4N biosynthesis and PmrAB-independent addition to the lipid A disaccharolipid. Therefore, $PhoPQ_{Ecl}$ contributes to regulation of colistin heteroresistance in some ECC clusters.

## INTRODUCTION

Gram-negative bacteria assemble a highly conserved outer membrane (OM) barrier. Glycerophospholipids comprise the periplasmic monolayer of the asymmetric lipid bilayer, while the surface-exposed monolayer is enriched with lipopolysaccharide (LPS). The LPS glycolipid is organized into three domains; an O-antigen carbohydrate repeat, core oligosaccharide, and the membrane anchor, lipid[89]. The lipid A domain is initially synthesized as a β-1',6-linked glucosamine disaccharide that is both phosphorylated and fatty acylated. Lipid A is the bioactive portion of LPS and robustly activates the human Toll-like receptor 4 (TLR-4) and myeloid differentiation factor 2 (MD-2) immune complex to induce immune reactivity[17,89,114,167]. Gram-negative pathogens encode highly conserved regulatory mechanisms that modify lipid A to prevent TLR-4/MD-2 recognition and to fortify the OM against immune effectors and antimicrobials, which promotes survival in the host[168].

Lipid A modification enzymes are transcriptionally regulated by two-component systems (TCS)[11,149]. The PmrAB and PhoPQ TCSs are well-studied phosphorelay signaling systems that regulate lipid A modifications in response to specific environmental signal[152,153,169]. PmrAB and PhoPQ are highly conserved among pathogenic Enterobacteriaceae[16]. PmrAB responds to high $Fe^{3+}$ concentrations, cationic antimicrobial peptides (CAMPs), and slightly acidic pH to directly activate *eptA* (also known as *pmrC*) and *arn* operon expression[155,170,171], which encode phosphoethanolamine (pEtN) and 4-amino-4-deoxy-L-arabinose (L-Ara4N) transferases, respectively[157,160,172]. Cationic amine addition to the lipid A domain of LPS neutralizes the surface charge to protect the cell from CAMP-mediated lysis[160,172].

PhoPQ is activated in response to depletion of divalent cations such as $Mg^{2+}$ and $Ca^{2+}$ and the presence of CAMPs[152,153,169]. PhoPQ phosphotransfer directly activates transcription of genes

encoding PagL (only in *Salmonella*[168]) and PagP, which add or remove acyl chains from lipid A, respectively[9,152,173,174]. Additionally, it directly activates *arn* expression in *Klebsiella* and *Yersinia spcs*.[175,176]. While the PmrAB and PhoPQ TCSs each regulate distinct subsets of genes, the independent signaling pathways also converge through the connector protein, PmrD[161,177,178]. PmrD binds phospho-PmrA, which prevents PmrB-mediated dephosphorylation[156,177,179,180]. Constitutive PmrA-dependent gene expression increases pEtN and L-Ara4N lipid A modifications. The *Enterobacter cloacae* complex (ECC) is composed of thirteen closely-related Gram-negative bacterial clusters (designated C-I to C-XIII)[181]. ECC are typically associated with the host microbiota. However, many clusters have been associated with hospital-acquired infections, especially in immunocompromised patients[182]. Infections manifest in a wide range of host tissues with symptoms including skin, respiratory tract, urinary tract, wound and blood infections[183]. ECC have increasingly emerged in nosocomial settings and are problematic because they harbor multidrug resistance (MDR) mechanisms, which limit treatment options[82,182,184,185]. Alternative last-line therapeutics used to treat MDR Gram-negative infections include the CAMP, colistin (polymyxin E), which binds the lipid A portion of LPS to perturb the outer membrane and lyse the bacterial cell. Despite success as a last-line therapeutic[186,187], many ECC clusters demonstrate heteroresistance, where a subset of the clonal population is colistin resistant[12,137,184,188]. We do not fully understand the underlying molecular mechanism(s) that regulate colistin heteroresistance in ECC; further characterization will advance our understanding of antimicrobial resistance and could help inform new treatment strategies.

A previous report showed that colistin heteroresistance naturally occurs within clonal ECC clusters[184]. Moreover, colistin heteroresistance in *E. cloacae* was induced by innate immune defenses within a murine infection model, which led to treatment failure[188]. Transcriptional

analysis of susceptible and resistant populations suggested that pEtN and L-Ara4N lipid A modifications contribute to heteroresistance[188] and PhoPQ contributed to regulation[184,188], as described in other Enterobacteriaceae[16]. However, it was not established that the lipid A modifications actually occur, nor has PhoPQ-dependent, PmrAB-independent regulation of colistin heteroresistance been fully described in *E. cloacae* or other ECC isolates.

Herein, we demonstrate that *E. cloacae* colistin heteroresistance involves PhoPQ$_{Ecl}$, which regulates L-Ara4N modification of lipid A. The PhoP$_{Ecl}$ response regulator directly binds to the promoter region of *arnB*$_{Ecl}$, which is the first gene of a seven-gene operon (*arnBCADTEF*$_{Ecl}$). Transcriptomics analysis supports a model of PhoPQ-dependent, PmrAB-independent *arn*$_{Ecl}$ regulation. Furthermore, L-Ara4N modification of lipid A increased in response to growth in limiting $Mg^{2+}$, which amplified colistin resistance in a PhoPQ$_{Ecl}$-dependent manner. Lastly, sequencing of twelve ECC colistin-susceptible isolates pinpointed mutations within the PhoPQ-dependent lipid A modification pathway that promoted colistin susceptibility. This study advances our understanding of the molecular mechanisms that mediate colistin heteroresistance in ECC.

## RESULTS

### Colistin heteroresistance in *E. cloacae* is regulated by PhoPQ$_{Ecl}$, but not PmrAB$_{Ecl}$.

To elucidate the underlying mechanisms that regulate colistin heteroresistance in ECC, we analyzed a collection of *E. cloacae* subsp. *cloacae* strain ATCC 13047 genetic mutants by calculating the colony forming units (CFUs) during exponential growth in the absence and presence of colistin (**Fig 1A**). While wild type and all mutant *E. cloacae* strains grew in standard growth media, Δ*phoPQ*$_{Ecl}$ was not viable when 10 μg/ml of colistin was added to the media. Clinical resistance to colistin is defined as >4 μg/ml[189]. The decrease in Δ*phoPQ*$_{Ecl}$ cell viability

suggested that PhoPQ$_{Ecl}$ contributes to colistin heteroresistance. Furthermore, wild type *E. cloacae* grown in colistin demonstrated approximately ten-fold less CFUs at hour two (P value <0.05), suggesting a survival defect in early logarithmic growth phase. However, the fitness defect was no longer significant at hour three. By hour four, CFUs were equivalent to growth without colistin (**Figure 1A**).

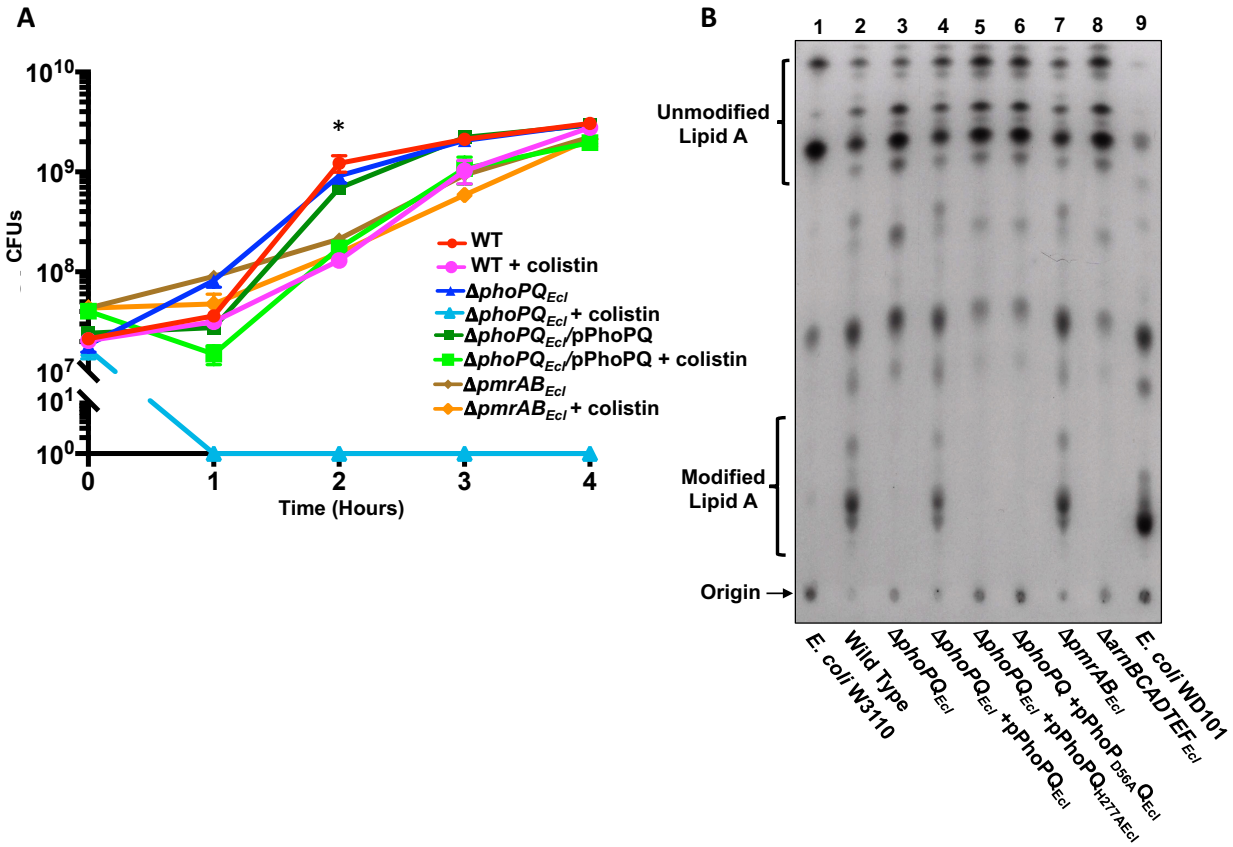


**Figure 1**: **Survival of colistin heteroresistant *E. cloacae* is dependent on PhoPQ$_{Ecl}$, but not PmrAB$_{Ecl}$-regulated lipid A modifications. (A)** *E. cloacae* logarithmic phase growth over time as measured by CFUs. At 2 h, the growth rate between wild type grown in LB was significantly (*) different from cells grown in LB + colistin (P value < 0.05). **(B)** $^{32}$P-radiolabeled lipid A was isolated from wild type and mutant *E. cloacae* strains and separated based on hydrophobicity using thin layer chromatography. Lipid A species are labeled as unmodified or modified as determined by *E. coli* W3110 (lane 1) and WD101 (lane 9) lipid A, respectively.

Due to reports of colistin heteroresistance in *E. cloacae* and other ECC strains (34, 39), we subjected wild type, Δ*phoPQ*$_{Ecl}$, Δ*phoPQ*$_{Ecl}$/pPhoPQ$_{Ecl}$, and Δ*pmrAB*$_{Ecl}$ *E. cloacae* to colistin E-test strip analysis, which provides a convenient method to observe heteroresistance. Squatter colonies within the zone of inhibition indicated colistin heteroresistance in wild type,

Δ*phoPQ*$_{Ecl}$/pPhoPQ$_{Ecl}$, and Δp*mrAB*$_{Ecl}$ strains, but not Δ*phoPQ*$_{Ecl}$. We confirmed colistin heteroresistance by population analysis profiling (PAP) (**Table 1**)[134]. Minimal inhibitory concentration (MIC) values were calculated using the broth microdilution (BMD) method (**Table 1**). Wild type, Δ*phoPQ*$_{Ecl}$/pPhoPQ$_{Ecl}$, and Δp*mrAB*$_{Ecl}$ *E. cloacae* all demonstrated MICs >256 μg/ml, while the Δ*phoPQ*$_{Ecl}$, Δ*phoPQ*$_{Ecl}$/pPhoPQ$_{H277A}$, Δ*phoPQ*$_{Ecl}$/pPhoP$_{D56A}$Q and Δ*arn*$_{Ecl}$ (*arnBCADTEF*$_{Ecl}$) MIC was 0.5 μg/ml. Together, these studies confirm that PhoPQ$_{Ecl}$ signal transduction and the *arn*$_{Ecl}$ biosynthetic operon (L-Ara4N) contribute to colistin heteroresistance in *E. cloacae*.

**Table 1**

| Isolate | MIC of colistin (μg/ml) by BMD[b] | MIC of colistin (μg/ml) by Etest | Frequency of appearance of subpopulations (PAPs[a]) — Concentration of colistin: 1 μg/ml | 2 μg/ml | 4 μg/ml | 8 μg/ml | 16 μg/ml | 32 μg/ml | 64 μg/ml |
|---|---|---|---|---|---|---|---|---|---|
| Wild type | ≥256* | 0.125** | $9.5\ 10^{-3}$ | $6.3\ 10^{-2}$ | $5.2\ 10^{-3}$ | $7.5\ 10^{-3}$ | $7.6\ 10^{-2}$ | $6.3\ 10^{-3}$ | $9.3\ 10^{-3}$ |
| ΔphoPQ$_{Ecl}$ | 0.5 | 0.125 | $2.6\ 10^{-3}$ | 0 | 0 | 0 | 0 | 0 | 0 |
| Δ*phoPQ*$_{Ecl}$ + pPhoPQ$_{Ecl}$ | ≥256* | 0.125** | $3.6\ 10^{-2}$ | $1.3\ 10^{-2}$ | $4.3\ 10^{-3}$ | $1.6\ 10^{-2}$ | $4.1\ 10^{-3}$ | $1.7\ 10^{-3}$ | $4.5\ 10^{-4}$ |
| Δ*phoPQ*$_{Ecl}$ + pPhoPQ$_{H277AEcl}$ | 0.5 | 0.125 | $3.1\ 10^{-2}$ | 0 | 0 | 0 | 0 | 0 | 0 |
| Δ*phoPQ* + pPhoP$_{D56A}$Q$_{Ecl}$ | 0.5 | 0.125 | $7.4\ 10^{-2}$ | 0 | 0 | 0 | 0 | 0 | 0 |
| Δ*pmrAB*$_{Ecl}$ | ≥256* | 0.125** | $2.9\ 10^{-2}$ | $1.8\ 10^{-3}$ | $7.7\ 10^{-2}$ | $9.2\ 10^{-3}$ | $5.5\ 10^{-2}$ | $1.3\ 10^{-3}$ | $2.3\ 10^{-4}$ |
| Δ*arnT*$_{Ecl}$ | 0.5 | 0.125 | $4.0\ 10^{-2}$ | 0 | 0 | 0 | 0 | 0 | 0 |

[a]PAP: Population Analysis Profile using an initial culture of $10^{10}$ CFU/ml.
[b]BMD: Broth microdilution method.
*Presence of skip wells.
**Presence of squatter colonies inside the zone of inhibition.

Since lipid A modifications induce colistin resistance in pathogenic Enterobacteriaceae[16], we analyzed wild type and mutant *E. cloacae* lipid A for modifications. $^{32}$P-radiolabelled lipid A was isolated and chromatographically separated based on hydrophobicity. As controls, we also analyzed lipid A from *E. coli* strain W3110 (**Figure 1B, lane 1**), which does not significantly modify its lipid A, and *E. coli* strain WD101 (**Figure 1B, lane 9**), which constitutively expresses *pmrA* to produce modified lipid A[172]. Thin layer chromatography (TLC) analysis indicated that wild type *E. cloacae* produced a mixture of lipid A consistent with modified and unmodified species (**Figure 1B, lane 2**). Δ*phoPQ*$_{Ecl}$ and the Δ*arn*$_{Ecl}$ strains did not produce modified lipid A (**Figure 1B, lanes 3 and 8**). PhoPQ complementation fully restored production of modified lipid

A in the *phoPQ* mutant (**Figure 1B, lane 4**). Furthermore, site-directed mutagenesis to substitute H277 in $PhoQ_{Ecl}$ or D57 in $PhoP_{Ecl}$ with alanine limited lipid A assembly to only unmodified species (**Figure 1B lanes 5 and 6**). These results confirm that $PhoPQ_{Ecl}$ phosphotransfer and L-Ara4N biosynthesis are essential for lipid A modification in *E. cloacae*. Interestingly, the $pmrAB_{Ecl}$ mutant assembled a modified lipid A, similar to wild type (**Figure 1B, lane 7**), and exhibited colistin heteroresistance (**Figure 1A, Table 1, Figure 2A**), suggesting that $PmrAB_{Ecl}$ does not regulate colistin heteroresistance in *E. cloacae.*

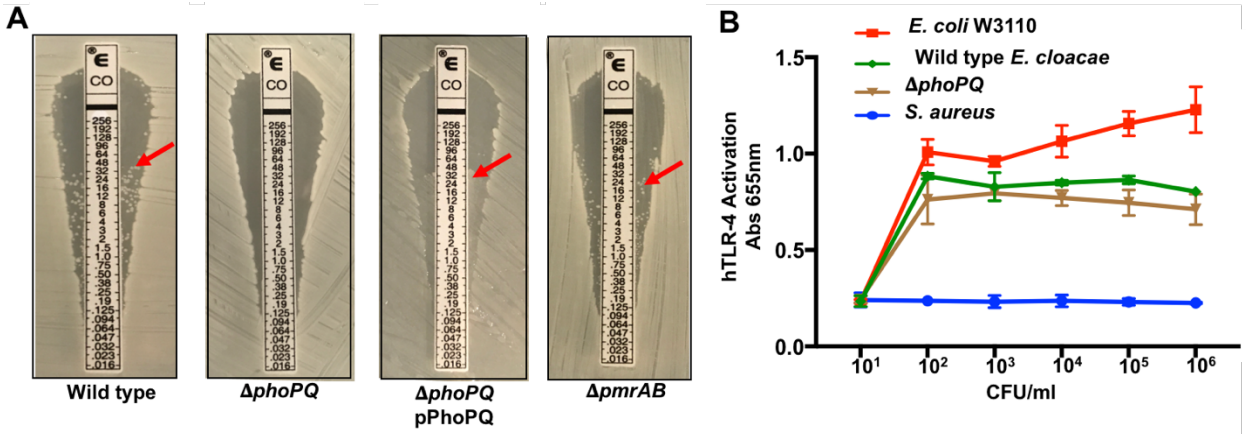


**Figure 2: (A)** E-test strips illustrate *E. cloacae* squatter colonies within the zone of inhibition, indicative of heteroresistance. Red arrows highlight colistin resistant colonies. **(B)** Stimulation of human TRL-4/MD-2 complex following incubation with bacterial cells (CFU/mL).

The lipid A anchor of LPS is a pathogen associated molecular pattern (PAMP) that is bound with high affinity by the mammalian host TLR-4/MD-2 complex[190], which activates a proinflammatory response to clear the bacterial infection[191]. Structural alterations to lipid A can dramatically alter TLR-4/MD-2-dependent host immune activation[167] and a previous report nicely demonstrated that *E. cloacae* colistin heteroresistance was induced by innate immune effectors[188]. Therefore, we examined if *E. cloacae* containing modified or unmodified lipid A would differentially activate TLR-4/MD-2 in a human embryonic kidney reporter cell line (HEK-blue)[167]. Wild type and $phoPQ_{Ecl}$ mutant strains stimulated TLR-4/MD-2-dependent activation equally

(**Figure 2B**), suggesting that lipid A modifications do not significantly alter host immune recognition. Reporter activation by *E. cloacae* lipid A was attenuated compared to *E. coli* lipid A at higher cell densities, suggesting differential recognition by the human TLR-4/MD-2 complex. The Gram-positive *Staphylococcus aureus,* which does not produce lipid A, did not stimulate the TLR-4/MD-2 complex (**Figure 2B**). Thus, while PhoPQ$_{Ecl}$-dependent lipid A modifications contribute to CAMP resistance in *E. cloacae*, they do not significantly affect innate immune recognition and reactivity.

## Determination of *E. cloacae* lipid A modifications.

In order to define outer membrane modifications, we isolated lipid A from wild type *E. cloacae* grown in media supplemented with 10 μg/ml of colistin and from Δ*phoPQ*$_{Ecl}$, which was grown without colistin. Purified lipid A was analyzed by direct infusion nanoESI. The MS1 spectra with a range of *m/z* 750-2000 are shown in online supplement The expanded MS1 spectrum (*m/z* 850-1200) of lipid A isolated from wild type *E. cloacae* demonstrated three distinct modifications: (i) addition of either one or two L-Ara4N moieties (red), (ii) palmitate ($C_{16:0}$) addition (green), and (iii) hydroxylation (**Figure 3A**) The MS1 spectrum of lipid A isolated from Δ*phoPQ*$_{Ecl}$ did not produce L-Ara4N modified lipid A (**Figure 3B**). Hydroxyl addition was not labeled for simplicity, but correlates with a *m/z* shift of 8 of the doubly-charged molecular ions. Higher-energy collisional dissociation (HCD) and ultraviolet photodissociation (UVPD) MS/MS spectra were obtained for the ions of *m/z* 1042.68 and 1161.79 from wild type and the ions of *m/z* 911.62 and 1030.73 from Δ*phoPQ E. cloacae*. Analysis of the MS/MS spectra from wild type (*m/z* 1042.68) indicated PhoPQ$_{Ecl}$-dependent addition of L-Ara4N at both the 1- and 4'-phosphates. The MS/MS spectra for the ion of *m/z* 1161.79 (wild type *E. cloacae*) showed addition of L-Ara4N at both the 1- and

4'-phosphates and palmitate addition to the *R*-2-hydroxymyristate. Analysis of lipid A from the *phoPQ*$_{Ecl}$ mutant (*m/z* 911.62) completely lacked L-Ara4N modified lipid A and analysis of the *m/z* 1030.73 ion from the *phoPQ*$_{Ecl}$ mutant demonstrated that palmitate addition at the *R*-2-hydroxymyristate position of lipid A occurred independent of PhoPQ$_{Ecl}$.

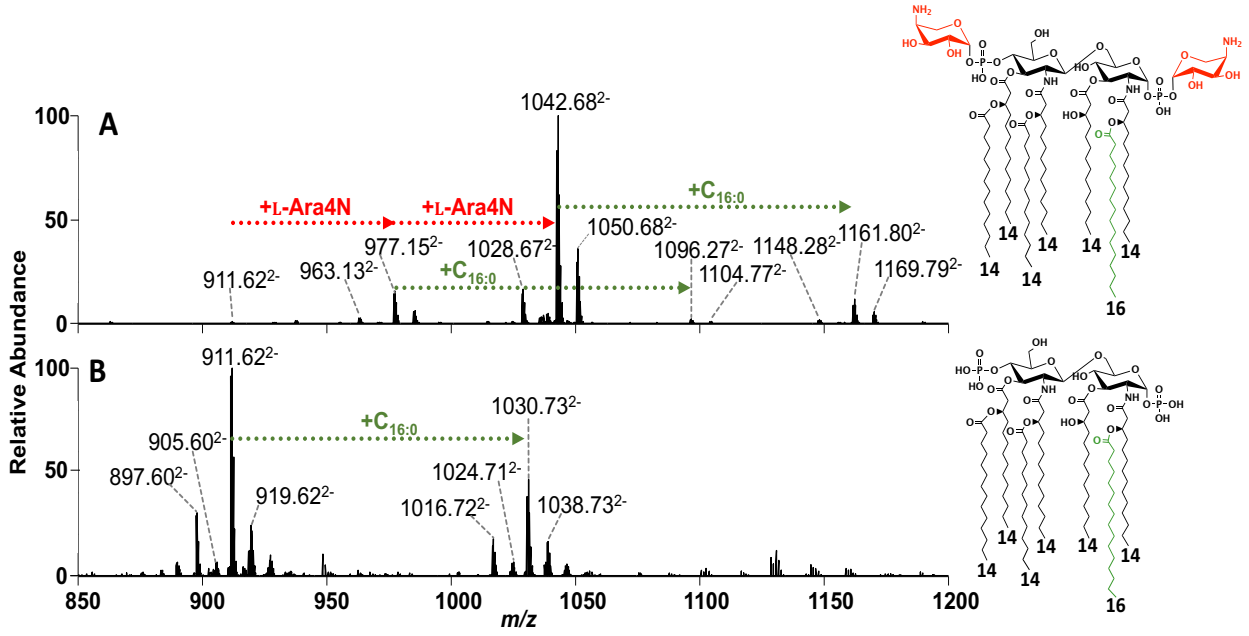


**Figure 3: Expanded MS1 spectra of lipid A** isolated from (**A**) wild type *E. cloacae* grown in media supplemented with 10 μg/ml colistin and (**B**) Δ*phoPQ*$_{Ecl}$, which was grown in media without antibiotics. The chemical structures associated with the MS1 spectra are illustrated on the right. The presence of aminoarabinose groups are denoted by L-Ara4N (red), while addition of palmitoyl groups are denoted by + C16:0 (green). Hydroxylation is not illustrated but is indicated by an m/z shift of eight relative to doubly charged lipid A ions in the spectra.

Based on transcriptomics studies, a previous report suggested that *E. cloacae* adds pEtN and L-Ara4N to lipid A to develop colistin heteroresistance[188]. However, our genetic and high-resolution mass spectrometry analysis demonstrate that only L-Ara4N modifies the 1- and 4'-phosphates of lipid A in a PhoPQ$_{Ecl}$-dependent manner (**Figure 3A and B**) and this amine-containing modification correlates with colistin heteroresistance (**Figure 1A and Table 1**).

## L-Ara4N lipid A modifications are dependent on PhoPQ$_{Ecl}$, but not PmrAB$_{Ecl}$.

To further characterize lipid A modifications in the Δ*pmrAB*$_{Ecl}$ mutant, we analyzed

purified lipid A from wild type and mutant *E. cloacae* using MALDI-TOF mass spectrometry. Wild type produced a lipid A mixture, which included L-Ara4N modified lipids (**Figure 4A and B**). In contrast, analysis of Δ*phoPQ*$_{Ecl}$ and Δ*arn*$_{Ecl}$ lipid A indicated that L-Ara4N modified lipids were not present. Expression of PhoPQ$_{Ecl}$ *in trans* from an IPTG-inducible promoter restored L-Ara4N modified lipid A in the *phoPQ*$_{Ecl}$ mutant. Furthermore, Δ*pmrAB*$_{Ecl}$ produced the L-Ara4N modification, similar to wild type (**Figure 4A**). The *m/z* of each prominent peak in our MALDI-MS analysis corresponded with the exact mass of an expected structure with only the L-Ara4N-containing structures demonstrating colistin resistance (**Figure 4B**). Here, we confirmed that L-Ara4N modification of lipid A in *E. cloacae* is not dependent on PmrAB$_{Ecl}$.

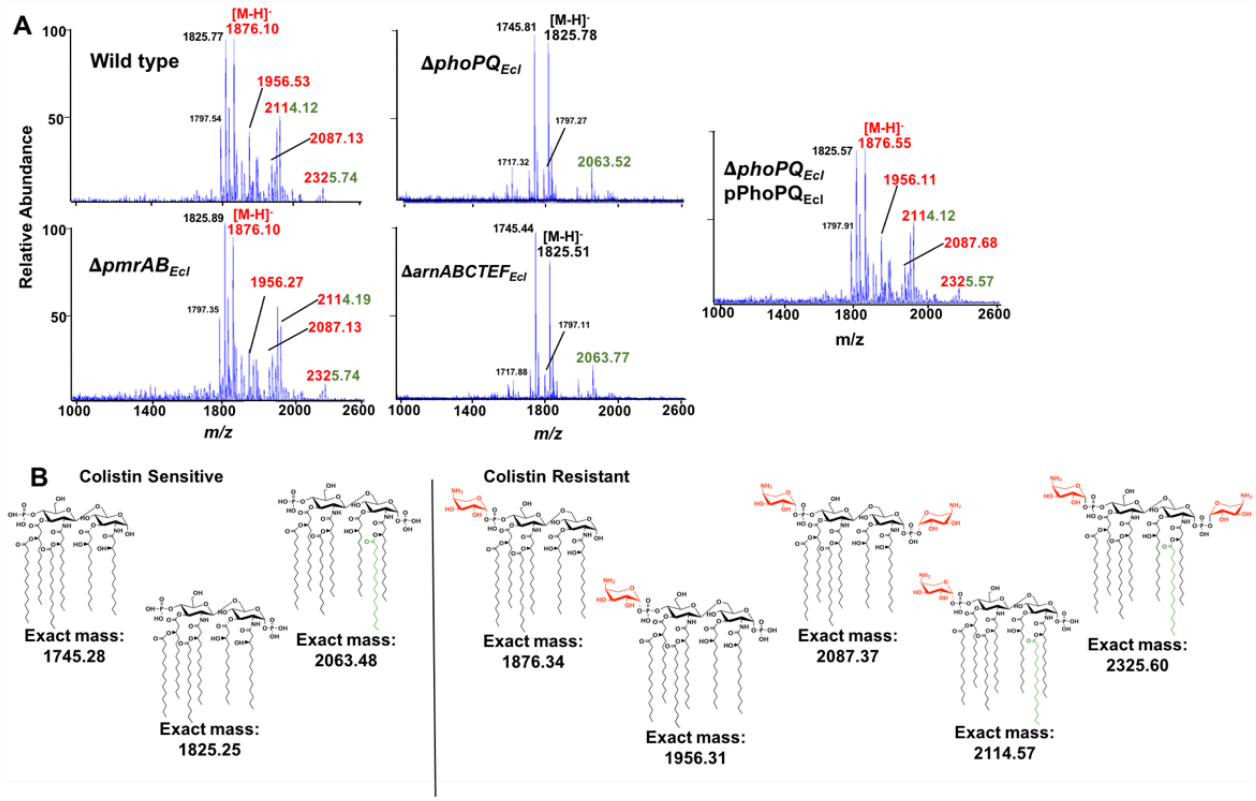


**Figure 4: Analysis of *E. cloacae* lipid A. (A)** MALDI-TOF MS analysis of lipid A isolated from wild type or mutant *E. cloacae* strains. l-Ara4N modifications are illustrated in red, while C16:0 additions are illustrated in green. Numbered labels that are both red and green contain both modifications. **(B)** lipid A chemical structures found in wild type and mutant *E. cloacae*.

## PhoP$_{Ecl}$ directly binds to the *arnB*$_{Ecl}$ promoter.

The *arn* operon is composed of seven genes and expression is driven by a promoter upstream of *arnB* (16). This genetic organization is conserved in *E. cloacae* as illustrated in **Fig 3A**. *phoP* expression is autoregulated in Enterobacteriaceae, where PhoP binds to the PhoP box to interact with RNA polymerase, which induces transcription[192]. The putative PhoP box in the *phoP* promoter region (P$_{phoP}$) is conserved in *E. coli, Salmonella*, and *E. cloacae* (**Figure 5B**). Alignment of the *E. cloacae arnB* promoter region (P$_{arnB}$) with *E. coli, Salmonella*, and *E. cloacae* P$_{phoP}$ suggested a putative PhoP box region. Importantly, *E. cloacae* P$_{arnB}$, which contains a putative PhoP box, is highly conserved among ECC. However, this feature was not conserved within *E. coli* P$_{arnB}$, suggesting regulatory mechanisms that control promoter activation are different (**Figure 5B**).

We performed electrophoretic mobility shifts (EMSAs) using *E. cloacae* P$_{arnB}$ to determine if PhoP$_{Ecl}$ directly binds the promoter to activate *arn*$_{Ecl}$ transcription. Increasing concentrations of purified PhoP$_{Ecl}$ (**Figure 6**) induced a shift of the biotinylated *arnB*$_{Ecl}$ promoter fragment, which contains the putative PhoP box binding motif (**Figure 5C**). Importantly, PhoP$_{Ecl}$ does not bind to *E. coli* P$_{arnB,}$ which does not encode the PhoP box motif (**Figure 5C**). Furthermore, the PhoP$_{Ecl}$-*arnB*$_{Ecl}$ promoter interaction was abrogated when unlabeled *E. cloacae* P$_{arnB}$ was added in increasing amounts, as a competitive inhibitor. We also show that the interaction is specific because addition of noncompetitive DNA (poly(dI-dC)) did not reduce the PhoP$_{Ecl}$ and *E. cloacae* P$_{arnB}$ interaction (**Figure 5D**). Lastly, PhoP$_{Ecl}$ bound *E. cloacae* and *E. coli* P$_{phoP}$, which both encode the nucleotide sequence specific to the PhoP box (**Figure 5E**). Together, these findings suggest that *E. cloacae* encodes a mechanism that enables L-Ara4N biosynthesis to respond directly to PhoPQ$_{Ecl}$.

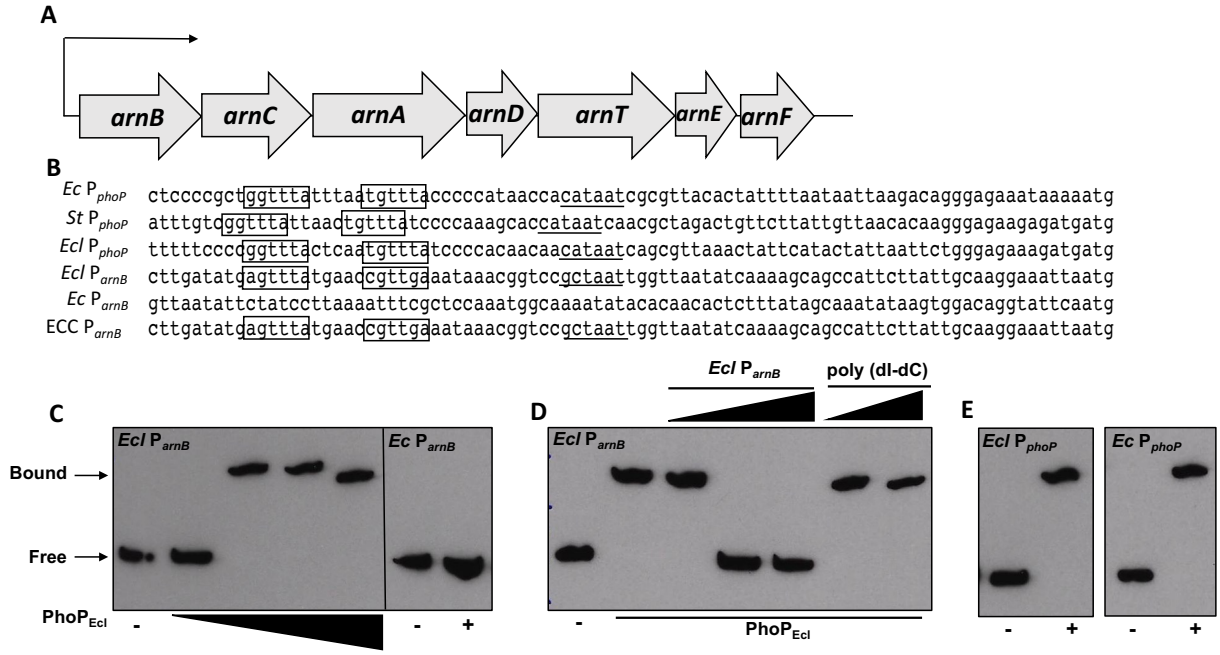


**Figure 5: PhoP$_{Ecl}$ binds to the *arnB* promoter of *E. cloacae* (*Ecl*), but not *E. coli* (*Ec*). (A)** Illustration of the *arn* operon organization. **(B)** Sequence alignment of the *phoP* promoter (*PphoP*) region in *Ec*, Salmonella (*St*), and *Ecl*, which each contain a PhoP box. The *arnB* promoter (*ParnB*) of *Ecl* contains a putative PhoP box binding site that is not present in Ec. The putative PhoP boxes have been boxed, while the −10 region is underlined. There were no putative PmrA boxes in the *Ecl arnB* or *phoP* promoter regions, so they were not included for simplicity. **(C)** Electrophoretic mobility shift assay (EMSA) of *Ecl ParnB* with increasing concentrations of PhoP$_{Ecl}$. PhoP$_{Ecl}$ was used at concentrations of 0, 0.1, 1.0, 5.0 and 10.0 µM. EMSA using *Ec ParnB* in the absence or presence of PhoP$_{Ecl}$ respectively. **(D)** EMSA competition experiments where increasing concentrations (1:1, 2:1, 5:1) of unlabeled *ParnB* competes with biotin-labeled *ParnB*, but nonspecific unlabeled poly(dI-dC) (2:1, 5:1) does not. E. PhoP$_{Ecl}$ binds to both the *Ecl* and *Ec phoP* promoters.

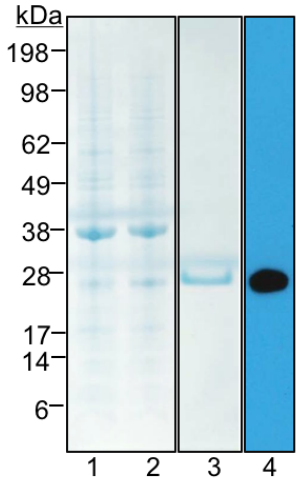


**Figure 6**: **Purification of PhoP$_{Ecl}$.** The PhoP$_{Ecl}$-His$_8$ construct was expressed in *E. coli* BL21 (DE3) using an inducible pT7 construct. A band at 26.64 kDa, the size of the predicted protein, was present upon induction. The protein was purified by affinity chromatography. An anti-penta histidine antibody was used to detect the purified protein.

1. Crude Extract-uninduced
2. Crude Extract-induced
3. Purified PhoP$_{Ecl}$-His$_8$
4. Detection using an anti-histidine antibody

## RNA-sequencing analysis of the *phoPQ*$_{Ecl}$ and *pmrAB*$_{Ecl}$ mutants.

To better understand PhoPQ$_{Ecl}$ and PmrAB$_{Ecl}$ transcriptional regulation, we isolated and sequenced total RNA from wild type and mutant *E. cloacae* strains. A heat map illustrates the fold change of *arn*$_{Ecl}$, *phoPQ*$_{Ecl}$, and *pmrAB*$_{Ecl}$ gene expression in the TCS mutants relative to wild type (**Figure 7**). Expression of the *arn*$_{Ecl}$ genes were significantly down regulated in Δ*phoPQ*$_{Ecl}$ compared to wild type, suggesting that activation of the pathway is dependent on PhoPQ$_{Ecl}$. In contrast, *arn*$_{Ecl}$ gene expression was not significantly altered in the Δ*pmrAB*$_{Ecl}$ mutant relative to wild type.

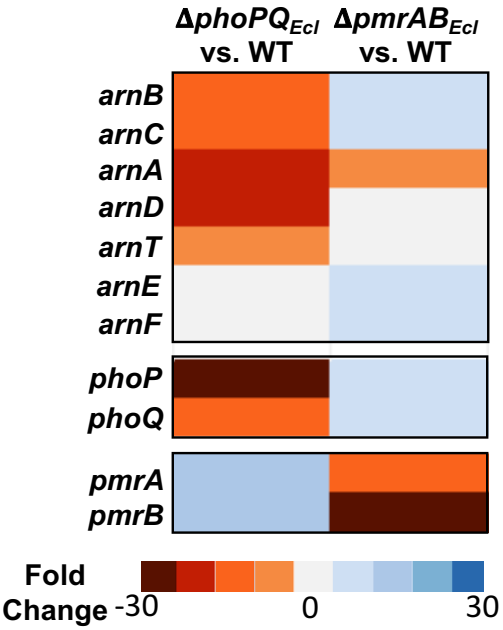


**Figure 7: RNA-sequencing analysis of *E. cloacae* genes.** Heat map illustrating the altered expression of select operons in Δ*phoPQ*$_{Ecl}$ and Δ*pmrAB*$_{Ecl}$ mutants. Expression is shown as a ratio of mutant to wild type expression ($P < 0.05$).

## *E. cloacae* colistin resistance is amplified in response to limiting $Mg^{2+}$.

Together, these analyses indicate colistin heteroresistance in wild type *E. cloacae* (**Figure 1A and Table 1**) is mediated by L-Ara4N modification of lipid A, which is regulated in a

PhoPQ$_{Ecl}$-dependent manner under standard growth conditions. In *E. coli* and *Salmonella*, PhoPQ is activated by various signals, including low $Mg^{2+}$ and CAMPs[9,152,153]. Here we analyzed if PhoPQ$_{Ecl}$ responds to similar physiological cues to induce colistin resistance in *E. cloacae*. Wild type and mutant *E. cloacae* were grown in N minimal medium with high (10 mM) or low (10 μM) $Mg^{2+}$ levels. All cultures were exposed to colistin at mid-logarithmic growth. Wild type and complemented *phoPQ$_{Ecl}$* mutant strains grown in high $Mg^{2+}$ demonstrated some susceptibility to 5 and 10 μg/ml of colistin (**Figure 8A, High $Mg^{2+}$**), suggesting colistin-susceptible and -resistant populations were present, which is indicative of heteroresistance. When grown under limiting $Mg^{2+}$ conditions, *E. cloacae* cells were more resistant (**Figure 8A, Low $Mg^{2+}$**). In contrast, *phoPQ$_{Ecl}$* demonstrated a fitness defect in either $Mg^{2+}$ concentration when exposed to colistin (**Figure 8A).** These data suggest that *E. cloacae* PhoPQ$_{Ecl}$ amplifies colistin resistance in response to limiting $Mg^{2+}$ growth conditions.

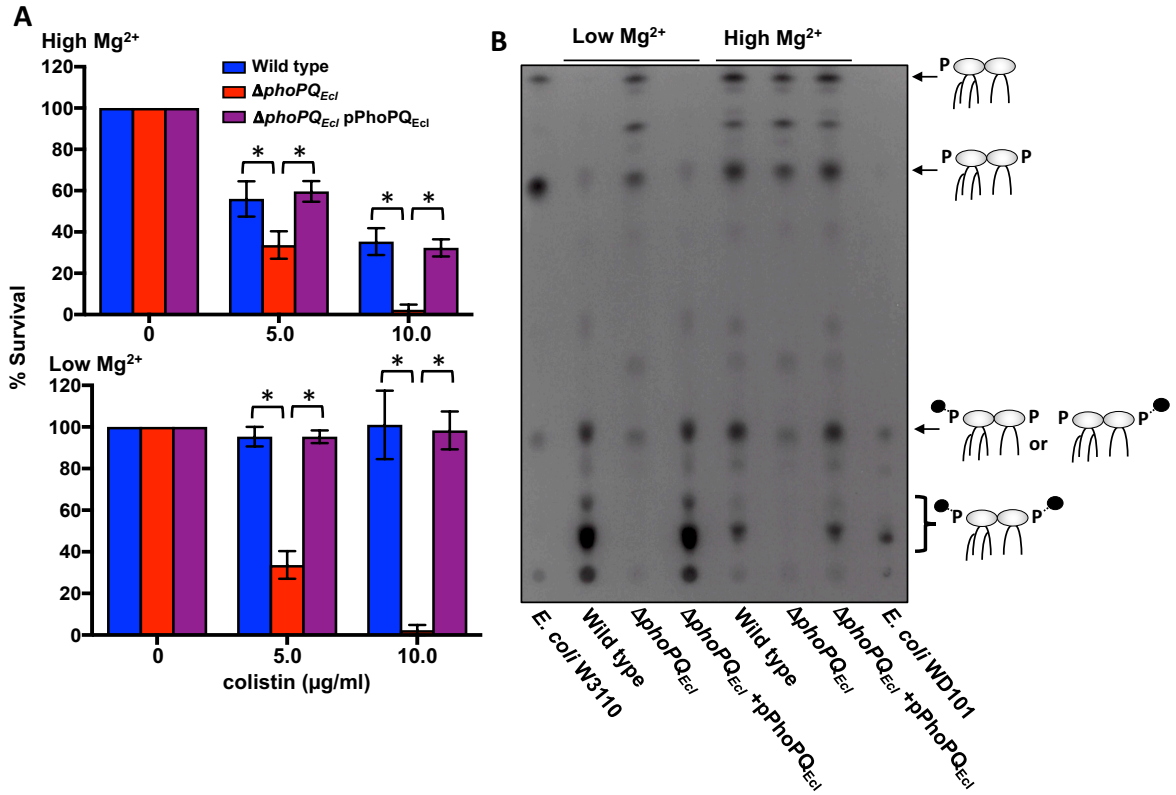


**Figure 8: PhoPQ$_{Ecl}$-dependent activation of L-Ara4N addition induces colistin resistance in low $Mg2^{+}$. (A)** Wild

type and mutant *E. cloacae* strains were grown in N minimal medium with high (10mM, top) or low (10 μM, bottom) $Mg2^{+}$. Strains were challenged with 0, 5 or 10 μg/ml of colistin for 1 h and plated for survival. Two biological replicates were each analyzed in triplicate with data from one representative set reported. P value < .05. **(B)** $^{32}$P-radiolabeled lipid A was isolated from wild type and mutant E. cloacae strains and separated based on hydrophobicity using thin layer chromatography. The associated lipid A structures (right) are illustrated (black circles indicating L-Ara4N addition). Lipid A species were labeled as determined by *E. coli* W3110 (unmodified) and WD101 (modified) lipid A.

## PhoPQ$_{Ecl}$ responds to limiting $Mg^{2+}$ conditions by inducing L-Ara4N lipid A modification.

To determine if increased colistin resistance was dependent on L-Ara4N modification of lipid A, we isolated lipid A after growth in either low or high $Mg^{2+}$. TLC analysis demonstrated that wild type and the complemented *phoPQEcl* mutant primarily produced L-Ara4N-modified lipid A when $Mg^{2+}$ concentrations were limiting (**Figure 8B, Low $Mg^{2+}$**). In contrast, the same strains grown in excess $Mg^{2+}$, produced a mixture of modified and unmodified lipid A, which is indicative of heteroresistance (**Figure 8B, High $Mg^{2+}$**). Interestingly, growth in excess $Mg^{2+}$ does not completely shut-off production of PhoPQ$_{Ecl}$-dependent lipid A modification in *E. cloacae*, as was previously shown in *E. coli*[177]. Together, these studies suggest that a subset of the clonal *E. cloacae* population activates PhoPQ$_{Ecl}$-dependent L-Ara4N modification of lipid A under standard growth conditions to promote heteroresistance. However, depletion of $Mg^{2+}$ amplifies L-Ara4N modification (**Figure 8B**) and colistin resistance (**Figure 8A**) throughout the population.

## Inactivation of colistin heteroresistance in ECC clinical isolates.

A previous report showed that while many ECC clinical isolates were colistin heteroresistant, some were susceptible to colistin–mediated lysis. Interestingly, ECC colistin heteroresistance was cluster dependent[184]. To determine the genetic basis for colistin sensitivity in ECC clusters, we examined twelve colistin susceptible clinical isolates (CI) and compared them

to heteroresistant wild type ATCC 13047. We confirmed colistin susceptibility in all isolates using the BMD method to determine MICs and sequenced each genome. We obtained ~70 X $10^6$ reads for each susceptible isolate and the wild type strain, which were mapped to the annotated ATCC 13047 genome[193]. The coverage region of each isolate varied between 82% to 99%, where most coverage variation occurred in plasmid DNA regions. Initial analysis of our wild type strain confirmed it did not encode mutations in the $phoPQ_{Ecl}$, $pmrAB_{Ecl}$, or the $arn_{Ecl}$ coding sequences, consistent with the published annotation. In contrast, multiple mutations were found in the $phoPQ_{Ecl}$ and $arn_{Ecl}$ operons of the colistin-susceptible isolates. Interestingly, ten of the twelve isolates encoded single nucleotide polymorphisms (SNPs) in the $phoPQ_{Ecl}$ promoter sequence immediately upstream of the $phoP_{Ecl}$ translational start codon (within 8 nucleotides), which indicated the SNPs likely disrupted the ribosome binding site (**Figure 9A**). To determine if the SNPs attenuated PhoPQ-dependent colistin resistance, CI-3 (cluster III), which did not encode amino acid changes in the $phoPQ_{Ecl}$ or $arn_{Ecl}$ genetic coding regions, was transformed with pPhoPQ$_{Ecl}$. Complementation restored colistin resistance, where the MIC increased from 0.5 in CI-3 to >256 μg/ml after PhoPQ$_{Ecl}$ signaling was restored (**Figure 9B**). Complementation suggested that SNPs in the $phoPQ_{Ecl}$ ribosome binding sites contributed to colistin susceptibility. SNP mutations, which abrogate translation of PhoPQ$_{Ecl}$, support a model where colistin heteroresistance is dependent on PhoPQ$_{Ecl}$ in diverse ECC isolates.

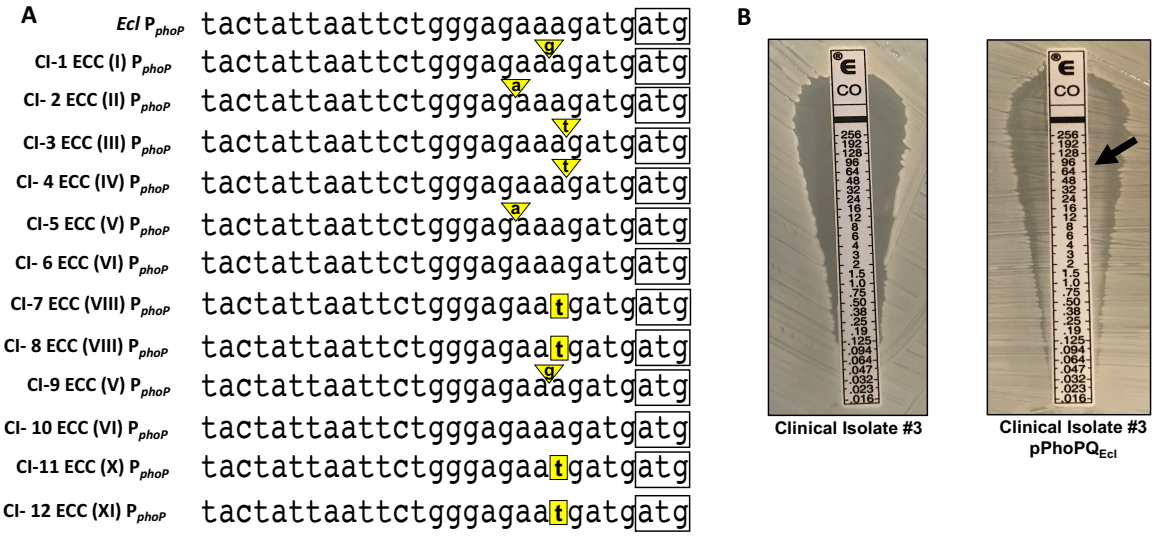


**Figure 9: PhoP$_{Ecl}$ single-nucleotide polymorphisms that attenuate colistin heteroresistance in ECC clinical isolates. (A)** Sequence alignment of E. cloacae and other ECC *phoP* promoter (*PphoP*) regions. The region includes 25 nucleotides upstream of the start codon (boxed). Gray boxes indicate single-nucleotide replacement mutations, while gray triangles indicate single-nucleotide insertion mutations. **(B)** E-test strips of CI-3 and CI-3/pPhoPQ$_{Ecl}$ to visualize heteroresistant colonies. The black arrow indicates colistin-resistant colonies.

## DISCUSSION

*E. cloacae* and other ECC members encode PmrAB$_{Ecl}$ and PhoPQ$_{Ecl}$ homologs. We hypothesized these TCS regulatory systems functioned together in a pathway to control L-Ara4N and pEtN modification of lipid A, based on previous transcriptomics analysis of resistant and susceptible populations[188] and because these lipid A modifications are highly conserved among Enterobacteriaceae[16]. However, our genetic and high-resolution mass spectrometry analysis of *E. cloacae* lipid A determined that colistin heteroresistance in *E. cloacae* was mediated by PhoPQ$_{Ecl}$-dependent, PmrAB$_{Ecl}$-independent L-Ara4N lipid A modification. Therefore, we identified a mechanism of ECC colistin heteroresistance that involves the PhoPQ system.

*E. cloacae* and other ECC members do not encode a PmrD homolog, which couples PhoPQ signal transduction to regulation of PmrA-dependent genes in many Enterobacteriaceae[16]. Moreover, PmrA$_{Ecl}$ shares only 52% identity with *E. coli* PmrA and PmrB$_{Ecl}$ shares only 57% identity with *E. coli* PmrB, suggesting the L-Ara4N lipid A modification pathway in *E. cloacae*

diverged from *E. coli* and *Salmonella*. We confirmed direct binding of $PhoP_{Ecl}$ to the $arnB_{Ecl}$ promoter, which supports a model where L-Ara4N addition to lipid A and colistin heteroresistance in *E. cloacae* is dependent on $PhoPQ_{Ecl}$, but not $PmrAB_{Ecl}$.

Research from other groups has outlined a complex regulatory network in *E. coli* and *Salmonella* that tightly regulates lipid A L-Ara4N and EptA modifications[157,160,172,177,194]. We hypothesize that uncoupling $PmrAB_{Ecl}$ regulation from L-Ara4N modification bypasses an important regulatory checkpoint, which likely promotes misregulated $PhoPQ_{Ecl}$-dependent $arn_{Ecl}$ expression. Furthermore, colistin heteroresistance has also been associated with *Klebsiella pneumoniae*[195], another Enterobacteriaceae family member that activates *arn* expression independently of PmrAB[175]. Since selection has driven ECC and other opportunistic pathogens to maintain an altered lipid A modification signaling network, we predict that it is advantageous to maintain a CAMP resistant subpopulation in some environments. Presumably, the alternative regulatory mechanism promotes bacterial fitness in environments specific to their commensal and pathogenic niches.

Colistin heteroresistance is not well-understood at the molecular level in Enterobacteriaceae. Our study indicates that $PhoPQ_{Ecl}$ signal transduction contributes to heteroresistance in ECC. However, additional studies are necessary to understand[143,196] if there is a genetic determinant within the heteroresistant subpopulation that promotes resistance. Alternatively, colistin heteroresistance could be a byproduct of promoter noise-induced bimodality, which has been linked to heteroresistance in other bacteria. Despite these two possibilities, our studies demonstrated that $PhoPQ_{Ecl}$ phosphotransfer ($PhoQ_{H227}$ and $PhoP_{D56}$) is required for colistin heteroresistance (**Table 1**), suggesting the phenotype is regulated by $PhoPQ_{Ecl}$.

## MATERIALS AND METHODS

### Bacterial Strains and Growth

*E. cloacae* subsp. *cloacae* ATCC 13047 and ECC strains were initially grown from freezer stocks on Luria-Bertani (LB) agar. Isolated colonies were used to inoculate LB broth or N minimal medium (0.1M Bis-Tris, pH 7.5 or 5.8, 5 mM KCl, 7.5 mM $(NH_4)_2SO_4$, 0.5 M $K_2SO_4$, 1 mM $KH_2PO_4$, 0.10% casamino acids 0.2% glucose, 0.0002% thiamine, 15 μM $FeSO_4$, 10 μM or 10 mM $MgSO_4$) at 37° C. Strains were grown into mid-logarithmic growth ($OD_{600}$ = 0.6) before analysis. Kanamycin was used at 25 μg/ml for selection and colistin was used at 5 μg/ml or 10 μg/ml where indicated.

All strains and plasmids used in this study are listed in Table S1 online. Briefly, *E. cloacae* subsp. *cloacae* 13047 mutant strains were constructed as previously described using recombineering with the plasmid pKOBEG[197]. Linear PCR products were introduced in to the *E. cloacae* ATCC 13047/pKOBEG strain by electroporation and plated on selective media. Selected clones were transformed with pCP20 to cure the antibiotic resistance cassette.

To complement *E. cloacae* mutants, the coding sequence from $phoPQ_{Ecl}$ was cloned into the SalI and KpnI sites in pMMBKn[17]. To generate point mutants in $PhoQ_{H277A}$ and $PhoQ_{D56A}$, site directed mutagenesis was performed using Pfu Turbo using primers that incorporated the associated alanine-encoded nucleotide replacements. All constructs were validated using Sanger sequencing. IPTG inducible constructs were transformed into the *phoPQ* mutant and grown in 2.0 mM IPTG to induce expression.

### Broth Microdilution assays

MICs of colistin were determined in triplicate by the broth microdilution (BMD) method. Briefly strains were inoculated from overnight cultures when $OD_{600}$ = 0.1. Various concentrations

(0 - 256 μg/ml) of colistin were added to each well and cultures were incubated overnight. Growth was measured by reading the $OD_{600}$. The lowest concentration at which growth was inhibited was recorded as the MIC. *E. coli* W3110 and WD101 were used as control strains. In some cases, 'skip wells' were observed suggesting a heteroresistance phenomenon and the MIC was determined disregarding the clear wells[184].

**Population Analysis**

Population analysis profiling was performed by plating 1 X $10^{10}$ CFU onto LB agar containing 1 to 64 μg/ml colistin (in 2-fold increments). Plates were incubated overnight at 37° C and frequency of the subpopulation was determined by dividing by the total number of cells[134].

**Isolation of Lipid A**

Isolation of lipid A for TLC analysis involved $^{32}$P-radiolabeling of whole cells was performed as previously described with slight modifications[198]. In brief, 12.5 ml of *E. cloacae* was grown at 37° C to $OD_{600}$ = 1.0. Bacteria were harvested by centrifugation at 10,000 X g for 10 min. Lipid A extraction was carried out by mild-acid hydrolysis as previously described[199].

**Mass Spectrometry**

MS1 spectra of lipid A in Figure 3 were collected on a MALDI-TOF/TOF (Axima Performance, Shimadzu) mass spectrometer in the negative mode. All other spectra were collected in the negative mode on a Thermo Scientific Orbitrap Fusion Lumos mass spectrometer (San Jose, CA, USA) modified with a Coherent ExciStar XS ArF excimer laser (Santa Clara, CA), as previously described[200]. HCD was performed with the normalized collision energy (NCE) of 25%. UVPD was performed with the laser emitting 193 nm photons at 5 mJ per laser pulse with 5 pulses per scan. The laser pulse repetition rate was 500 Hz. The instrument was operated at 120000 resolving power with a precursor isolation window of 3 *m/z*. All samples were dissolved in 50:50

MeOH:$CHCl_3$ and directly infused into the mass spectrometer via a static nano-electrospray ionization source. The presented spectra are an average of 50 scans.

**TLR-4 Signaling Assays**

HEK-Blue hTLR4, cell line was maintained according to the manufacturer specifications (Invivogen). Overnight bacterial cultures in stationary phase were serial diluted for assays as previously described[17,167]. At least two biological replicates were each done in triplicate and one representative set was shown.

**Colony Forming Unit Counts and Colistin Survival Assays**

For colony forming unit counts (CFUs), *E. cloacae* subsp. *cloacae* 13047 and mutant strains were initially grown from freezer stocks on Luria-Bertani (LB) agar. Isolated colonies were resuspended and used to inoculate LB broth with 10 μg/ml or without colistin at an $OD_{600}$ = 0.01. Cells were plated at designated time points on LB agar. Plates were grown overnight at 37° C and colony forming units (CFU) were counted and reported.

Colistin survival assays were performed as previously described with slight modifications[177]. Briefly, wild type and mutant *E. cloacae* strains were grown overnight on LB agar. The following day, N minimal media pH = 7.5 containing either 10 μM $MgSO_4$ (low $Mg^{2+}$) or 10 mM $MgSO_4$ (high $Mg^{2+}$) were inoculated at $OD_{600}$ = 0.05 with bacteria from overnight cultures after cells were washed with N minimal media without $Mg^{2+}$. Cultures were grown until $OD_{600}$ = 0.6, when they were split and treated with 0, 5 or 10 μg/ml of colistin (Polymyxin E). Cultures were incubated for 1 h at 37° C and then colony-forming units were plated on LB, grown, and calculated. Percent survival was calculated by dividing the number of bacteria after treatment with colistin relative to those incubated in the absence of colistin and then multiplied by 100.

**Protein Purification**

To purify the PhoP$_{Ecl}$ protein, the coding sequence was cloned into pT7-7Kn, as previously described[201]. Briefly, the *phoP$_{Ecl}$* coding sequence was amplified from *E. cloacae* cDNA with primers that added a C-terminal His$_{8X}$ tag. From an overnight starter culture, 1 Liter of LB broth containing 25 μg/ml of kanamycin was inoculated at 1:50 and grown at 37° C until the $OD_{600}$ = 0.5. IPTG was added to a final concentration of 1mM, and the culture was incubated at 37° C for an additional 4 h. Bacteria were recovered by centrifugation at 10,000 x g for 10 min, and the bacteria were resuspended in lysis buffer. Bacteria were lysed using sonication and the soluble fraction was recovered by centrifugation at 10,000 x g for 30 min. PhoP$_{Ecl}$-His$_{8X}$ was purified on a Ni-nitrilotriacetic acid (NTA) beads according to the manufactures instructions (Qiagen).

**Electrophoretic Mobility Shift Assay**

PhoP$_{Ecl}$-His$_{8X}$ proteins were purified as described above. EMSAs were performed based on a modified protocol[202]. 250-bp DNA fragments of *phoP$_{Ecl}$* and *arnB$_{Ecl}$* spanning −230 to +20 relative to the translational start site were amplified from *E. cloacae* or *E. coli* cDNA using 5'-biotinylated primers. PhoP$_{Ecl}$-His$_{8X}$ proteins were incubated with biotinylated DNA at 25° C for 20 min. For competition experiments, unlabeled *E. cloacae* P$_{arnB}$ and poly(dI-dC) were added at 1:1, 2:1, or 5:1 ratios relative to biotin-labeled P$_{arnB}$ DNA. 0.1 - 10 μM of PhoP$_{Ecl}$-His$_{8X}$ proteins were used. After electrophoresis at 4° C, protein/DNA was transferred onto a positively charged nylon membrane. Blots were blocked in 5% milk in TBS for 20 min and streptavidin conjugated HRP was used at a 1:300 dilution.

**Nucleic Acid Extraction**

Total RNA was extracted using the Direct-Zol RNA MiniPrep Kit (Zymo Research) from *E. cloacae* grown to a final $OD_{600}$ = 0.6. Isolated RNA was treated with DNA-free DNA removal

kit (Thermo-Fisher Scientific) to eliminate genomic DNA contamination. DNase-depleted RNA was used for qRT-PCR and RNA-seq.

**RNA-sequencing**

RNA-sequencing was performed as previously described[203]. Briefly, DNA-depleted RNA was processed for Illumina sequencing using the NEB Next Ultra Directional RNA Library Prep kit for Illumina as described by the manufacturer (NEB). Sequencing was performed using Illumina HiSeq. Sequencing data was aligned to the *E. cloacae* subs. *cloacae* ATCC 13047 published genome annotations[193] using CLC genomic workbench software (Qiagen) and RPKM expression values were determined. The weighted proportions fold change of expression values between samples was determined and a Baggerley's test on proportions was used to generate a false discovery rate corrected P-value. We then used a cut-off of 2-fold weighted proportions absolute change with a false-discovery rate corrected P-value of $\leq 0.05$ to identify significantly differentially regulated genes between samples. The sequencing data for the clinical isolates has been deposited in the Nation Center for Biotechnology's Gene Expression Omnibus (GSE127802).

**Genomic-sequencing**

Genomic sequences were analyzed as previously done[17]. Briefly, samples were processed for Illumina sequencing using the NEB Next Ultra DNA Library Prep kit (NEB). Sequencing was performed using Illumina HiSeq. Reads were aligned to *E. cloacae* strain ATCC 13047 published genome annotations using CLC genomic workbench software (Qiagen) with 90% length fraction and 90% similarities parameters. Mapped reads were locally realigned and fixed ploidy detection identified low and high frequency variants. *E. cloacae* variant tracks were compared to identify mutations. Mutations not present in strain ATCC 13047 were called if 95% of aligned reads

contained the variant. The sequence data have been submitted to the GenBank under accession number SUB4176618.

# CHAPTER 4: Septal Class A Penicillin-Binding Protein Activity and LD-Transpeptidases Mediate Selection of Colistin-Resistant Lipooligosaccharide-Deficient *Acinetobacter baumannii*

Katie N. Kang[a], Misha I. Kazi[a], Jacob Biboy[b], Joe Gray[c], Hannah Bovermann[a] Jessie Ausman[a], Cara C. Boutte[a], Waldemar Vollmer[b], Joseph M. Boll[a,#]

Affiliations:

[a]Department of Biology, University of Texas Arlington, Arlington, TX, USA

[b]Centre for Bacterial Cell Biology, Biosciences Institute, Newcastle University, Newcastle upon Tyne, United Kingdom

[c] Biosciences Institute, Newcastle University, Newcastle upon Tyne, United Kingdom

[#]Correspondence:

Joseph M. Boll

The University of Texas at Arlington

Arlington TX, 76010

Phone (817) 272-4045

Email: joseph.boll@uta.edu

** Published as: Kang KN et al. Septal Class A Penicillin-Binding Protein Activity and LD-Transpeptidases Mediate Selection of Colistin-Resistant Lipooligosaccharide-Deficient *Acinetobacter baumannii*. *mBio.* 2021 Jan 5;12(1):e02185-20. doi:10.1128/mBio.02185-20.

## ABSTRACT

Despite dogma suggesting lipopolysaccharide/lipooligosaccharide (LOS) was essential for viability of Gram-negative bacteria, several *Acinetobacter baumannii* clinical isolates produced LOS$^-$ colonies after colistin selection. Inactivation of the conserved class A penicillin-binding protein, PBP1A, was a compensatory mutation that supported isolation of LOS$^-$ *A. baumannii*, but the impact of PBP1A mutation was not characterized. Here, we show that the absence of PBP1A causes septation defects and that these, together with LD-transpeptidase activity, support isolation of LOS$^-$ *A. baumannii*. PBP1A contributes to proper cell division in *A. baumannii*, and its absence induced multiple septa and cell filamentation and/or chaining. Only isolates producing three or more septa supported selection of colistin resistant LOS$^-$ *A. baumannii*. PBP1A was enriched at the midcell, where the divisome complex facilitates daughter cell formation, and its localization was dependent on glycosyltransferase activity. Transposon mutagenesis showed that genes encoding two putative LD-transpeptidases (LdtJ and LdtK) became essential in the PBP1A mutant. Both LdtJ and LdtK were required for selection of LOS$^-$ *A. baumannii*, but each had distinct enzymatic activities in the cell. Together, these findings demonstrate that defective septation and LD-transpeptidase activity remodel the cell envelope to support selection of colistin resistant LOS$^-$ *A. baumannii*.

## INTRODUCTION

The Gram-negative cell envelope is tripartite with an inner (cytoplasmic) membrane, a periplasm that includes a thin peptidoglycan layer and an outer membrane, which is enriched with surface-exposed lipopolysaccharide (LPS) or lipooligosaccharide (LOS). The cell envelope maintains cell shape[204,205], supports the mechanical load caused by the turgor[106] and enables the cell to rapidly adapt to environmental challenges. Specialized macromolecular complexes span the cell envelope and coordinate peptidoglycan biosynthesis and LPS/LOS localization.

LPS/LOS is assembled at the inner membrane[85,98,99] and transported to the outer membrane via LptA-G, which bridges the periplasm and peptidoglycan cell wall[100–103,206]. LPS/LOS glycolipids are based on a highly conserved lipid A moiety that anchors them on the surface-exposed face of the outer membrane. LPS/LOS disruption leads to rapid lysis and death; therefore, it has been targeted with antimicrobials[25]. For example, colistin (polymyxin E) is a last resort antimicrobial used to treat multidrug resistant bacteria, including the ESKAPE pathogen *Acinetobacter baumannii*[207,208]. Colistin binds the lipid A phosphate groups to perturb the outer membrane barrier, which rapidly kills the bacterium[209,210]. Surprisingly, several *A. baumannii* clinical isolates inactivate LOS biosynthesis and rapidly establish resistance to otherwise toxic colistin concentrations[17,91]. However, certain *A. baumannii* clinical isolates could not develop such resistance. Previous work showed that inactivation of PBP1A (encoded by *mrcA*) is a compensatory mutation that supports colistin selection of LOS$^-$ *A. baumannii*[17], but the role of PBP1A in *A. baumannii* physiology and how PBP1A mutation alters the cell envelope, have not been reported.

In *Escherichia coli*, PBP1A and PBP1B (encoded by *mrcB*) are semi-redundant class A penicillin-binding proteins (aPBPs). aPBPs are bifunctional enzymes, catalyzing both

polymerization of glycans via glycosyltransferase (GTase) activity and crosslinking of stem peptides by DD-transpeptidase (DD-TPase) activity. The DD-TPase activity of aPBPs depends on ongoing GTase reactions[39] and in *E. coli* aPBP activity contributes to a substantial amount of the peptidoglycan synthesized per generation[41]. PBP1B not only contributes to peptidoglycan maintenance[47], but also interacts with the divisome complex[35,44], which forms the septum and constricts the cell envelope at the midcell[35,211]. PBP1A interacts with PBP2, which suggests it has a role in cell elongation during growth[42]. While PBP1A and PBP1B have distinct roles in growth, only one enzyme is required for growth because the other can compensate[38,42,212]. Specifically, in the absence of PBP1B, PBP1A was enriched at the midcell[42], which implies PBP1A compensates to rescue cell division defects.

In *E. coli*, the majority of transpeptidation reactions in peptidoglycan are catalyzed by PBPs to result in 4-3 crosslinks. However, LD-transpeptidases (LD-TPases) such as LdtD and presumably LdtE and LdtF, form 3-3 crosslinks[20,67,213]. 3-3 crosslinking becomes essential for *E. coli* survival when LPS transport or biosynthesis is disrupted, presumably because LdtDEF repair peptidoglycan defects together with the GTase function of PBP1B and the DD-carboxypeptidase PBP6a[20]. In contrast, LdtA, LdtB and LdtC attach the outer membrane-anchored Braun's lipoprotein (Lpp) to peptidoglycan, which stabilizes the cell envelope[64].

*A. baumannii* encodes two aPBPs, PBP1A and PBP1B, and two putative LD-TPases (LdtJ and LdtK), but their roles in growth and division have not been characterized. Here, we show that only multiseptated *A. baumannii* strains can support LOS$^-$ colony formation. In contrast to *E. coli*[42], *A. baumannii* PBP1A is required for proper cell division and PBP1B is unable to compensate in its absence, which enables PBP1A mutants to assemble multiple septal sites. Specifically, disruption of PBP1A GTase activity produces the septation defect, which is also characteristic of

LOS$^-$ *A. baumannii*. PBP1A-mCherry and PBP1A$_{S459A}$-mCherry (DD-TPase mutant) localize at the midcell during growth, where PBP1A potentially interacts with divisome components to synthesize septal peptidoglycan during division. In contrast, PBP1A$_{E92Q}$-mCherry (GTase mutant) did not localize at the midcell, suggesting GTase activity is required for septal localization. In addition to a role in cell division, the PBP1A mutant was resistant to several β-lactam antibiotics relative to wild type and the PBP1B mutant, indicating PBP1A contributes to intrinsic β-lactam susceptibility. Furthermore, *ldtJ* and *ldtK* gene deletions were synthetically lethal in Δ*mrcA* and were essential for selection of colistin resistant LOS$^-$ *A. baumannii*. LdtJ forms 3-3 crosslinks and incorporates D-amino acids onto peptidoglycan stem peptides, while LdtK stabilizes the outer membrane. Together, slowed septation, alternative crosslinking and outer membrane stabilization supported colistin selection of LOS$^-$ *A. baumannii*.

## RESULTS

### Isolation of colistin resistant LOS$^-$ *A. baumannii* is dependent on defective septation.

We examined *A. baumannii* clinical isolates and found morphological differences between strain ATCC 19606, which produces LOS$^-$ populations after colistin selection, relative to strain ATCC 17978, which cannot[17]. Cells in logarithmic growth phase were treated with a fluorescent derivative of D-alanine (NADA)[214], which is incorporated into the peptidoglycan cell wall by PBPs and LDTs[215–218]. Wild type 17978 cells were coccobacilli with septal assembly localized at the midcell (**Figure 10A**), where septal peptidoglycan synthesis produced two daughter cells during division. In contrast, wild type 19606, which demonstrated an 80-fold reduction in PBP1A expression during mid-logarithmic growth[17], were bacilli containing multiple septal sites (**Figure 10B**). LOS$^-$ cells derived from 19606 also contained multiple septal sites (**Figure 10C**). Unlike

17978, 19606 and LOS$^-$ subpopulations contained three or more septa (**Figure 10D**), indicating a septation defect. Consistent with previous findings[17], 19606 produced LOS$^-$ colonies after colistin selection, whereas 17978 did not (**Figure 10E, Table 2**). The average lengths and widths of 17978, 19606 and 19606 LOS$^-$ were also calculated (**Figure 11A**) and showed that defective septation in wild type 19606 and 19606-derived LOS$^-$ *A. baumannii* resulted in subsets of elongated cells within the population.

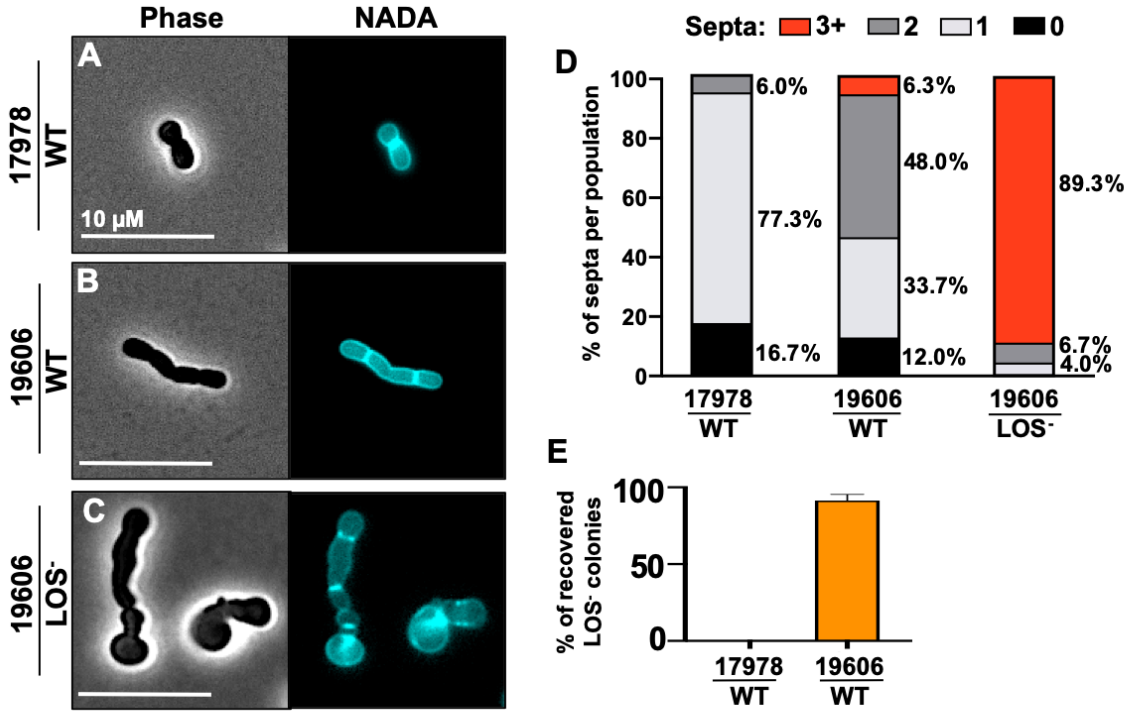


**Figure 10: Microscopy of *A. baumannii* 17978 and 19606 in logarithmic growth phase. (A to C)** Phase and fluorescence microscopy of wild type (WT) 17978 **(A)**, 19606 (reduced levels of PBP1A expression relative to 17978) **(B)**, and 19606 LOS- **(C)** cells. Cells in mid-logarithmic growth were labeled with NADA. **(D)** Septa were quantified using ImageJ software (n= 300) and reported as a percentage of the whole. Data were collected from three experiments, and one representative image and dataset were reported. **(E)** Percentage of LOS- *A. baumannii* recovered after colistin selection using 109 CFU in logarithmic growth phase.

To determine if the septation defect was conserved among isolates that support LOS$^-$-mediated colistin resistance, we analyzed several additional *A. baumannii* clinical isolates. Consistent with strain 19606, *Ab* 5075 (**Figure 11C**) and *Ab* AYE (**Figure 11D**) also produced multiseptated bacilli and yielded LOS$^-$ colistin resistant isolates (**Figure 11B**). In contrast, *Ab*

ACICU (**Figure 11E**) and *Ab* SDF (**Figure 11F**) assembled a single septum at the midcell. Like 17978, we could not recover LOS$^-$ isolates from either ACICU or SDF parent strains (**Figure 11B, Table 2**). Septal quantification showed that *Ab* 5075 and *Ab* AYE had subpopulations that produced three or more septa, while *Ab* ACICU and *Ab* SDF did not (**Figure 11G**). The average length and width of each clinical isolate was reported (**Figure 11H**). Strains that assembled three or more septa also produced elongated cell subpopulations.

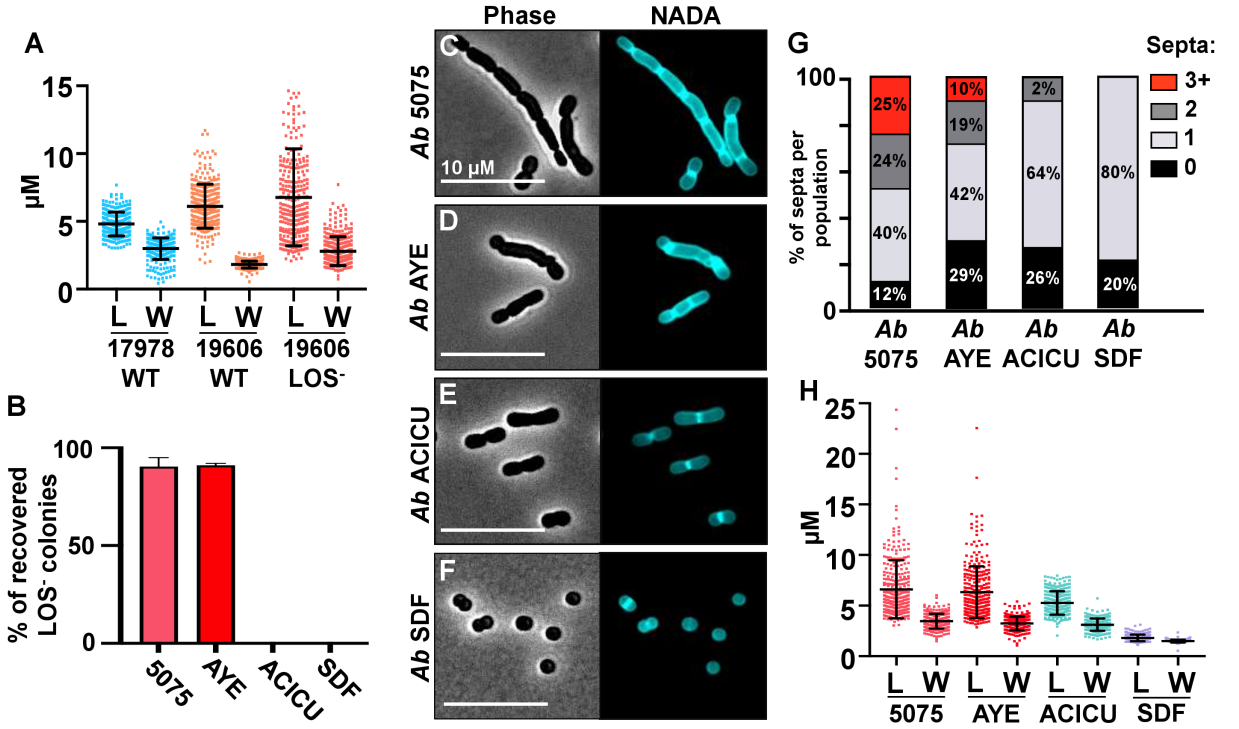


**Figure 11**: **Quantification of *A. baumannii* cell morphology**. **(A)** Wild type (WT) 17978, 19606 and LOS- isolates derived from 19606. **(B)** *A. baumannii* clinical isolates. **(A, H)** Cell lengths (L) and widths (W) were calculated using ImageJ software (n = 300). Each dot on the graph represents one cell. **(G)** Septa were quantified using ImageJ software (n = 300) and reported as a percentage of the whole.

To determine if elongated cell morphologies were consistent in growth phases, we also analyzed stationary phase cultures. Only 19606 (**Figure 12A**), 5075 (**Figure 12B**) and AYE (**Figure 12C**) formed filamented populations and yielded colistin resistant LOS$^-$ isolates in stationary phase (**Figure 12G, Table 2**). 17978 (**Figure 12D**), ACICU (**Figure 12E**) and SDF (**Figure 12F**) maintained a coccobacilli morphology and failed to produce a single LOS$^-$ isolate

after colistin selection (**Figure 12G, Table 2**). The length and width of each isolate in stationary phase were calculated (**Figure 12H**). Strains 19606, *Ab* 5075, and *Ab* SDF were elongated relative to 17978, *Ab* ACICU and *Ab* AYE. While it was previously shown that only select strains supported isolation of LOS$^-$ *A. baumannii* after colistin selection[17], here we show a correlation between strains with defective septation and selection of colistin resistant LOS$^-$ isolates.

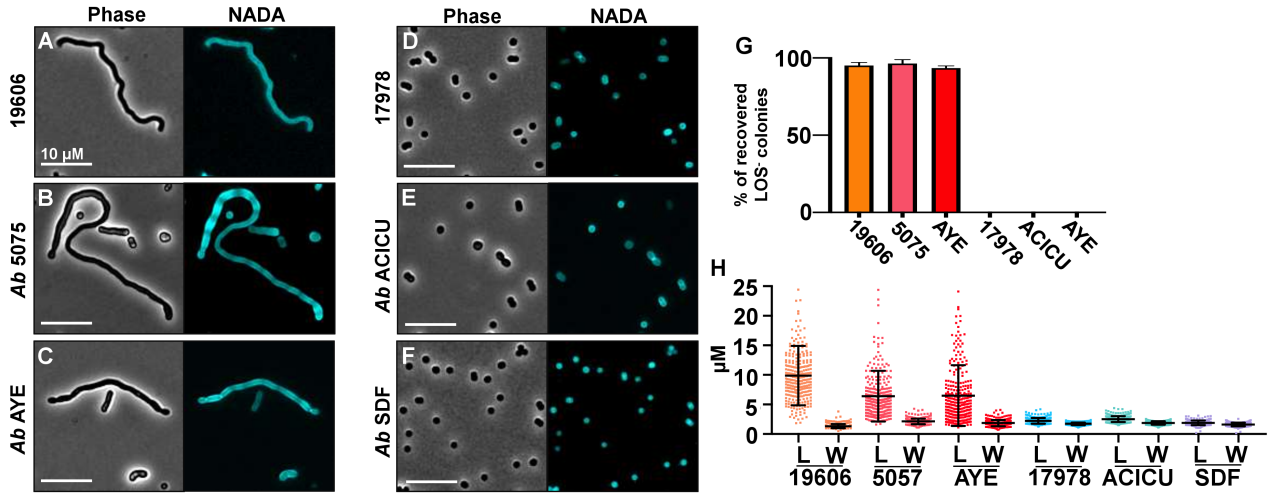


**Figure 12: Microscopy of *A. baumannii* clinical isolates in logarithmic growth phase.** NADA stained **(A)** Ab 5075, **(B)** Ab AYE, **(C)** Ab ACICU **and (D)** Ab SDF were visualized using phase and fluorescent microscopy. **(E)** Percent of recovered LOS- *A.baumannii* after colistin selection using CFU in logarithmic growth phase **(F)** Septa were quantified using ImageJ software (n = 300) and reported as a percentage of the whole.

**Table 2: *A. baumannii* develops colistin resistance through inactivation of lipooligosaccharide (LOS) biosynthesis**

| ***Ab* Strain** | **Recovery Frequency of LOS$^-$ *Ab*** |
|---|---|
| **Logarithmic Growth Phase** | |
| *Ab* 5075 | 2.33E-08 |
| *Ab* 5075 **Δ***ldtJ::Tn* | N/A[a] |
| *Ab* 5075 **Δ***ldtK::Tn* | N/A |
| *Ab* ACICU | N/A |
| *Ab* AYE | 8.09E-08 |
| *Ab* SDF | N/A |
| ATCC 17978 | N/A |
| ATCC 17978 **Δ***mrcA* | 9.19E-08 |
| ATCC 17978 **Δ***mrcA*/pPBP1A | N/A |
| ATCC 17978 **Δ***mrcA*/pPBP1A$_{S459A}$ | N/A |
| ATCC 17978 **Δ***mrcA*/pPBP1A$_{E92Q}$ | 9.19E-08 |
| ATCC 17978 **Δ***mrcB* | N/A |
| ATCC 19606 | 1.47E-07 |
| ATCC 19606 **Δ***ldtJ* | N/A |
| ATCC 19606 **Δ***ldtJ* /pLdtJ | 8.99E-06 |
| ATCC 19606 **Δ***ldtK* | N/A |
| ATCC 19606 **Δ***ldtK*/pLdtK | 2.11E-07 |
| **Stationary Phase** | |
| *Ab* 5075 | 1.93E-07 |
| *Ab* ACICU | N/A |

| | |
|---|---|
| *Ab* AYE | 9.59E-07 |
| *Ab* SDF | N/A |
| ATCC 17978 | N/A |
| ATCC 17978 **Δ***mrcA* | 1.06E-08 |
| ATCC 17978 **Δ***mrcA*/pPBP1A | N/A |
| ATCC 17978 **Δ***mrcA*/pPBP1A$_{S459A}$ | N/A |
| ATCC 17978 **Δ***mrcA*/pPBP1A$_{E92Q}$ | 2.01E-08 |
| ATCC 17978 **Δ***mrcB* | N/A |
| ATCC 17978 + 8 g/L Amoxicillin | N/A |
| ATCC 17978 + 64 g/L Ampicillin | N/A |
| ATCC 17978 + 4 g/L Carbenicillin | N/A |
| ATCC 17978 + 32 g/L Mecillinam | N/A |
| ATCC 17978 + 16 g/L Mezlocillin | N/A |
| ATCC 17978 + 256 g/L Cefoxitin | N/A |
| ATCC 17978 + 64 g/L Cefoperazone | N/A |
| ATCC 17978 + 8 g/L Cefotaxime | N/A |
| ATCC 17978 + 8 g/L Aztreonam | N/A |
| ATCC 17978 + 8 g/L Moenomycin | N/A |
| ATCC 19606 | 2.13E-07 |

[a]N/A indicates no LOS$^-$ isolates were recovered

## PBP1A mutation induced septal defects to support isolation of colistin resistant LOS$^-$ *A. baumannii*.

Inactivation of the gene encoding PBP1A, Δ*mrcA*, is a compensatory mutation that enables colistin selection of LOS$^-$ 17978 (19). Relative to wild type and two complementation strains with different promoter comstructs, 17978 Δ*mrcA* produced multiseptated cell populations in mid-logarithmic growth phase (**Figure 13A-13D**), resembling 19606, 5075 and AYE morphotypes. Consistent with previous analysis showing that PBP1A GTase activity inhibited colistin selection of LOS$^-$ colonies[17], Δ*mrcA*/pPBP1A$_{E92Q}$ also produced elongated multiseptated cells (**Figure 13E**), similar to Δ*mrcA* LOS$^-$ (**Figure 13F**). In contrast, point mutation of S459A, a residue essential for PBP1A DD-TPase activity (**Figure 13G**), and Δ*mrcB* (encoding PBP1B) (**Figure 13H**) produced septal patterns indistinguishable from wild type 17978, ACICU and SDF. Only PBP1A mutations that induced three or more septal sites (i.e., Δ*mrcA* and Δ*mrcA*/pPBP1A$_{E92Q}$) (**Figure 13I**) were sufficient to produce colistin resistant LOS$^-$ isolates (**Figure 13J, Table 2**). We also measured the lengths and widths of each mutant (**Figure 13K**). Only strains with cell populations containing

three or more septal sites were elongated. Relative to wild type, Δ*mrcA* had a growth defect in logarithmic phase (**Fig 13L**) when grown in Luria broth at 37° C.

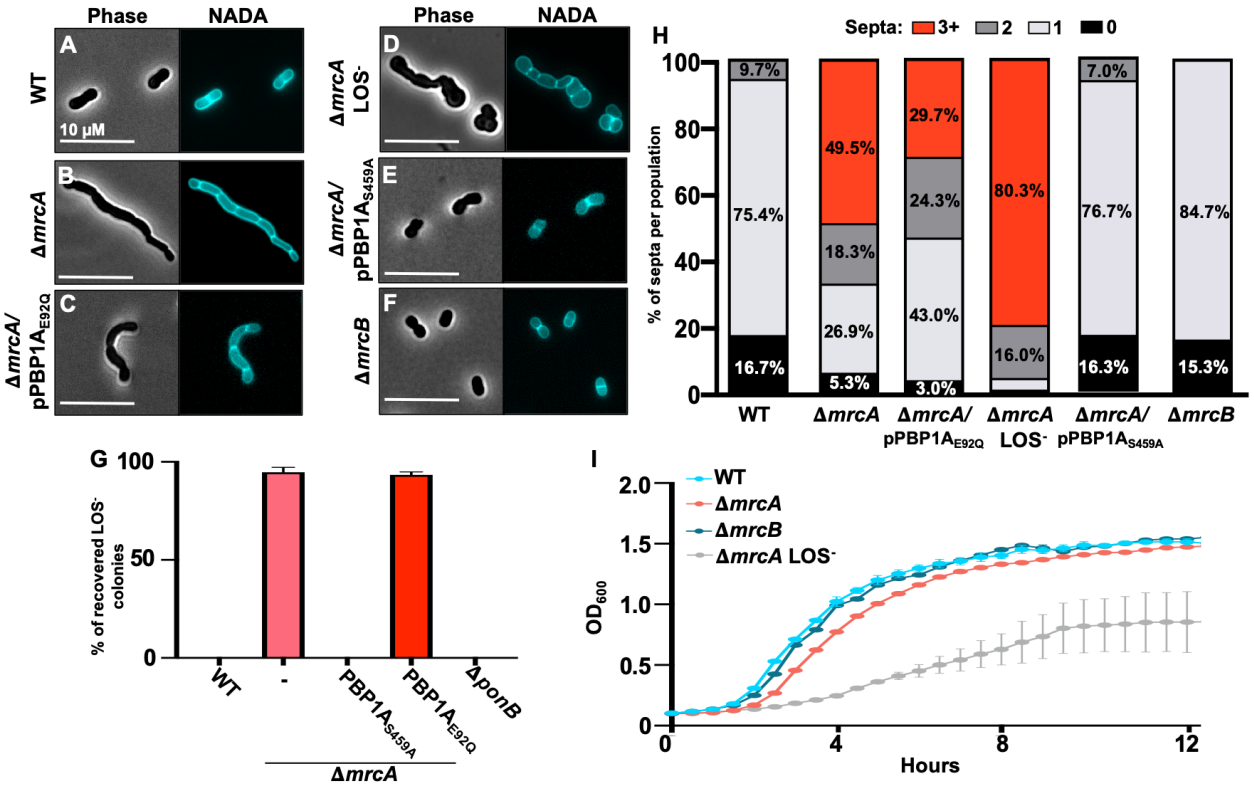


**FIGURE 13: Microscopy of *A. baumannii* strain 17978 mutants in logarithmic growth phase. (A to H)** Phase and fluorescence microscopy of NADA-treated wild type (WT) **(A)** *mrcA* **(B)**, *mrcA*/pPBP1A **(C)**, *mrcA*/pPBP1A OE (over expression) **(D)**, *mrcA*/pPBP1A$_{E92Q}$ **(E)**, *mrcA* LOS- **(F)**, *mrcA*/pPBP1A$_{S459A}$ **(G)**, and *mrcB* **(H)** cells. **(I)** Septa were quantified using ImageJ software (n= 300) and reported as a percentage of the whole. Each experiment was independently replicated three times, and one representative data set was reported. **(J)** Percentage of recovered LOS- *A. baumannii* after colistin selection using CFU in logarithmic growth phase. **(K)** Quantification of length **(L)** and width (W) of each cell population (n= 300) was calculated using ImageJ software. Each experiment was independently replicated three times, and one representative data set was reported. Each dot on the graph represents one cell. **(L)** CFU/ml of wild type and aPBP mutants in rich medium at 37°C.

Unlike wild type 17978, Δ*mrcA*/pPBP1A$_{S459A}$ and Δ*mrcB* (**Figure 14A-C**), Δ*mrcA* and Δ*mrcA*/pPBP1A$_{E92Q}$ demonstrated a filamentous morphology in stationary phase (**Figure 14D-E**) that resembled Δ*mrcA* LOS$^-$ (**Figure 14F**) and supported recovery of LOS$^-$ colistin resistant isolates (**Figure 14G, Table 2**). The cell lengths, which indicate defective septation, and widths of stationary phase cultures were measured (**Figure 14H**). Consistent with our initial observation

that only *A. baumannii* clinical isolates producing cell populations with three or more septal sites support LOS$^-$ selection, PBP1A mutations that induced multiseptate cell morphotypes also supported LOS$^-$ isolation. Together, these data indicate that septal defects correlate with isolation of colistin resistant LOS$^-$ *A. baumannii*.

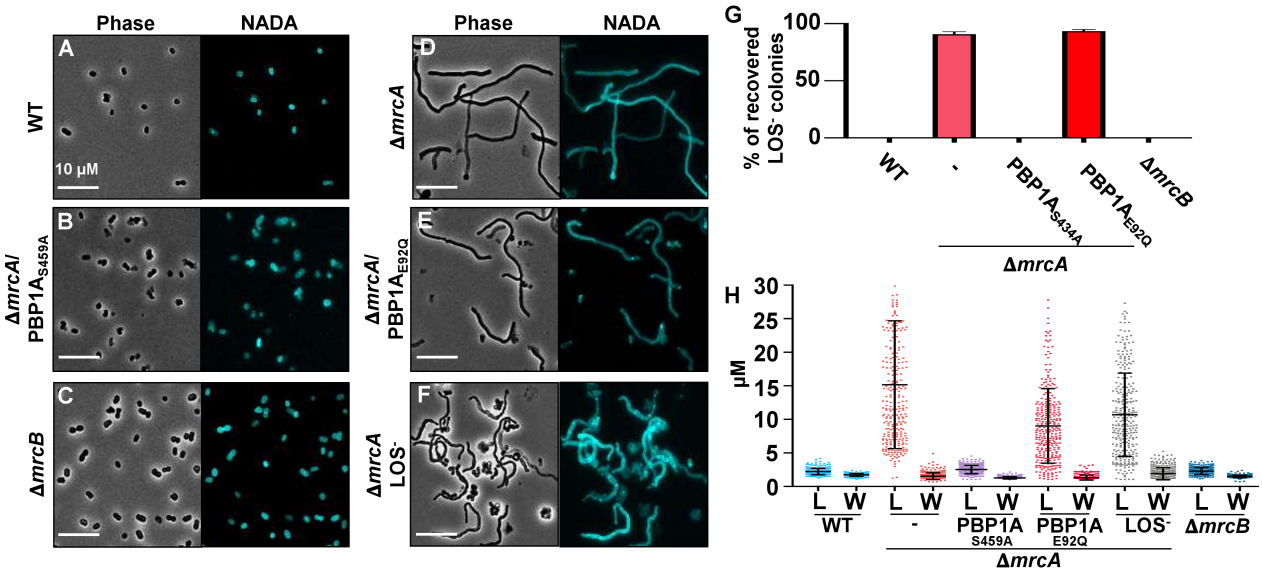


**Figure 14: Microscopy of *A. baumannii* clinical isolates in stationary phase.** NADA stained **(A)** 19606, **(B)** *Ab* 5075, **(C)** *Ab* AYE, **(D)** 17978, **(E)** *Ab* ACICU and **(F)** *Ab* SDF were visualized using phase and fluorescent microscopy. **(G)** Quantification of length (L) and width (W) of each cell population ($n$ = 300) was calculated using ImageJ software. Each dot on the graph represents one cell. **(H)** Percent of recovered LOS$^-$ *A. baumannii* after colistin selection using $10^9$ CFU in stationary phase.

## PBP1A localizes to the division site in *A. baumannii.*

Due to the septation defect in Δ*mrcA* and Δ*mrcA*/pPBP1A$_{E92Q}$, we hypothesized that PBP1A contributes to daughter cell formation in *A. baumannii.* To determine PBP1A localization, we fused mCherry to the C-terminus of PBP1A (PBP1A-mCherry) and expressed in Δ*mrcA.* Expression of each PBP1A-mCherry fusion protein in Δ*mrcA* was equivalent and PBP1A was required for mCherry signal. While mCherry fluorescent signal was observed throughout cells when pPBP1A (**Figure 15A**) or pPBP1A$_{S459A}$ (**Figure 15B**) fusion proteins were expressed, increased intensity was evident at the midcell, where the septum forms. These findings indicate

that PBP1A localizes at the septal site and potentially interacts with the divisome complex in *A. baumannii*. Phase microscopy showed pPBP1A-mCherry and pPBP1A$_{S459A}$-mCherry expression fully complemented the Δ*mrcA*-induced division defect to restore the signature *A. baumannii* coccobacilli morphology. In contrast, pPBP1A$_{E92Q}$-mCherry (**Figure 15C**) did not localize at the midcell and cells contained multiple septal sites, showing that GTase-defective PBP1A was not sufficient to complement Δ*mrcA*.

We also treated cells expressing PBP1A-mCherry proteins with NADA, which is incorporated into the peptidoglycan. pPBP1A-mCherry and pPBP1A$_{S459A}$-mCherry co-localized with septal peptidoglycan at the midcell, but pPBP1A$_{E92Q}$-mCherry did not (**Figure 15A-C**). To quantify, intensity localization was graphed along the cell axis (**Figure 15D-E**). PBP1A and PBP1A$_{S459A}$ co-localized with septal peptidoglycan, whereas PBP1A$_{E92Q}$ did not. These analyses not only show the GTase activity of PBP1A is required for proper division in *A. baumannii*, but also that enzyme activity is required for PBP1A septal site localization.

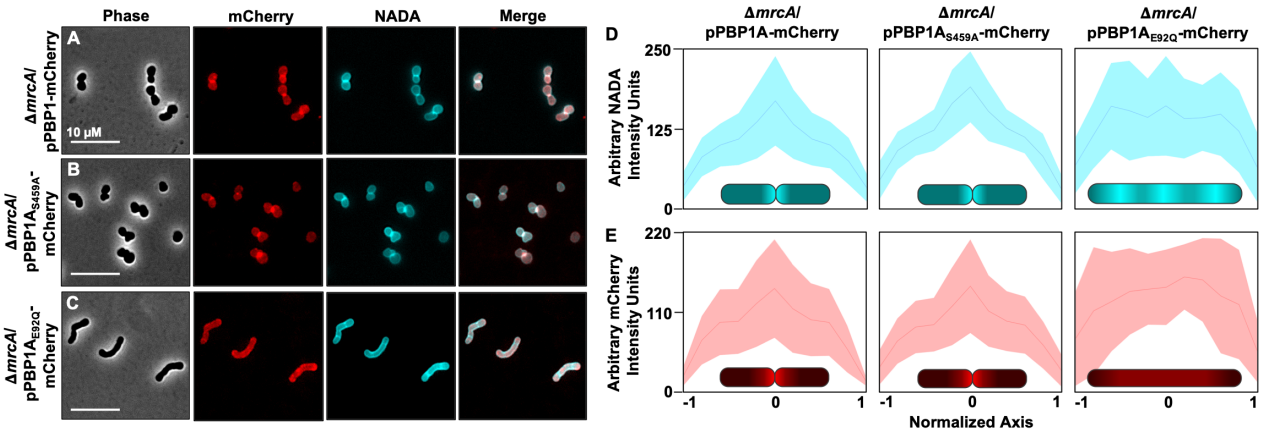


**FIGURE 15: Localization of PBP1A in *A. baumannii*. (A to C)** Phase and fluorescence microscopy of 17978 *mrcA* expressing PBP1A **(A)**, PBP1A$_{S459A}$ **(B)**, or PBP1A$_{E92Q}$ **(C)** fused to a C-terminal mCherry protein. Cells were labeled with NADA. Merged images are color composites of mCherry and NADA images. **(D and E)** Localization intensity of NADA **(D)** and PBP1A-mCherry **(E)** in cells. Shading indicates standard deviation. Intensity localization graphs generated using ImageJ software with MicrobeJ plugin (n = 50). Each experiment was independently replicated three times, and one representative data set was reported. Fluorescence localization intensity within cells is illustrated at the bottom.

## Antimicrobial susceptibility in *A. baumannii* aPBP mutants.

To determine the impact of aPBP deletions on antimicrobial susceptibility, minimal inhibitory concentrations (MIC) were calculated after wild type and the aPBP mutants were treated with several antimicrobials (**Table 3**). Relative to wild type, Δ*mrcA* showed increased resistance all β-lactam antibiotics tested except for carbapenems, which not only target DD-TPase, but also LD-TPase[219]. These data suggest that PBP1A DD-TPase activity is an intrinsic target that contributes to β-lactam susceptibility. Both aPBP mutants showed increased susceptibility to moenomycin, which inhibits GTase activity. No differences in MIC were observed when strains were treated with colistin. Lastly, both aPBP mutants demonstrated increased susceptibility to vancomycin.

**Table 3: *A. baumannii* MICs (mg/L)**

| Antimicrobial | WT | Δ*mrcA* | Δ*mrcB* | Δ*ldtJ* | Δ*ldtK* |
|---|---|---|---|---|---|
| **β-lactams** | | | | | |
| Penicillin Derivatives | | | | | |
| Amoxicillin | 16.0 | >512.0 | <8.0 | 128.0 | 128.0 |
| Ampicillin | 128.0 | >1024.0 | 128.0 | 16.0 | 16.0 |
| Carbenicillin | 8.0 | >64.0 | 8.0 | 4.0 | 4.0 |
| Mecillinam/Amdinocillin | 64.0 | >512.0 | 64.0 | 16.0 | 16.0 |
| Mezlocillin | 32.0 | >256.0 | 32.0 | 128.0 | 128.0 |
| Cephalosporin Derivatives | | | | | |
| Cefoxitin | >512.0 | 64.0 | 16.0 | 128.0 | 128.0 |
| Cefoperazone | 128.0 | >512.0 | 128.0 | >512.0 | >512.0 |
| Cefotaxime | 8.0 | 32.0 | 4.0 | 16.0 | 8.0 |
| Carbapenems | | | | | |
| Imipenem | 0.3 | 0.3 | 0.3 | <0.01 | <0.01 |
| Meropenem | 0.1 | 0.1 | 0.1 | <0.01 | <0.01 |
| Monobactam | | | | | |
| Aztreonam | 16.0 | 2.0 | 2.0 | 8.0 | 8.0 |
| **Phosphoglycolipid** | | | | | |

| | | | | | |
|---|---|---|---|---|---|
| Moenomycin | 16.0 | 2.0 | 2.0 | 4.0 | 4.0 |
| **Lipopeptide** | | | | | |
| Colistin | 1.0 | 1.0 | 1.0 | 1.0 | 1.0 |
| **Glycopeptide** | | | | | |
| Vancomycin | >512.0 | 64.0 | 64.0 | 64.0 | 64.0 |
| **Metal (mM)** | | | | | |
| Copper chloride | 5.0 | 4.5 | 4.0 | 3.5 | 3.0 |

## Filamentation is not sufficient for isolation of colistin resistant LOS- A. baumannii.

While PBP1A GTase activity is required for proper *A. baumannii* division, septation is also correlated with isolation of colistin resistant LOS$^-$ *A. baumannii*. We next tested if filamentation was sufficient to recover colistin resistant LOS$^-$ *A. baumannii*. Previous studies showed that treatment with DD-TPase-targeting β-lactams induced filamentation in Gram-negative bacteria[33,75]. Therefore, we treated wild type 17978 with several β-lactams and moenomycin (**Table 3**). Wild type 17978 was grown overnight in 0.5 X MIC concentrations of each antibiotic and cultures were treated with NADA to visualize morphological changes (**Figure 16A-J**). Amoxicillin, cefoperazone, and cefotaxime, aztreonam, moenomycin and cefoxitin treatment induced filamentation (**Figure 16K**), likely because they inhibit DD-TPase or glycosyltransferase activity required for cell division. In contrast, cells treated with ampicillin, carbenicillin, mecillinam, and mezlocillin formed spheres (**Figure 16K**), suggesting the β-lactams target primarily DD-TPases associated with cell elongation. We next performed colistin selection on treated cells to isolate LOS$^-$ *A. baumannii*; however, we were unable to recover LOS$^-$ isolates from all treated cultures (**Figure 16L, Table 3**), indicating that filamentation/elongation alone is not sufficient for colistin selection of LOS$^-$ *A. baumannii*.

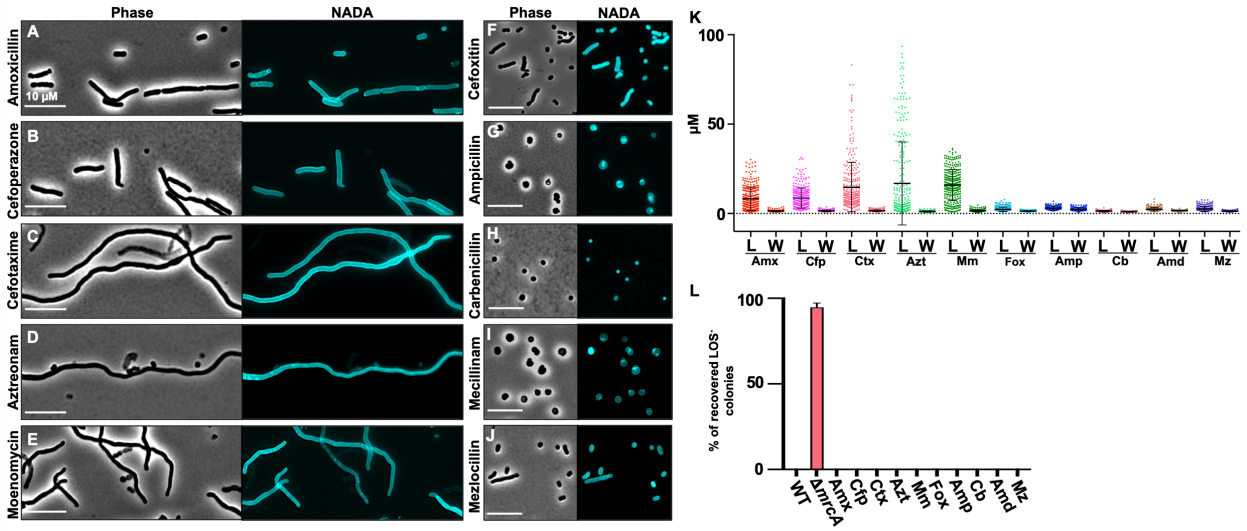


**Figure 16: Quantification of *A. baumannii* cell morphology at sub-MIC antibiotic treatment.** Cell lengths (L) and widths (W) were calculated using ImageJ software (n = 300). Each dot on the graph represents one cell. Amoxicillin (Amx), cefoperazone (Cfp), cefotaxime (Ctx), aztreonam (Azt), moenomycin (Mm), cefoxitin (Fox), ampicillin (Amp), carbenicillin (Cb), mecillinam/amdinocillin (Amd), mezlocillin (Mz).

## Peptidoglycan modifications resulting from PBP1A mutation.

Since we found that Δ*mrcA* showed increased resistance against several DD-TPase-targeting β-lactam antibiotics, we next sought to determine if the mutation altered the muropeptide composition in logarithmic and stationary phase. Muropeptide compositions of both wild type and Δ*mrcA* were analyzed and showed modifications increased in stationary phase relative to logarithmic growth phase. Specifically, 3-3 crosslinking and D-amino acid modification of peptidoglycan were increased (**Figure 17A-B**). Both modifications are characteristic of increased LD-TPase activity, which is growth phase dependent in *E. coli*[69]. We also found that relative to wild type, Δ*mrcA* generated 2-fold more 3-3 crosslinks in logarithmic growth phase (**Fig 17A**).

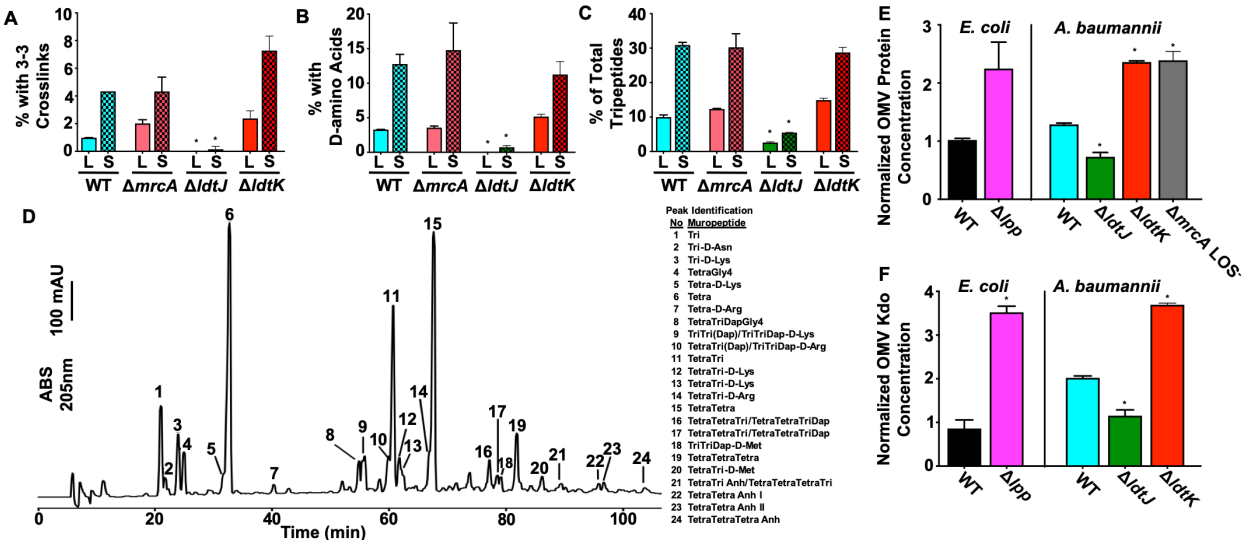


**FIGURE 17: LD-Transpeptidase activity is required for cell envelope modifications in *A. baumannii*. (A to C)** Percentage of total muropeptide content with 3-3 crosslinks **(A)**, D-amino acid addition **(B)**, and muro-tripeptide formation **(C)**. L, logarithmic growth phase; S, stationary phase. Error bars indicate variation of two biological replicates. An asterisk indicates significant differences relative to the corresponding wild type (WT) strain ($P<0.05$). **(D)** Chromatogram of the muropeptide content of stationary-phase 17978 *ldtK*. The muropeptides are labeled. **(E and F)** Relative quantification of *E. coli* and *A. baumannii* total protein **(E)** and Kdo **(F)** concentrations of outer membrane vesicles (OMVs) in *ldtJ* and *ldtK* strains relative to wild type (WT) *A. baumannii* and *E. coli.* WT *E. coli* was normalized to 1. Each experiment was independently replicated three times, and one representative data set was reported. Error bars indicate standard deviations. An asterisk indicates significant differences relative to the corresponding WT strain ($P<0.05$).

## LD-TPases are essential for selection of colistin resistant LOS$^-$ *A. baumannii.*

Next, we performed transposon-sequencing in Δ*mrcA* to determine genes that contribute to fitness relative to wild type. We discovered that two genes encoding putative LD-TPases (LdtJ and LdtK) were essential in Δ*mrcA*, but not in wild type (**Figure 17A**). As a control, we also show that mutations in *mrcB* were also synthetically lethal in *A. baumannii*, as previously reported in *E. coli*[220,221]. Since PBP1A inactivation supports colistin selection of LOS$^-$ *A. baumannii*[17], and mutation of *ldtJ* and *ldtK* are synthetically lethal in Δ*mrcA*, we hypothesized that LD-TPase activity could support viability of LOS$^-$ *A. baumannii*. LdtJ and LdtK both encode YkuD domains, which rely on essential cysteine residues to catalyze LD-TPase reactions (**Figure 17B**). To test if LdtJ and LdtK contribute to selection of colistin resistant LOS$^-$ *A. baumannii*, we engineered *ldtJ*

and *ldtK* mutations in strain 19606, which produced LOS$^-$ isolates without compensatory *mrcA* mutations[17,91]. Colistin selection of each mutant failed to recover LOS$^-$ *A. baumannii* after multiple attempts (**Figure 17C, Table 2**), showing each putative LD-TPase gene is required for LOS$^-$ viability. Complementation fully restored production of LOS$^-$ *A. baumannii* to wild type levels. Furthermore, we also performed colistin selection experiments using *ldtJ* and *ldtK* mutants in strain *Ab* 5075. These data showed *Ab* 5075 LD-TPase mutants were also unable to produce LOS$^-$ isolates relative to wild type (**Figure 17C, Table 2**), which suggests a conserved role for LD-TPases in viability of LOS$^-$ *A. baumannii*.

To determine the LD-TPase activities of LdtJ and LdtK, mutants were first treated with NADA and visualized. Δ*ldtJ* (**Figure 17E**) and Δ*ldtJ*/pLdtJ$_{C390}$ (**Figure 17F**) showed a severe defect in NADA incorporation relative to wild type (**Figure 17D**) and the mutant complemented with a wild type allele (**Figure 17G**), suggesting LdtJ is an LD-TPase that modifies peptidoglycan with D-amino acids. Δ*ldtK* (**Figure 17H**) and Δ*ldtK*/pLdtK$_{C138S}$ (**Figure 17I**) showed a slight reduction in NADA incorporation relative to wild type (**Figure 17D**) and the complemented strain (**Figure 17J**). More strikingly, Δ*ldtK* had a rounded cell morphology, suggesting a role for LdtK in elongation. Fluorescence intensity (**Figure 17K**) and cell shape from NADA-treated cultures were quantified. The LD-TPase mutants were also defective in growth in Luria broth at 37° C relative to the wild type and complemented strains.

## LdtJ forms 3-3 crosslinks and incorporates D-amino acids into peptidoglycan.

To define LD-TPase-dependent peptidoglycan modifications, we isolated peptidoglycan from strains 17978 and 19606. Muropeptides were generated by treatment with muramidase, separated by high-performance liquid chromatography and, if necessary, analyzed by MS/MS[17,69].

Peptidoglycan composition from Δ*ldtJ* showed it was unable to generate 3-3 crosslinks (**Figure 18A**) or incorporate D-amino acids (**Figure 18B**). Δ*ldtJ* also had reduced pools of tripeptides (**Figure 18C**) with a concomitant increase in tetrapeptide abundance. Peptidoglycan isolated from stationary phase Δ*ldtJ* showed similar structures, where 3-3 crosslinking, D-amino acid incorporation and tripeptide pools were significantly reduced relative to wild type (**Figure 18A-D**). Similar trends were also found in 19606. These studies indicate that LdtJ is an LD-TPase required for 3-3 crosslink formation and D-amino acid incorporation in *A. baumannii*, while its presence also promotes LD-carboxypeptidase activity. While a previous report showed that D-Lys is incorporated into some strains of *A. baumannii* peptidoglycan during stationary phase to protect the cell from effector proteins[69], here we confirmed via MS/MS that D-Asn, D-Arg and D-Met are also used to modify *A. baumannii* peptidoglycan via LdtJ activity in stationary phase.

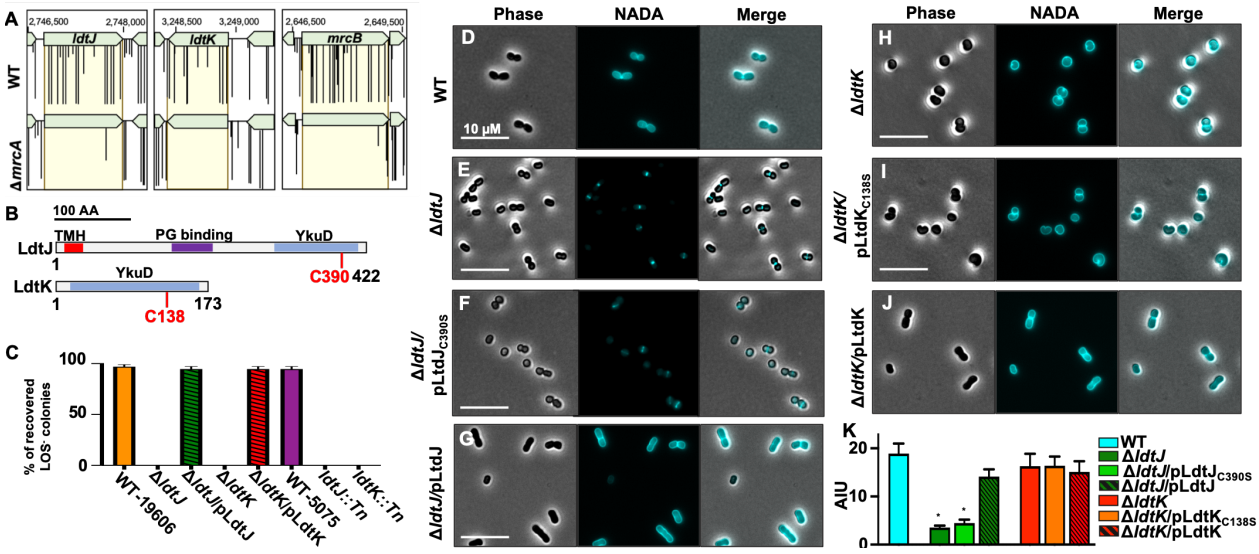


**FIGURE 18: LD-Transpeptidases are required for isolation of LOS- *A. baumannii*. (A)** Transposon sequencing analysis of *ldtJ*, *ldtK*, and *mrcB* in wild type (WT) and *mrcA* 17978 *A. baumannii*. Yellow-highlighted areas indicate genes of interest. Black lines indicate transposon insertion sites and abundance. **(B)** Schematic of domain organization of LdtJ and LdtK. **(C)** Percentage of recovered LOS- colonies after colistin selection of wild type and mutant 19606 and Ab5075 strains in logarithmic phase. **(D to J)** Phase and fluorescence microscopy of NADA-treated wild type and *ldtJ* **(D to G)** and *ldtK* **(H to J)** 17978. Each experiment was independently replicated three times, and one representative data set was reported. **(K)** Quantification of fluorescent signal intensity in arbitrary intensity units (AIU) (n= 300). Error bars indicate standard deviations. An asterisk indicates significant differences relative to WT (P<0.05).

## LdtK regulates outer membrane vesiculation.

In contrast to Δ*ldtJ*, the muropeptide composition of Δ*ldtK* showed slight increases of D-amino acid modification, 3-3 crosslinking and tripeptide pools relative to wild type in logarithmic growth phase (**Figure 18A-D**), indicating that LdtJ activity may increase in the absence of LdtK. We did not observe direct changes to LOS or lipid A structures in either Δ*ldtJ* or Δ*ldtK*. However, we found that Δ*ldtK* formed significantly more outer membrane vesicles relative to wild type when total outer membrane vesicle protein content (**Figure 18E**) or 3-deoxy-D-*manno*-oct-2-ulosonic acid (Kdo) concentrations (**Figure 18F**) were quantified from outer membrane vesicles. In *E. coli*, LdtABC catalyzes transpeptidation between the outer membrane-anchored Braun's lipoprotein (Lpp) to peptidoglycan stem peptides, which stabilize the outer membrane lipid bilayer[64]. We found that deletion of Lpp in *E. coli* resulted in hypervesiculation of the outer membrane, similar to Δ*ldtK A. baumannii* (**Figure 18E-F**). These studies suggest that LdtK functions to stabilize the outer membrane, possibly by linking it to other structures within the cell envelope. Interestingly, LOS$^-$ *A. baumannii* also produced significantly more outer membrane vesicles relative to wild type (**Figure 18E**), suggesting the LOS-deficient outer membrane is unstable. Therefore, mechanisms that stabilize the outer membrane and cell envelope likely contribute to LOS$^-$ viability.

## DISCUSSION

The molecular factors that support *A. baumannii* survival without LOS are not well understood. LOS$^-$ *A. baumannii* assemble multiple septal sites to produce cell chains or filaments. A previous study found that PBP1A GTase activity inhibited isolation of colistin resistant LOS$^-$ *A. baumannii*[17]. Here, we showed that PBP1A GTase activity, which is presumably also required for its TPase activity, is required for proper cell division in *A. baumannii*. GTase inactivation resulted

in septal accumulation that correlated with selection of LOS$^-$ *A. baumannii*. *E. coli* cells are also known to form multiseptated chains upon LptC depletion or treatment with the LpxC inhibitor, LPC-058, which compromised LPS transport and biosynthesis, respectively[20]. Together, these studies support a model where defective septation supports Gram-negative survival when LPS/LOS assembly and/or localization are compromised. Since we know outer membrane biogenesis limits the rate of LOS$^-$ *A. baumannii* growth[220], slowed septation via PBP1A mutation could reduce the growth rate enough to support LOS$^-$ outer membrane biogenesis. Even more intriguing is the idea that increased formation of septal sites supports LOS$^-$ *A. baumannii* growth through outer membrane stabilization. In *E. coli*, transenvelope complexes with the Tol system and CpoB promote outer membrane constriction and septum PG cleavage[35,221,222]. While LPS/LOS is the major stabilizing factor in the outer membrane[25], we do not understand how the lipid bilayer remains intact when LPS/LOS is compromised. However, increasing outer membrane attachment sites via septal site accumulation could increase LOS$^-$ outer membrane stability by directly linking it to other components within the cell envelope.

Cell division in *E. coli* is facilitated by the divisome complex, which includes more than twenty essential and accessory proteins that facilitate and regulate septal peptidoglycan synthesis, constrict the cell envelope and separate the daughter cells. Divisome assembly is an ordered process where the Z-ring initially recruits class A PBPs via the FtsZ membrane anchors, FtsA-FtsN and ZipA for a preseptal phase of PG synthesis[223]. Only after some delay, the next cell division proteins are recruited, including FtsQLB, FtsW-PBP3 and FtsN, which are required for constriction and daughter cell separation[224,225]. PBP1B associates with ZipA and FtsN (the latter interacts with FtsA) during the preseptal phase and later with FtsW/PBP3 and PBP3[35,44] and both its GTase and DD-TPase activities are stimulated by LpoB[221,226,227] and FtsN[43,228].

Cell division in *A. baumannii* has not been well studied; however, we showed the GTase activity of PBP1A is required for daughter cell formation. In *E. coli*, PBP1A localizes at the midcell in the absence of PBP1B, where it seems to compensate during division[42]. Therefore, it is not unreasonable to suggest a primary role for PBP1A in septation in *A. baumannii*. Based on the formation of viable, but chained *A. baumannii* in the *mrcA* mutant, PBP1A GTase activity likely plays an accessory role to FtsW-PBP3 in septal peptidoglycan synthesis. Since the $PBP1A_{E92Q}$ mutant forms a septum and constricts, but daughter cell separation is delayed, the GTase activity likely contributes a terminal step in division. PBP1A-mediated *de novo* PG synthesis could be required for sealing the new pole at the septum. Furthermore, PBP1A is known to complex with hydrolases[229], which could couple daughter cell separation with septal resolution. Moreover, it appears as if GTase activity is required for PBP1A localization at the midcell in *A. baumannii*. PBP1A interaction with the FtsW/PBP3 could be disrupted in the mutant, inhibiting septal localization. In *E. coli*, PBP1B GTase activity is regulated by many proteins (LpoB, FtsN, FtsW/PBP3, FtsQLB and PgpB[230]) so PBP1A mutations that disrupt GTase activity may result in mislocalization because it cannot associate with a specific regulatory factor. Further investigation is needed to understand if PBP1A directly contributes to septation via interactions with divisome components.

Since PBP1A inactivation supports colistin selection of $LOS^-$ *A. baumannii*[17], and *ldtJ* and *ldtK* are synthetically lethal in Δ*mrcA*, each LD-TPase activity likely fortifies the cell envelope to support $LOS^-$ *A. baumannii* growth. Furthermore, Δ*mrcA* demonstrated a significant increase in 3-3 crosslinking relative to wild type (**Fig 18A**). We showed that LdtJ is required for incorporation of D-amino acids, 3-3 crosslinking and increased carboxypeptidase activity, while *ldtK* mutation decreased outer membrane stability. These distinct phenotypes indicate separate LD-TPase

activities coordinate to stabilize the cell envelope. LdtJ and LdtK have homology to *E. coli* LdtD and LdtB, respectively. LdtD works in complex with PBP1B and a D-alanyl-D-alanine carboxypeptidase (PBP6a) to increase the ratio of 3-3 to 4-3 crosslinks, a mechanism that fortifies the cell envelope to enable *E. coli* survival when LPS transport is disrupted[20]. LdtB catalyzes covalent linkage of outer membrane-anchored Braun's lipoprotein (Lpp) to peptidoglycan[64], which stabilizes the cell envelope. Our data indicate that LdtJ and LdtK could contribute to comparable enzymatic activities in *A. baumannii*. Together, inactivation of PBP1A could support LOS$^-$ *A. baumannii* growth by inducing a septation defect, peptidoglycan remodeling and outer membrane lipoprotein to peptidoglycan crosslinking to collectively stabilize the cell envelope when the major outer membrane stabilizing factor, LPS/LOS, is compromised.

Intrinsic antimicrobial resistance is not well-understood in *A. baumannii*, but our analysis indicates that PBP1A is an important component for β-lactam susceptibility. Our antimicrobial susceptibility studies suggest PBP1A DD-TPase activity contributes to 4-3 crosslinks in both the Rod-complex and divisome, where Δ*mrcA* showed increased susceptibility to Rod-complex- and divisome-targeting β-lactams. This is further supported by our PBP1A localization studies, where PBP1A is enriched at the midcell, where the divisome assembles, but also localizes along the lateral cell wall (**Figure 15**), where the Rod-complex regulates peptidoglycan insertion to elongate rod shaped bacteria. However, further studies are necessary to determine PBP1A contributions to both division and elongation in *A. baumannii*.

LD-TPases are targeted by carbapenems[217] and copper chloride[231] and we observed altered susceptibility to both in the *ldtJ* and *ldtK* mutants (**Table 3**). While we performed these studies in the single LD-TPase mutants, we were not able to engineer a *ldtJ ldtK* double mutant after several attempts, indicating that one of the genes may be required for *A. baumannii* survival. A more

detailed analysis is needed to characterize the LdtJ and LdtK proteins to understand their contribution to resistance against clinically important antimicrobial compounds, which will inform more effective treatment strategies to combat *A. baumannii* infections.

## MATERIALS AND METHODS

### Bacterial Strains and Growth

All strains and plasmids used in this study are listed in Table S3 online. All *A. baumannii* strains were grown from freezer stocks initially on Luria-Bertani (LB) agar at 37° C. For selection, 7.5 μg/ml of kanamycin, or 10 μg/ml of colistin were used when appropriate. Strains that harbored the pABBRKn plasmid for complementation or over expression were supplemented with 30 μg/ml of kanamycin.

### Construction of PBP1A-mCherry fusions and over expression vector

Primers used in this study are listed in Table S4 online. The mCherry2B gene was amplified from pMV261[232], purified and cloned into the KpnI and SacI sites of pABBRKn[17] to generate pABBRKn::mCherry. The *mrcA* coding sequence (encoding PBP1A) from *A. baumannii* strain ATCC 17978 was amplified from plasmids pPBP1A, pPBP1A$_{E92Q}$, pPBP1A$_{S459A}$[17], purified and cloned into the XhoI and SacI sites in pABBRKn::mCherry, to create pPBP1A-mCherry, pPBP1A$_{E92Q}$-mCherry and pPBP1A$_{S459A}$-mCherry, respectively. Plasmids were transformed into Δ*mrcA* for localization studies.

To construct the IPTG-inducible pPBP1A vector, the *mrcA* coding sequence (encoding PBP1A) was amplified from *A. baumannii* strain ATCC 17978 cDNA, digested with KpnI and SalI restriction enzymes and cloned into pMMB67EHKn. The plasmid was transformed into Δ*mrcA* and induced with 2 mM IPTG for over expression studies.

**Construction of LD-TPase genetic mutants**

All *A. baumannii* mutations were isolated as previously described[233]. Briefly, $REC_{Ab}$ (pAT03) was expressed in *A. baumannii* ATCC 17978 or 19606. A linear PCR product containing the FRT-flanked kanamycin resistance cassette with flanking 125 bp regions of homology to either *ldtJ* or *ldtK* was transformed. Transformants were recovered in Luria broth, collected via centrifugation and plated on LB supplemented with kanamycin. PCR and Sanger sequencing verified all genetic mutations.

Removal of the pMMB67EH::$REC_{Ab}$ $Tet^R$ plasmid following isolation of mutants was performed as previously described[114]. pMMB67EH carrying the FLP recombinase was transformed into cured mutants. Cells were recovered in Luria broth and plated on LB agar supplemented with IPTG to induce expression of the FLP recombinase. PCR was used to confirm excision of the kanamycin cassette.

For complementation, *ldtJ* or *ldtK* coding sequences were cloned into the XhoI and KpnI sites in pMMB67EHKn[17]. Plasmids were transformed into the respective mutant to complement. For site-directed mutagenesis, complementation plasmids were amplified with primers to change the active-site cysteine residue to serine. Constructs were confirmed by Sanger sequencing and transformed into the respective mutant. *A. baumannii* mutants expressing complementation plasmids were grown in 2 mM IPTG to induce expression.

**Isolation of $LOS^-$ *A. baumannii* and determination of mutation frequency**

Isolation of $LOS^-$ *A. baumannii* colonies was done as previously described[17] with slight alterations. Briefly, cultures were grown to mid-logarithmic growth phase or stationary phase with or without antibiotics. 1 mL of $OD_{600}$ 1.0 (~$10^9$ colony forming units (CFU)) was collected via centrifugation at 1,500 X g. Cells were washed with 1 ml of Luria broth and plated on LB agar

supplemented with 10 μg/ml of colistin. Isolated colonies were picked and replica plated on LB agar supplemented with vancomycin (10 μg/ml) and LB agar supplemented with colistin (10 μg/ml). Colonies sensitive to vancomycin, but resistant to colistin were deemed LOS-deficient.

Determination of the mutation frequency was done as previously described[17]. The mutation frequency was calculated for three biological replicates and one representative set was reported.

**Western blotting**

Western blot analysis was carried out via gel transfer to PVDF (Thermo Fisher Scientific). All blots were blocked in 5% milk for 2 h. The primary antibodies α-PBP1A and α-NADH chain L were used at 1:1000 and 1:500[17], respectively followed by α-rabbit-HRP secondary antibody at 1:10,000 (Thermo Fisher Scientific). Supersignal West Pico PLUS (Thermo Fisher Scientific) was used to measure relative protein concentrations.

**Peptidoglycan analysis**

Biological replicates were grown to either stationary or mid-logarithmic growth phase in 400 mL LB. Cells were collected at 4° C and suspended in 6 mL chilled 1 X PBS and lysed with drop-wise addition to 6 mL boiling 8% SDS. Peptidoglycan was prepared from cell lysate as previously described[234]. Briefly, muropeptides were released from peptidoglycan by the muramidase Cellosyl (Hoechst, Frankfurt am Main, Germany), reduced by sodium borohydride, and separated on a 250 × 4.6 mm 3 μm Prontosil 120-3-C18 AQ reversed phase column (Bischoff, Leonberg, Germany). The eluted muropeptides were detected by absorbance at 205 nm. Eluted peaks were assigned based on published chromatograms[17,69]; new peaks were subjected to MS/MS analysis. Peak means and variation of two independent biological repeats were reported for all samples.

**Fluorescent NADA staining**

Overnight cultures were back-diluted to $OD_{600}$ of 0.05 and grown at 37°C in LB media until they reached stationary or mid-logarithmic growth phase. Cells were washed once with Luria broth and resuspended in 1 ml Luria broth. 3 µl of 10 mM of NBD-(linezolid-7-nitrobenz-2-oxa-1,3-diazol-4-yl)-amino-D-alanine (NADA) (ThermoFisher) was added to the resuspension. Cells were incubated with NADA at 37°C for 30 minutes. Following incubation, cells were washed once and fixed with 1x phosphate buffered saline containing a (1:10) solution of 16% paraformaldehyde.

**Microscopy**

Fixed cells were immobilized on agarose pads and imaged using an inverted Nikon Eclipse Ti-2 widefield epifluorescence microscope equipped with a Photometrics Prime 95B camera and a Plan Apo 100 m X 1.45 numerical aperture lens objective. Green fluorescence and red fluorescence images were taken using a filter cube with a 470/40 nm or 560/40 nm excitation filters and 632/60 or 535/50 emission filters, respectively. Images were captured using NIS Elements software.

**Image analysis**

All images were processed and pseudo-colored with ImageJ FIJI[235] and MicrobeJ plugin was used for quantifications. Cell lengths, widths, and fluorescence intensities as a function of length were quantified in MicrobeJ[236]. Cell length, width and fluorescence data were plotted in Prism 8 (GraphPad 8.4.1). NADA stain was pseudo-colored using MicrobeJ cyan look-up table. Phase and fluorescent channels were merged in MicrobeJ. Fluorescence localization graphs of dividing cells were generated using MicrobeJ XStatProfile. MicrobeJ feature detection was used to calculate the number of septal sites per cell stained with NADA as described above. Septal site percentages were represented with dot plots generated in Prism. 50 cells were analyzed for fluorescent localization and 300 cells were analyzed for all other experiments. Each experiment

was independently replicated three times, one representative dataset was reported in the quantification and one representative image included in the figure.

**Growth curves**

Growth curves were performed as previously described[237]. Briefly, overnight cultures were back diluted to $OD_{600}$ of 0.01 and set up as triplicate biological replicas in a 96 well plate (BrandTech BRAND). A BioTek SynergyNeo$^2$ microplate reader was used to record optical density, which was read at $OD_{600}$ every half hour. The microplate reader was set to 37°C with continuous shaking. Growth curves were plotted in Prism 8. Each growth curve experiment was independently replicated three times and one representative dataset was reported.

**CFU growth curve**

Triplicate overnight cultures were diluted back to $OD_{600}$ of 0.01 and grown for 12 hours at 37°C in LB broth. Cells were plated at designated time points on LB agar. LB agar plates were grown overnight at at 37°C and the CFUs were enumerated and reported. Growth curve created in Graphpad Prism 8. Each growth curve experiment was independently replicated twice in triplicate and one representative dataset was reported.

**MIC calculation**

MIC assays were performed as previously described with slight modifications[166,184]. A small number of bacteria from an overnight plate were used to inoculate 5 mL LB at $OD_{600}$ 0.05 and grown to mid-logarithmic growth phase. Cells were washed twice with LB media and diluted to $OD_{600}$ 0.01. 150 μL of cells were added to each well of a 96-well plate. Antimicrobials and copper chloride (VWR) were diluted in water and serial diluted. Two-fold dilutions of each compound were added to each well. Plates were incubated at 37°C overnight with shaking. MICs

were determined by $OD_{600}$ measurements where cell density was 0. Each experiment was performed twice in triplicate and a representative MIC was reported.

**Transposon-sequencing**

Transposon-sequencing was performed as previously described[238]. Briefly pJNW684 was conjugated into wild type and **Δ***mrcA A. baumannii* strain ATCC 17978. A library of approximately 400,000 mutants was screened for growth in Luria broth. After 6 doublings, gDNA from cultures was isolated, sheared and transposon junctions were amplified and sequenced. Transposon insertions from wild type and **Δ***mrcA* were compared to determine factors that influence fitness. The transposon insertion maps for *ldtJ* and *ldtK* genes in wild type and **Δ***mrcA* were reported.

**Outer membrane vesicle isolation**

Overnight cultures were back diluted to $OD_{600}$ of 0.01 and grown to stationary phase in 100 ml Luria broth as biological duplicates. Cultures were pelleted and the supernatant was filtered through a 0.45 μM filter (Fisherbrand). Equivalent volumes of filtered supernatant were subjected to ultracentrifugation (Sorvall WX 80+ Ultracentrifuge with AH-629 Swinging Bucket Rotor) at 4° C for one hour and 151,243 x g. The outer membrane vesicle pellet was resuspended in 500 μl of cold buffer (Tris 50mM, NaCl 5mM, $MgSO_4$ 1mM; 7.5 pH). Outer membrane vesicles from each strain were isolated three times in biological duplicates.

**Quantification of outer membrane vesicles**

For Bradford assays, a standard curve was prepared from dilution of bovine serum albumin (0 – 20 mg/ml) in Pierce Coomassie Plus Assay Reagent (Thermofisher) to a final volume of 1 ml. In parallel, outer membrane vesicles (15, 20, and 30 μl) were diluted in reagent to a final volume of 1 ml. Absorbance ($OD_{595}$) was measured in a 96 well plate (BrandTech) using a microplate

spectrophotometer (Fisherbrand AccuSkan). Optical densities of samples were compared to the standard curve plotted in Excel (Microsoft) and quantifications were graphed in Prism 8. Experiments were reproduced three times from each outer membrane vesicle isolation and one representative dataset was reported.

Kdo assays were performed as previously described (68). Briefly, 0-100 μg/ml Kdo (Sigma) standards were diluted in parallel with isolated outer membrane vesicles (2, 5, 8, and 10 μl) in 0.5M $H_2SO_4$ (Sigma). OMV isolates were boiled for 10 minutes. 0.1 M periodic acid (Sigma), 0.2 M sodium arsenite (Sigma) in 0.5 M HCl (Sigma), and 0.6% thiobarbituric acid (Sigma) were incubated with Kdo standards and OMV isolates. All samples were boiled and n-butanol (Sigma) was used to extract the purified Kdo prior to optical density measurements taken at $OD_{552}$ and $OD_{509}$ (Microplate Spectrophotometer Fisherbrand AccuSkan) in cuvettes (FisherBrand). Readings at $OD_{552}$ were subtracted from $OD_{509}$ and used to generate a linear Kdo standard curve in Excel (Microsoft). Optical densities of samples were compared to the standard curve to quantify. Values were graphed in Prism 8. Each experiment was reproduced three times from each outer membrane vesicle isolation and one representative dataset was reported.

**Statistical Analysis**

Tests for significance in differences of muropeptide composition and outer membrane vesicle production were conducted using the Student's *t* test (two-tailed distribution with two-sample, equal variance calculations). Statistically significant differences between relevant strains possessed $P < 0.05$.

# CHAPTER 5: PBP1A is required for proper division and fitness in *Acinetobacter baumannii*

Katie N. Kang[a] and Joseph M. Boll[a,#]

Affiliations:

[a]Department of Biology, University of Texas Arlington, Arlington, TX, USA

[#]Correspondence:

Joseph M. Boll

The University of Texas at Arlington

Arlington TX, 76010

Phone (817) 272-4045

Email: joseph.boll@uta.edu

** In preparation as: **Kang KN** and Boll JM. PBP1A is required for proper division in *A. baumannii*. *J Bacteriol*. In preparation. Estimated submission May 2022

## Abstract

The class A penicillin-binding proteins (aPBPs), PBP1A and PBP1B, are major cell wall synthases that synthesize more than half of the peptidoglycan per generation in *E. coli*. Studies in *E. coli* determined that aPBPs have distinct roles in peptidoglycan biosynthesis during elongation and division; however, disruption of either enzyme is rescued by the other to maintain cell homeostasis and promote proper growth. *Acinetobacter baumannii* is a nosocomial pathogen with high propensity to overcome antimicrobial treatment. *A. baumannii* encodes both PBP1A (encoded by *mrcA*) and PBP1B (encoded by *mrcB*), but only *mrcA* deletion decreased fitness, suggesting that PBP1B activity was not semi-redundant with PBP1A. Herein we show that *A. baumannii* PBP1A has a specific role in division and fitness. PBP1A localizes to sites of septum biogenesis early in division where it directly interacts with transpeptidase, PBP3, an essential component of the divisome complex, a multiprotein complex that regulates daughter cell formation. PBP3 overexpression was sufficient to rescue the division defect in Δ*mrcA*; however, it did not restore the fitness defect. PBP5 overexpression also restored the canonical *A. baumannii* coccobacilli morphology in Δ*mrcA*. Together, these data support a direct role for PBP1A *A. baumannii* division and also suggest that PBP1A indirectly regulates elongasome activity. The distinct septal activity of PBP1A along with its role in growth have proven important for antibiotic efficacy and resistance, which contrasts with model systems, where aPBPs demonstrate semi-redundant PBP1A and PBP1B activities. Together, our data suggest that PBP1A, PBP3 and PBP5 interact at the divisome and promote division through distinct activities in *A. baumannii*.

## Introduction

Gram-negative bacteria are in enclosed in a tripartite envelope consisting of the inner membrane (IM), a peptidoglycan (PG) wall and an outer membrane (OM). The PG sacculus determines cell morphology, where distinct elongasome and divisome protein complexes dictate rod length and septation, respectively. Dogma suggests that elongation and division activities are in direct competition; therefore, cell[239,240] and septal[241] morphologies are the result of PG biogenesis trade-offs between the two complexes. Increased elongation activity favors a narrow, extended cylindrical area[240] with V-shaped division constrictions[241] whereas increased divisome activity results in wide, short cells[240] with blunted septal sites[241].

In some Proteobacteria like *E. coli*, the divisome and elongasome complexes contain over 30 proteins that contribute to regulation, PG biogenesis and membrane constriction[33,34]. PG synthases include two primary synthases, the class *A* penicillin-binding proteins (aPBPs), PBP1A and PBP1B (encoded by *mrcA* and *mrcB*, respectively). The aPBPs are bifunctional and catalyze transpeptidase (TPase) and glycosyltransferase (GTase) activities. In *E. coli,* PBP1A and PBP1B are thought to be functionally semi-redundant as only one is required for viability[22] and individual *mrcA* and *mrcB* deletions do not contribute to substantial morphological defects[35,42]. Additionally, neither aPBP is specifically required for elongation[41] or division[45] in this model organism.

aPBPs directly interact with specific monofunctional synthases in the elongasome or divisome complexes. PBP1A associates with the monofunctional TPase, PBP2, in the elongasome[42] and PBP2 interacts with the monofunctional elongation GTase, RodA[242]. Elongasome activities are regulated by MreBCD through interaction with the cytoplasmic domain of PBP2[242]. In contrasts, PBP1B associates with PBP3 in the divisome[43,243] and with FtsN[43], an essential bitopic membrane protein necessary to promote divison[244] by inducing PBP3 activity[245].

PBP1B forms a trimeric complex with PBP3 and FtsW, the monofunctional divisome GTase[243]. FtsW inhibits PBP1B-mediated PG polymerization in the absence of PBP3[243]. While PBP1A and PBP1B interact with distinct PG assembly complexes, when an aPBP is inactivated, the other is thought to compensate for the missing activity[42].

Our understanding of the PG synthase machineries in Gram-negative bacteria are largely on based studies in the model organism *E. coli*. However, accumulating evidence clearly shows distinct PBP1A and PBP1B activities in *A. baumannii*[17,73,74]. Deletion of the gene encoding PBP1A induced septation defects, which induced cell chaining and filamentation in *A. baumannii*[73]. Consistent with a role in division, PBP1A was enriched at the midcell in growth, where divisome components assemble to regulate daughter cell formation[73]. While phenotypes were consistent with a role for PBP1A in *A. baumannii* division, a conclusive role was not assigned. Here, we show that PBP1A and PBP1B are not functionally redundant in *A. baumannii*. PPB1A distinctly localizes to the midcell prior to septum formation where it activates division. Instead, PBP1A distinctly localizes to the midcell prior to division, where it presumably activates septation. PBP1A directly associates with PBP3 in growth, strongly suggesting that it interacts with the divisome to regulate septation. While PBP3 overexpression rescued the Δ*mrcA* division defect, it did not compensate for the growth defect, suggesting that PBP1A and PBP3 have distinct roles in septation. Together, these studies uncover a unique role for PBP1A in *A. baumannii* and show that it promotes proper growth and fitness.

## Results

### PBP1B cannot compensate for loss of PBP1A in *A. baumannii*

PBP1A is associated with cylindrical PG biogenesis in the elongasome and PBP1B interacts with members of the divisome. However, single deletions of aPBPs do not affect cellular morphology[42] though one is required for viability in *E. coli*[22]. This led to the hypothesis that PBP1A and PBP1B are functionally semi-redundant in rod shaped bacteria. Intriguingly, our previous data suggested wild type levels PBP1B cannot compensate for PBP1A activity in *A. baumannii*[73]. We observed Δ*mrcA* but not Δ*mrcB* contained division abnormalities and reduced fitness[73]. Similarly, TPase-disrupted Δ*mrcA* but not Δ*mrcB* was recently shown to impair growth rates in *A. baumannii*[74]. Here, we sought to determine if over expression of PBP1B could rescue the defects previously observed in Δ*mrcA*.

We generated a growth curve of wild type, Δ*mrcA,* Δ*mrcB* and Δ*mrcA* over expressing PBP1B with optical density measurements. As previously reported[73,74], Δ*mrcB* did not demonstrate significant growth defects compared to wild type. Additionally, PBP1B over expression was not sufficient to rescue impaired growth in Δ*mrcA* (**Figure 18A**). We next asked if PBP1B over expression could rescue Δ*mrcA* division defects. *A. baumannii* Δ*pbp1A* over expressing PBP1B were grown to logarithmic phase and stained with the fluorescent derivative of D-alanine (NADA) to visualize PG[21,214]. Length quantifications of Δ*pbp1A* $PBP1B_{OE}$ with respect to wild type demonstrate increased expression of PBP1B was not sufficient to rescue Δ*pbp1A* division (**Figure 18B, D**). This suggests the proposed functional redundancy of aPBPs in division is not conserved in *A. baumannii*.

Further, if PBP1A and PBP1B were functionally redundant for fitness, we hypothesized we would observe increased protein levels in one when the other was deleted. Cultures of wild

type, Δ*mrcA* and Δ*mrcB* were grown to logarithmic or stationary phase and normalized and collected for western blotting. Protein levels of PBP1A and PBP1B were assessed in each whole cell lysate with protein-specific anti-sera. In both logarithmic growth and stasis, protein levels of either aPBP did not increase with respect to wild type to compensate for the deletion of the other (**Figure 18C**). While it is possible that *A. baumannii* aPBPs correct imbalance when the other is defective, our data suggests PBP1B cannot compensate for defective PBP1A activity.

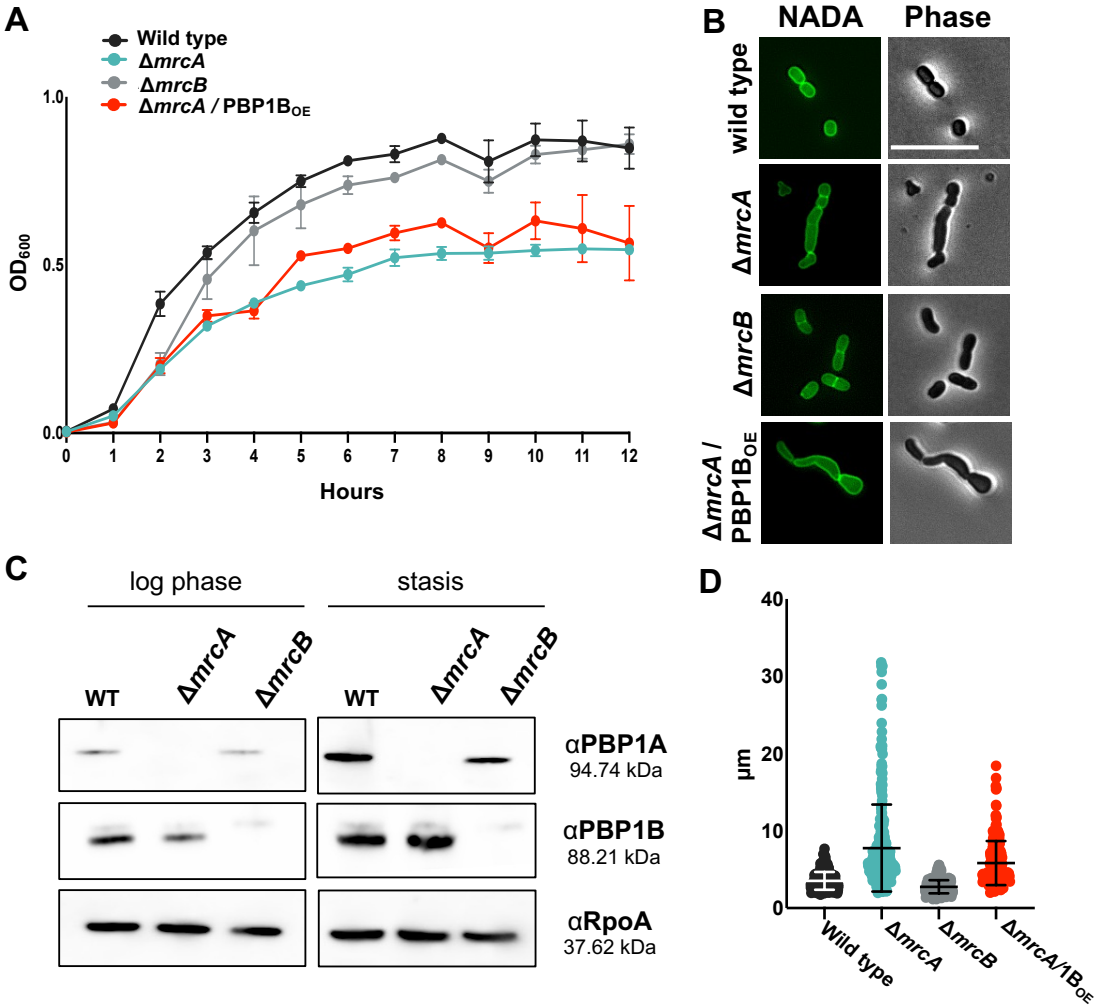


**Figure 18: PBP1B cannot compensate for the division defect when PBP1A is defective**. (A) Optical density growth curve of wild type (WT), Δ*mrcA,* Δ*mrcB* and Δ*mrcA*/pPBP1B$_{OE}$ (overexpression). (B) Fluorescence and phase microscopy of WT, Δ*mrcA,* Δ*mrcB* and Δ*mrcA*/PBP1B$_{OE}$. Scale bar 10 μm. (C) Length (pole to pole) quantifications of each cell population ($n \geq 300$) in 1B was calculated using ImageJ software. Each dot represents one cell. Significance testing conducted using Student *t* test with two-tailed distribution assuming equal variance. **** $P < 0.0001$. *** $= P = 0.0002$. (D) Western blot of WT, Δ*mrcA* and Δ*mrcB* whole cell lysates collected in mid-logarithmic growth (left) and stasis (right). PBP1A is 94.74 kDa; PBP1B is 88.21 kDa and RpoA is 37.62 kDa.

## PBP1A over expression shifts PG biogenesis towards division

Previously, we reported that PBP1A fused to the fluorescent protein, mCherry, was diffuse throughout *A. baumannii* but increased fluorescence intensity was apparent at the midcell, where the divisome regulates septal formation and divsion[73]. Further investigation of PBP1A localization shows PBP1A concentrates at the midcell prior to septal biogenesis (**Figure 19A,B**). This suggests PBP1A may contribute to early steps of septal PG biogenesis or regulation and contribute to the shift from elongation PG synthesis to septum synthesis.

Intriguingly, recent studies showed over expression of PBP1A in *A. baumannii* causes cell rounding[61,73]. Visually, the phenotype is strikingly similar to mecillinam-mediated PBP2 inhibition[246] and was therefore hypothesized that PBP1A activity in *A. baumannii* inhibits the elongasome complex[61]. We next determined if cellular rounding through increased PBP1A expression and PBP2 inhibition acted in the same pathway. We grew wild type over expressing PBP1A, wild type incubated sub-minimum inhibitory concentrations (sub-MIC) of mecillinam, wild type over expressing PBP1A incubated with sub-MIC mecillinam and Δ*mrcA* treated with sub-MIC mecillinam to logarithmic growth phase and measured cells pole to septa. Intriguingly, PBP2 inhibition through mecillinam treatment produced statistically significant shorter cells than over expressing PBP1A (**Figure 19C,D**), suggesting PBP1A may shift PG biogenesis towards division but likely does not directly inhibit elongasome activity. Interestingly, Δ*mrcA* treated with sub-MIC mecillinam still contained defective septation (**Figure 19C,D**), suggesting PBP2 inhibition was not sufficient to shift PG biosynthesis towards division when PBP1A was inhibited.

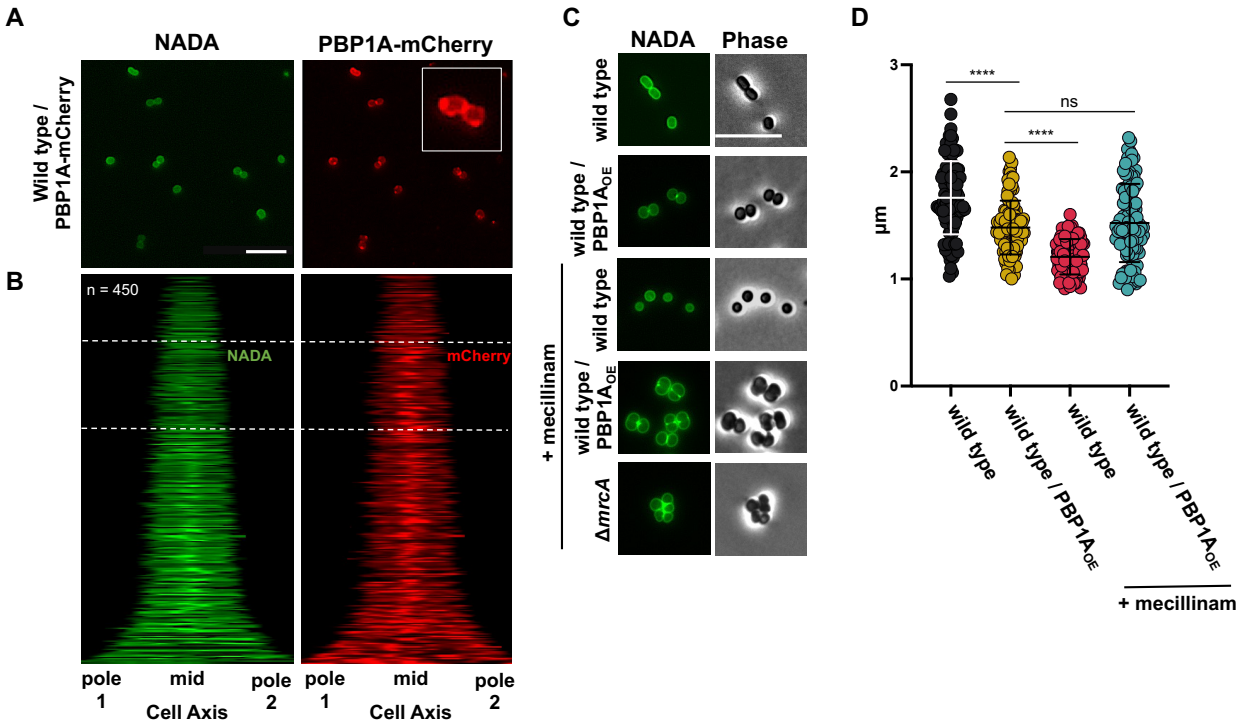


**Figure 19: PBP1A shifts balance towards division. (A)** Fluorescence microscopy of wild type PBP1A-mCherry. PBP1A-mCherry is expressed from its native promoter. Scale bar = 10µm. **(B)** Kymographs depicting fluorescence of NADA (left) and PBP1A-mCherry (right) intensity localization along the cell axis. Cells are ordered by increasing length. **(C)** Fluorescence and phase microscopy of wild type, wild type PBP1A$_{OE}$ (over expression), wild type treated with half-MIC mecillinam, wild type PBP1A$_{OE}$ (over expression) treated with half-MIC mecillinam and Δ*mrcA* treated with half-MIC mecillinam. Scale bar = 10µm. **(D)** Length (pole to septa in dividing cells or pole to pole in non-diving cells) (n = 100) was calculated using ImageJ software with segmentation code (see Appendix 1). Significance testing conducted using Student *t* test with two-tailed distribution assuming equal variance. **** $P < 0.0001$. ns = $P = 0.3263$.

## PBP1A directly interacts with PBP3 at the divisome during growth

*A. baumannii* Δ*mrcA* has defective division (**Figure 18B**) and recent work from our laboratory shows Δ*mrcA* contains multiple sites of incomplete septal biogenesis[73]. While our study implies PBP1A is necessary for division, it remains unclear if PBP1A directly interacts with the divisome in *A. baumannii.* Next, we tested for direct associations between PBP1A, PBP2 and PBP3 with a *co*-*i*mmuno*p*recipitation (coIP) assay previously developed by our laboratory[201]. Initially, wild type cells expressing Flag-tagged PBP1A were incubated with the amine-reactive crosslinker, formaldehyde. To capture interactions between PBP1A and adjacent proteins, crosslinked PBP1A-Flag protein complexes were immunoprecipitated with Flag-affinity beads.

Protein-specific anti-sera were used to interrogate the PBP1A-Flag complex. However, we were unable to identify interactions with this method. Formaldehyde crosslinking requires the amine groups of adjacent proteins to be within 2 Å. We postulated large PBP1A complexes may exist outside of this narrow range. To overcome the size limitations of formaldehyde crosslinking, we next used Lomant's reagent (dithiobis succinimidylpropionate or DSP). DSP is similarly membrane-permeable and reactive to primary amine groups; however, DSP contains a 12.0 Å spacer arm. coIPs with DSP crosslinking revealed PBP1A directly interacts with PBP3 but not PBP2 during growth (**Figure 20**). These studies show that PBP1A directly interacts with PBP3, a highly conserved protein known to contribute to daughter cell formation during septation. Contrary to what is understood in *E. coli*, our data show PBP1A associates directly with the divisome and not the elongasome in *A. baumannii* during growth.

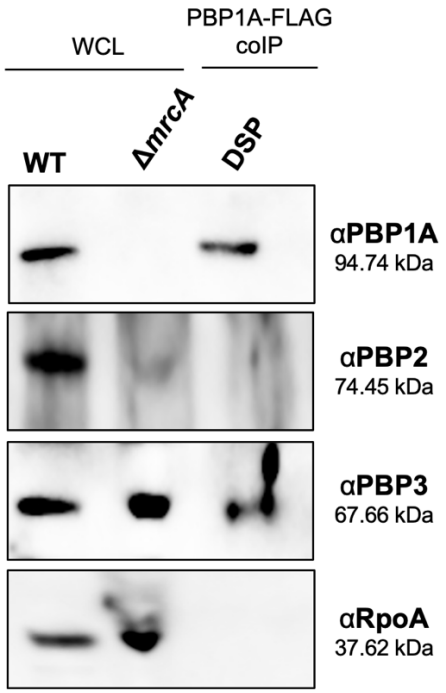


**Figure 20: PBP1A directly interacts with PBP3, but not PBP2.** Whole cell lysates (WCL) of wild type (WT) and Δ*mrcA* next to PBP1A-Flag coIP crosslinked with DSP. Anti-sera used to detect specific proteins in the complex are labeled on the right. PBP1A is 94.74 kDa; PBP2 is 74.45 kDa; PBP3 is 67.66 kDa; RpoA is 37.62 kDa.

**PBP3-dependent rescue of Δ*pbp1A* division defects**

Prompted by the finding that PBP1A directly interacts with PBP3 in the divisome, we next investigated if PBP1A and PBP3 or its GTase partner, FtsW, share redundant roles in septal PG biogenesis. We over expressed PBP3 or FtsW in Δ*pbp1A* to determine if either divisome synthase could promote wild type septation in Δ*mrcA.* Quantifications of cell lengths show PBP3 but not FtsW compensated for the loss of *mrcA* and rescued septation (**Figure 21 A,B**).

Similar to the *A. baumannii* Δ*pbp1A* phenotype, disruption of PBP3 activity produces filamentous, nondividing cells in Gram-negative bacteria[73,247]. Interestingly, several studies show PBP5, a DD-carboxypeptidase, rescues division defects in PBP3-depleted *E. coli*[239,248] and other bacteria[249]. Considering PBP3 rescued septation defects in *A. baumannii* Δ*mrcA,* we asked if PBP5 could similarly promote division when PBP1A activity is lost. Here, we show Δ*mrcA* over expressing PBP5 has wild type morphology (**Figure 21 A,B**). Taken together these studies imply that PBP1A, PBP3 and PBP5 work together in *A. baumannii* to regulate PG biogenesis during septation.

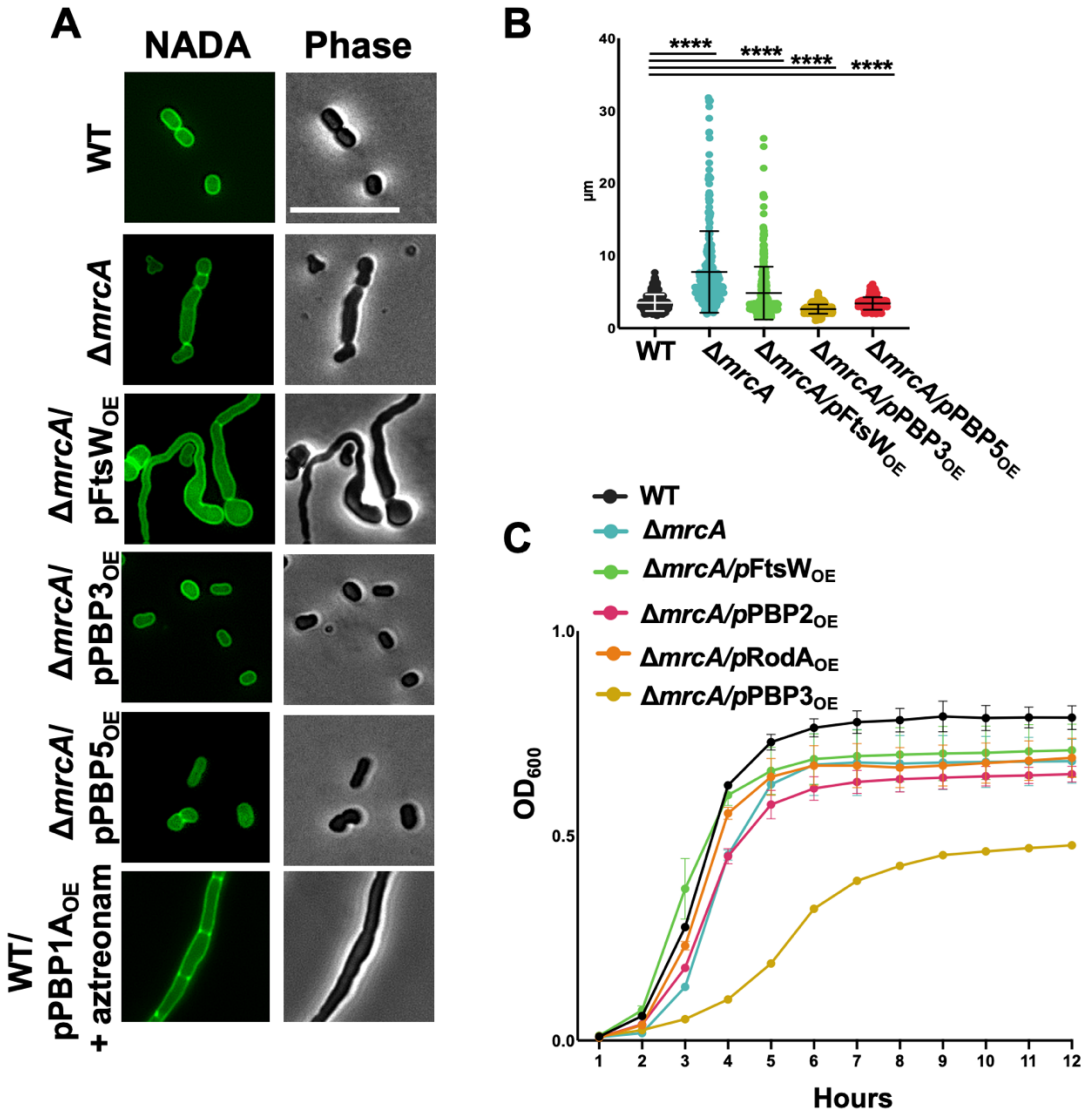


**Figure 21: PBP3 and PBP5 rescue division but not fitness. (A)** Fluorescence and phase microscopy of wild type, Δ*mrcA,* Δ*mrcA* FtsW$_{OE}$ (over expression), Δ*mrcA* PBP3$_{OE}$ and Δ*mrcA* PBP5$_{OE}$. Scale bar = 10μm. **(B)** Length (pole to pole) (n ≥ 300) was calculated using ImageJ software. Each dot represents one cell. **(C)** Optical density growth curve of Δ*mrcA* and monofunctional PG synthaeses over expressed in Δ*mrcA*. Each dot represents one cell. Significance testing conducted using Student t test with two-tailed distribution assuming equal variance. **** P < 0.0001.

## PBP3 and PBP1A do not share redundant roles in the divisome

Previous studies from our lab[73] and others[74] have demonstrated a significant fitness defect in *A. baumannii* Δ*mrcA*. We asked if restoring productive septation in Δ*mrcA* would be sufficient

to rescue fitness. We over expressed each of the monofunctional synthases in Δ*mrcA* and assessed fitness with optical density growth curves. However, over expression of all of the monofunctional synthases tested failed to rescue fitness in Δ*mrcA*. Although PBP3 was sufficient to rescue the septation defect, PBP1A activity is required for fitness **(Figure 21C)**.

We next asked if PBP1A over expression would similarly rescue division when PBP3 is disrupted. To disrupt PBP3, we treated cells with sub-MIC of aztreonam which has high specificity for PBP3[247] relative to other PBPs and effectively prevents division in *A. baumannii*[73]. When PBP1A was over expressed in aztreonam treated cells, the filamentous phenotype remained **(Figure 21A)**. In contrast to our data showing PBP3 is sufficient to promote division in Δ*mrcA* (**Figure 21A,B**), PBP1A cannot rescue division when PBP3 is disrupted (**Figure 21A**). This points to a role for PBP3 in septal PG biogenesis that cannot be compensated for by PBP1A. Together, these data suggest that while both PBP1A and PBP3 interact in the divisome, they do not share redundant roles.

## Discussion

Emerging studies have highlighted the importance of PBP1A activity for proper division and fitness in *A. baumannii*[73,74]. Here we add to that model, where PBP1B activity does not compensate for *mrcA* inactivation in *A. baumannii*. While aPBP activity was thought to be functionally redundant based on studies in other model organisms, we show that *A. baumannii* PBP1A localizes to the midcell before septum formation, where it directly interacts with the divisome to promote septal site and daughter cell formation. Moreover, PBP3 but not FtsW rescued division in Δ*mrcA*. PBP3 and FtsW are cooperative partners in the divisome; however, it is not unexpected that PBP3 alone would rescue the division defect. Monofunctional GTases require

TPases for functionality[40], likely to prevent PG glycan polymerization without crosslinking if the TPase is defective or absent. In this context, it is not surprising that only over expression of the TPase, PBP3, was capable of shifting PG biogenesis towards division and compensating for the loss of PBP1A activity.

Interestingly, PBP5 also rescues division defects in *A. baumannii* Δ*mrcA*. PBP5 is a DD-carboxypeptidase found in both Gram-negative and Gram-positive bacteria that localizes to PG biogenesis sites, where it catalyzes the formation of tetrapeptides by cleaving the terminal D-alanine from pentapeptides[248,250]. While amidation of pentapeptides to tetrapeptides is important for the maturation of PG, it is not clear why PBP5 over expression resolves division problems in PBP3-depleted organisms[239,248,249]. One report hypothesized that following tetrapeptide formation by PBP5, an unidentified LD-carboxypeptidase further modified the tetrapeptides to tripeptides[239], which was proposed to be the primary substrate of PBP3[251,252]. The authors proposed that when *E. coli* encoding thermolabile PBP3 is grown at 42° C, the over expression of PBP5 would lead to increased PBP3-substrate; therefore, the remaining PBP3 was sufficient to shift biogenesis towards division and away from elongation, since PBP3 activity is specific to the divisome complex[239]. However, another possibility that PBP5 is directly providing LD-transpeptidases with tetrapeptide substrate at the divisome, allowing alternative 3-3 crosslinking to compensate for PBP3 depletion in the divisome.

Interestingly, over expressed PBP1A was not sufficient compensate for aztreonam-inhibited PBP3 activity. Whereas PBP1A and PBP3 are both necessary for productive septation in wild type *A. baumannii*, these findings suggest they have independent roles in the division. Considering PBP1A localizes to the site of septal PG biogenesis early, it is intriguing to speculate that PBP1A may build the recently described septal PG wedge that forms after cellular constriction

and prior to septation[241]. The wedge is thought to prevent lysis during division[241] and may be one possible mechanism for the fitness defect we[73] and others[74] have observed in *A. baumannii* Δ*mrcA*. Moreover, TPase inactivated PBP1A, but not PBP1B or PBP2, increased cellular lysis in *A. baumannii* under standard growth conditions[74], suggesting PBP1A is a major contributor to PG biogenesis and stability in wild type during division.

Another possible mechanism for PBP1A contribution to the divisome as an important component of the feedback network in PG hydrolase activity. In *E. coli*, several elongasome, divisome and hydrolytic enzymes, including PBP1A, are loosely associated with the OM lipoprotein, NlpI[229]. NlpI is thought to act as a scaffold for hydrolase and synthase complexes[229] and is important for regulating proteolysis of the hydrolytic endopeptidase, MepS[253]. NlpI phenotypes in *E. coli* have striking similarities to PBP1A phenotypes in *A. baumannii*, where deletion leads to filamentation and over expression produces rounded, ovoid cells[254]. While *A. baumannii* does not encode an NlpI homolog, the phenotypic similarities are intriguing and suggest PBP1A may have an additional, indirect role in localization or regulation of hydrolase activity. Consistent with this hypothesis, Δ*mrcA* forms multiple division sites, but is slow to septate.

## MATERIALS AND METHODS

### Bacterial Strains and Growth

All *A. baumannii* strains were grown from freezer stocks initially on Luria-Bertani (LB) agar at 37° C. For selection, 25 μg/ml of kanamycin was used when appropriate. Strains that harbored the pMMB plasmid for coIP, complementation or over expression were supplemented with 25 μg/ml of kanamycin and 2 mM isopropylthio-β-galactoside (IPTG).

### Fluorescent NADA staining

Overnight cultures were back-diluted to $OD_{600}$ of 0.05 and grown at 37°C in LB media until they reached stationary or mid-logarithmic growth phase. Cells were washed once with Luria broth and resuspended in 1 ml Luria broth. 3 µl of 10 mM of NBD-(linezolid-7-nitrobenz-2-oxa-1,3-diazol-4-yl)-amino-D-alanine (NADA) (ThermoFisher) was added to the resuspension. Cells were incubated with NADA at 37°C for 30 minutes. Following incubation, cells were washed once and fixed with 1x phosphate buffered saline containing a (1:10) solution of 16% paraformaldehyde.

**Microscopy**

Fixed cells were immobilized on agarose pads and imaged using an inverted Nikon Eclipse Ti-2 widefield epifluorescence microscope equipped with a Photometrics Prime 95B camera and a Plan Apo 100 m X 1.45 numerical aperture lens objective. Green fluorescence and red fluorescence images were taken using a filter cube with a 470/40 nm or 560/40 nm excitation filters and 632/60 or 535/50 emission filters, respectively. Images were captured using NIS Elements software.

**Image analysis**

All images were processed and pseudo-colored with ImageJ FIJI (63) and MicrobeJ plugin was used for quantifications of pole-to-pole lengths (64). For pole-to-septa length quantifications, a segmentation code written for Image J was used (see Apendix 1). Cell length, width and fluorescence data were plotted in Prism 9 (GraphPad 9.3.1). 100 cells were analyzed for pole-to-septa lengths and 300 cells were analyzed for all other experiments. Each experiment was independently replicated three times, and each replication was used in the dataset. One representative image from the datasets were included in the figure.

**Growth curves**

Growth curves were performed as previously described (65). Briefly, overnight cultures were back diluted to $OD_{600}$ of 0.01 and set up as triplicate biological replicas in either a 96-well plate or 24-well plate (BrandTech BRAND). A BioTek SynergyNeo$^2$ microplate reader was used to record optical density, which was read at $OD_{600}$ every hour. The microplate reader was set to 37°C with continuous shaking. Growth curves were plotted in Prism 9. Each growth curve experiment was independently replicated three times and one representative dataset was reported.

**Western blotting**

Western blot analysis was carried out via gel transfer to PVDF (Thermo Fisher Scientific). All blots were blocked in 5% milk for 2 h. The primary antibodies α-PBP1A, α-PBP3, α-PBP2, and α-RpoA were used at 1:1000, 1:500, 1:300, and 1:1000, respectively followed by α-rabbit-HRP secondary antibody at 1:10,000 (Thermo Fisher Scientific). Supersignal West Pico PLUS (Thermo Fisher Scientific) was used to measure relative protein concentrations.

**Co-immunoprecipitation**

Protocol was adapted from previous work by our laboratory[201]. Cultures were initially grown on LB agar with overnight at 37° C. A single colony was used to inoculate 5 ml LB broth and grown overnight at 37° C. The overnight broth was diluted back to $OD_{600}$ of 0.05 and grown to midlog at 37° C in 50 ml LB broth. Culture was collected, washed with 1x PBS and incubated with 25 mM DSP (Thermofisher) in a total volume of 1 ml PBS for one hour with shaking at 37° C. Reaction quenched with room temperature incubation of 400 µl 1 M glycine with rocking for 15 minutes. Cells were lysed and solubilized overnight at 4° C with rocking. Lysates supernatant was centrifuged twice at 10,000 X g for 20 minutes and the pellet was discarded. 30 µl of ANTI-FLAG® M2 Affinity Resin (Sigma) was added to the supernatant and incubated overnight at 4° C with rocking. Resin was harvested at 6,000 x G and washed 4 times with RIPA buffer. Pellet

resuspended in 100 µl 1x SDS-Page loading buffer with 5% BME. Samples boiled for 7 minutes and used for western blotting.

# CHAPTER 6: CONCLUSIONS

## Overview

The principal objective of this work was to determine the mechanistic basis for envelope remodeling in response to severe OM defects originating from polymyxin insults and depletion of lipid A. Despite the lipid A domain of LOS being an important target for some antibiotics[115,119] and those still in the development pipeline[96], the physiological requirements to support lipid A-deficient ($LOS^-$) viability remain poorly understood. Thus, a better understanding of OM stress-induced envelope remodeling, including the depletion of lipid A in the outer leaflet, would provide greater insights into combating resistance to LOS-targeting antimicrobials and better define the minimum envelope requirements for viability in Gram-negative bacteria.

## Uncoupled regulation of lipid A modification promotes colistin-heteroresistance in *E. cloacae*

Colistin-heteroresistance was observed in *E. cloacae* clinical specimens, raising concerns over resistance detection failure during routine ASTs. Prior to our work, there was no detailed understanding of the molecular mechanisms behind this observation. In some γ-proteobacteria, the PhoPQ and PmrAB TCSs work synergistically to detect lipid A perturbation by polymyxins and activate *arn* operon transcription which upregulates the biosynthesis and conjugation of charge-neutralizing L-Ara4N to lipid A. Here, we showed *E. cloacae* PhoP binds directly to *ParnB* with high specificity. Thus, PhoPQ is necessary and sufficient to detect periplasmic stress and activate

the transcription of the *arn* operon to modify lipid A. In uncoupling the regulatory TCSs, PhoPQ and PmrAB, *E. cloacae* is primed for colistin-heteroresistance. Importantly, our findings uncovered the previously unknown mechanism underlying the emergence of colistin-resistant subpopulations in colistin-sensitive *E. cloacae*. Furthermore, our data suggest *E. cloacae* infections are poor candidates for colistin monotherapy.

## Defining the minimum envelope requirements to support LOS$^-$ viability

Colistin resistance research to date has tended to focus on lipid A remodeling rather than lipid A depletion. One hurdle for studying fitness requirements in LOS$^-$ Gram-negative bacteria is the challenge of finding a viable, LOS$^-$ model organism. While two LOS-depleted strains have been bioengineered under laboratory conditions[90,92], *A. baumannii* is the first bacteria to arrest lipid A biosynthesis as a drug-resistance mechanism[91,93], positioning it as an ideal model to study envelope remodeling under the extreme biophysical stress of LOS deficiency.

The search for LOS$^-$ fitness requirements in *A. baumannii* revealed two previously unstudied Ldts, LdtJ and LdtK. Characterizing LdtJ provided insights into how the cell must remodel PG to meet the increased mechanical stability demands during LOS deficiency. In Gram-negative bacteria, both lipid A in the OM and the single-layered PG contribute equally to resistance of turgor forces[106]; thus, in the absence of lipid A, PG alone would bear the entire mechanical stress of the cell. PG is an antistrophic material that consists of rigid glycan chains along the cell circumference and elastic peptide stems on the long axis[204,255]. Considering the glycan polymers are already rigid, additional stiffness would need to be contributed via peptide stem reconfiguration. Here, we showed LdtJ catalyzes alternative, 3-3 crosslinking between PG peptide stems, which produces PG mesh with a smaller pore diameter than the standard, 4-3 crosslinks catalyzed by

PBPs. We hypothesize that tighter crosslinking by LdtJ increases PG stiffness and compensates for the loss of rigidity previously provided by lipid A.

Additionally, we identified LdtJ-dependent NCDAA incorporation in PG peptide stems. Incorporation of NCDAAs plateaus the growth of logarithmically dividing bacteria[71]. LOS$^-$ cells may depend on slow biogenesis of nascent PG so synthesis and hydrolysis do not outpace protective remodeling. Another intriguing possibility involves the role of NCDAAs in resistance to osmotic stress[71]. This role is likely conserved in *A. baumannii* as our data shows Δ*ldtJ* is sensitive to hypoosmotic stress. In line with this, we found LOS$^-$ *A. baumannii* are highly sensitive to osmotic fluctuations, likely due to increased OM permeability and reduced cellular stiffness. Interestingly, MS/MS analysis of LOS$^-$ PG suggests it contains D-amino acid modifications in log phase, unlike wild type. We hypothesize NCDAA incorporation is required for PG to withstand turgor and osmotic forces in lipid A-depleted cells. Supporting this hypothesis, our lab previously found PNAG exopolysaccharides are upregulated in LOS$^-$ *A. baumannii*[17]. While there is no literature directly correlating PNAG with osmoprotection, it does have significant hydroscopic properties[256]. Therefore, it is not unreasonable to hypothesize PNAG functions as an additional, external buffer against hypo/hyperosmotic stress in LOS$^-$ cells.

Characterization of the second Ldt identified, LdtK, demonstrated the importance of PG recycling and envelope stability in LOS$^-$ cells. Despite homology predictions positioning LdtK as a PG lipoprotein crosslinker, our localization studies revealed LdtK is the first known cytoplasmic Ldt[60]. Further investigation characterized LdtK as an LD-carboxypeptidase involved in the early phases of PG recycling[60]. Amidation of PG fragments catalyzed by LdtK produces anhydro Mur*N*ac-tripeptides[60]. Subsequent PG recycling enzymes have high specificity for tripeptides and therefore productive PG recycling is dependent on LdtK activity.

Interestingly, we observed severe hypervesiculation in Δ*ldtK*. This phenotype is characteristic of *E. coli* Δ*lpp*, wherein the OM and PG are no longer covalently linked via Lpp lipoprotein attachment catalyzed by *E. coli* Ldts homologous to LdtK. Lpp contains a C-terminal arg-lys residue that is crosslinked to PG, whereas putative lipoproteins in *A. baumannii* contain a C-terminal lys-lys residue. Intriguingly, our MS/MS analysis of the Δ*ldtK* PG proteome revealed depletion of lys-lys residues compared to wild type. While it is possible LdtK catalyzes cytoplasmic lipoprotein attachment to nascent PG through a yet-unknown mechanism, Δ*ldtK* hypervesiculation is likely a secondary stress response to the accumulation of toxic Mur*N*Ac-tetrapeptides in the cytoplasm. These data suggest LdtK-mediated PG recycling is critical for envelope stability in wild type and becomes necessary for viability in lipid A-depleted cells.

In characterizing the activities of two putative Ldts essential for LOS$^-$ viability, we gained greater insight into necessary envelope remodeling and maintenance requirements in lipid A-depleted cells. These data point to a role for Ldts in promoting envelope stability and structural support required for LOS$^-$ survival. This work highlights the importance of increased cellular rigidity, protection against osmotic fluctuations and productive PG recycling in maintaining the stability of the LOS$^-$ envelope. Lastly, we identified a previously unrecognized role for Ldts in early-phase PG recycling.

## PBP1A is the major aPBP synthase in *A. baumannii* and contributes to both division and fitness

Gram-negative bifunctional aPBPs, PBP1A and PBP1B, are best understood in *E. coli* and are largely considered semi-redundant for cell wall biogenesis in this model organism[22]. Here, PBP1A is considered an elongasome synthase based on protein-protein interactions with PBP2[42]

and PBP1B is thought to be involved in division due to associations with PBP3[39]. However, we show the roles of PBP1A and PBP1B differ significantly in *A. baumannii* and are not obviously functionally redundant. We demonstrated Δ*mrcA* but not Δ*mrcB* promotes significant resistances to different classes of medically important antimicrobials[73], which has concerning implications for *A. baumannii* clinical isolates that do not transcribe PBP1A. Additionally, we found PBP1A but not PBP1B activity important for division and fitness in *A. baumannii*.

Unexpectedly, we observed that Δ*mrcA* chained into filaments[73], a phenotype indicative of defective or slowed division. Using a fluorescent protein fusion, we demonstrated PBP1A concentrates at the septum in dividing cells. In contrast to literature precedent[33,42], we identified direct protein-protein interactions between PBP1A and PBP3 at the divisome. Intriguingly, over expression of PBP3 in Δ*mrcA* rescued division, but not growth defects. We also demonstrated PBP1A localizes diffusely along the lateral cell wall. This lateral localization suggests PBP1A may contribute to both elongation and division in *A. baumannii*. However, we were unable to confirm direct interactions between PBP1A and PBP2. Together, these data strongly suggest PBP1A is necessary for productive septation but has a different role than PBP3 in the divisome. Importantly, such significant contributions to fitness and division by PBP1A have not been documented before in other Gram-negative bacteria.

Our study[73] and others[61] found over expression of PBP1A in wild type *A. baumannii* promotes cellular rounding. The study hypothesized that PBP1A directly interferes with elongasome activity[61]. It was further posited but not experimentally shown that PBP1A toxicity in $LOS^-$ cells is a direct result of elongasome interference[61]. However, we did not find direct interaction between PBP1A and PBP2 in the elongasome. While we acknowledge the possibility that PBP1A may indirectly inhibit the elongasome complex, it is unlikely that native levels of

PBP1A are sufficient to wholly attenuate elongasome activity and lead to LOS$^-$ lethality. Intriguingly, preliminary data suggests PBP1A over expression in LOS$^-$ cells promotes significant elongation within one cell cycle prior to lysis, suggesting PBP1A activity may instead lead to LOS$^-$ death via other mechanisms. Together, our data do not support a model for PBP1A as an elongasome antagonist in wild type cells.

# FUTURE DIRECTIONS

Our work found PBP1A over expression in LOS$^-$ cells promotes rapid elongation prior to lysis, suggesting PBP1A polymerizes PG at a rate that outpaces envelope reinforcement in LOS$^-$ bacteria. One intriguing PG fortification mechanism is a recently described repair complex found to form between PBP1B and an Ldt providing alternative crosslinks[20], like LdtJ. MS/MS analysis of Δ*pbp1A* PG showed increased 3-3 crosslinking, suggesting a PBP1B-LdtJ repair complex may be more likely to form in the absence of PBP1A. To investigate this hypothesis, we performed a co-immunoprecipitation assay. However, under standard laboratory conditions in wild type and Δ*pbp1A*, we were not able to confirm the formation of a PG repair complex between PBP1B and LdtJ. However, future work in Δ*lpxC*, a strain with defective lipid A transport, may be more tractable for co-immunoprecipitation studies looking to identify PG repair complexes.

Considering the PBP1B-Ldt complex previously identified in *E. coli* depends on PBP1B GTase activity and disruption of the PBP1A GTase domain is sufficient for toxicity attenuation in LOS$^-$ *A. baumannii*, it is tempting to speculate that PBP1A and PBP1B GTase domains may directly compete for the same PG precursor substrate, lipid II. Thus, further contributing to the incompatibility between PBP1A activity and LOS$^-$ viability. Additional studies are needed to

determine if lipid II is the rate-limiting step in PG repair necessary for Gram-negative survival without LOS.

Likewise, dependence on freely available lipid II may contribute to LdtK essentiality in LOS$^-$ cells. Preliminary data suggests disruption to early phase PG recycling is deleterious in LOS$^-$ *A. baumannii*. However, it is still unknown if later stage recycling enzymes are required for LOS$^-$ viability. If late-stage PG recycling abrogation does not cause hypervesiculation yet remains deleterious in LOS$^-$ cells, it suggests that OM sloughing is not the primary cause of death, and that lipid II availability is the rate-limiting step for LOS$^-$ survival.

Another unresolved question is whether the Δ*ldtK* hypervesiculation phenotype is needed to eliminate toxic tetrapeptide build-up or if it is a way to remove nonspecific solutes and restore the isotonic balance during the build-up of PG precursors. Mass spectrometry analysis of filtered OMV contents would provide insight into their function. Additionally, it would be interesting to determine if Δ*ldtK* cells remain viable over several passages. In *E. coli*, deletion of the LD-carboxypeptidase involved in PG recycling, LdcA, is immediately deleterious in stationary phase[257] whereas *A. baumannii* likely compensates for LdtK deletion via hypervesiculation. If the OMVs of Δ*ldtK* contain only solutes and not anhydro Mur*N*ac-tetrapeptide fragments, the unresolved PG precursor build-up would likely become lethal during serial passage of Δ*ldtK*.

Lastly, our heteroresistance study[166] provided a detailed understanding of the colistin-heteroresistance mechanism in *E. cloacae.* Concerningly, heteroresistant subpopulations may fall under the detection limit of standard clinical ASTs at approximately 1e-7[13,135,188,258]. Undetected heteroresistance is hypothesized to lead to treatment failure in humans[135,258] and has been shown to facilitate colistin therapeutic failure in a mouse model[188]. Together, these data suggest *E. cloacae* infections are poor candidates for colistin monotherapies and highlights an unmet clinical

need uncover colistin synergistic therapeutics. However, colistin increases cellular permeability[259], suggesting it may facilitate the passage of hydrophobic or high molecular weight drugs including rifampicin into the cell. Rifampicin is hydrophobic drug that inhibits DNA-dependent RNA synthesis and is used to treat *Mycobacterium* and other Gram-positive infections[260,261]. Although Gram-negative bacteria are intrinsically resistant to rifampicin, recent studies have shown it is effective against Gram-negative bacteria if co-administered with a sensitizer[262,263]. Several studies, including a randomized control trial[264], in Gram-negative ESKAPE pathogens demonstrated synergy between colistin and rifampicin, using Etest strips and antibiotic enriched agar plates[264–266]. The observed synergy between colistin and rifampicin suggests colistin may synergize with other traditionally narrow-spectrum antibiotics that are unable to breach the OM to potentiate killing. As demonstrated by previous studies[264–266], combining antibiotic enriched agar with Estrips is one method to screen for potential synergistic therapeutic combinations. However, Estrips may fail to detect heteroresistance[135]. We propose that combining PAP, the gold standard AST for detecting heteroresistance, with high throughput screens of colistin combination therapies in 96-well microtiter plates, would identify synergistic drug combinations that are effective against colistin-heteroresistant strains. Moreover, screening currently approved drugs would allow for immediate implementation of successful combinatorial therapies.

# APPENDIX

## Appendix 1
### Segmentation Quantification Code

```
macro "Measure Segmented Distances [1]" {
   if (!(selectionType==6||selectionType==10))
      exit("Segmented line or point selection required");
   getSelectionCoordinates(x, y);
   if (x.length<2)
      exit("At least two points required");
   getPixelSize(unit, pw, ph);
   n = nResults;
   distance = 0;
   for (i=1; i<x.length; i++) {
     dx = (x[i] - x[i-1])*pw;
     dy = (y[i] - y[i-1])*ph;
     distance = sqrt(dx*dx + dy*dy);
     setResult("D"+i, n, distance);
   }
   updateResults;
}
```

# REFERENCES


1. Sikora, A. & Zahra, F. Nosocomial Infections. in *StatPearls Continuing Education Activity* (StatPearls Publishing, 2021).

2. Storr, J. *et al.* Core components for effective infection prevention and control programmes: new WHO evidence-based recommendations. *Antimicrob Resist In* 6, 6 (2017).

3. Collaborators, A. R. *et al.* Global burden of bacterial antimicrobial resistance in 2019: a systematic analysis. *Lancet Lond Engl* 399, 629–655 (2022).

4. *ANTIBIOTIC RESISTANCE THREATS in the United States, 2013*. https://www.cdc.gov/drugresistance/pdf/ar-threats-2013-508.pdf (2013).

5. *Antibiotic resistance threats in the United States, 2019.* https://www.cdc.gov/drugresistance/pdf/threats-report/2019-ar-threats-report-508.pdf (2019).

6. Roberts, R. R. *et al.* Hospital and Societal Costs of Antimicrobial-Resistant Infections in a Chicago Teaching Hospital: Implications for Antibiotic Stewardship. *Clin Infect Dis* 49, 1175–1184 (2009).

7. Schmid, A. *et al.* Monotherapy versus combination therapy for multidrug-resistant Gram-negative infections: Systematic Review and Meta-Analysis. *Sci Rep-uk* 9, 15290 (2019).

8. Sheu, C.-C., Chang, Y.-T., Lin, S.-Y., Chen, Y.-H. & Hsueh, P.-R. Infections Caused by Carbapenem-Resistant *Enterobacteriaceae*: An Update on Therapeutic Options. *Front Microbiol* 10, 80 (2019).

9. Richards, S. M., Strandberg, K. L., Conroy, M. & Gunn, J. S. Cationic antimicrobial peptides serve as activation signals for the *Salmonella Typhimurium* PhoPQ and PmrAB regulons in vitro and in vivo. *Front Cell Infect Mi* 2, 102 (2012).

10. Lee, J.-Y. & Ko, K. S. Mutations and expression of PmrAB and PhoPQ related with colistin resistance in *Pseudomonas aeruginosa* clinical isolates. *Diagn Micr Infec Dis* 78, 271–276 (2014).

11. Prost, L. R. & Miller, S. I. The Salmonellae PhoQ sensor: mechanisms of detection of phagosome signals. *Cell Microbiol* 10, 576–582 (2008).

12. Napier, B. A., Band, V., Burd, E. M. & Weiss, D. S. Colistin Heteroresistance in *Enterobacter cloacae* Is Associated with Cross-Resistance to the Host Antimicrobial Lysozyme. *Antimicrob Agents Ch* 58, 5594–5597 (2014).

13. Band, V. I. *et al.* Colistin Heteroresistance Is Largely Undetected among Carbapenem-Resistant Enterobacterales in the United States. *Mbio* 12, e02881-20 (2021).

14. Fusco, D. N. *et al.* Clinical failure of vancomycin in a dialysis patient with methicillin-susceptible vancomycin-heteroresistant *S. aureus*. *Diagn Micr Infec Dis* 65, 180–3 (2009).

15. Band, V. I. *et al.* Carbapenem-Resistant *Klebsiella pneumoniae* Exhibiting Clinically Undetected Colistin Heteroresistance Leads to Treatment Failure in a Murine Model of Infection. *Mbio* 9, e02448-17 (2018).

16. Needham, B. D. & Trent, M. S. Fortifying the barrier: the impact of lipid A remodelling on bacterial pathogenesis. *Nat Rev Microbiol* 11, 467–481 (2013).

17. Boll, J. M. *et al.* A penicillin-binding protein inhibits selection of colistin-resistant, lipooligosaccharide-deficient *Acinetobacter baumannii*. *Proc National Acad Sci* 113, E6228–E6237 (2016).

18. Aliashkevich, A. & Cava, F. LD-transpeptidases: the great unknown among the peptidoglycan cross-linkers. *Febs J* (2021) doi:10.1111/febs.16066.

19. Stankeviciute, G. *et al.* Differential modes of crosslinking establish spatially distinct regions of peptidoglycan in *Caulobacter crescentus. Mol Microbiol* 111, 995–1008 (2019).

20. Morè, N. *et al.* Peptidoglycan Remodeling Enables Escherichia coli To Survive Severe Outer Membrane Assembly Defect. *Mbio* 10, e02729-18 (2019).

21. Silva, A. M. *et al.* The Fluorescent D-Amino Acid NADA as a Tool to Study the Conditional Activity of Transpeptidases in *Escherichia coli*. *Front Microbiol* 09, 2101 (2018).

22. Yousif, S. Y., Broome-Smith, J. K. & Spratt, B. G. Lysis of *Escherichia coli* by beta-lactam antibiotics: deletion analysis of the role of penicillin-binding proteins 1A and 1B. *J Gen Microbiol* 131, 2839–45 (1985).

23. Magiorakos, A. -P. *et al.* Multidrug-resistant, extensively drug-resistant, and pandrug-resistant bacteria: an international expert proposal for interim standard definitions for acquired resistance. *Clin Microbiol Infec* 18, 268–281 (2012).

24. Hawkey, P. M. *et al.* Treatment of infections caused by multidrug-resistant Gram-negative bacteria: report of the British Society for Antimicrobial Chemotherapy/Healthcare Infection Society/British Infection Association Joint Working Party. *J Antimicrob Chemother* 73, iii2–iii78 (2018).

25. Nikaido, H. Molecular Basis of Bacterial Outer Membrane Permeability Revisited. *Microbiol Mol Biol R* 67, 593–656 (2003).

26. Tacconelli, E. *et al. GLOBAL PRIORITY LIST OF ANTIBIOTIC-RESISTANT BACTERIA TO GUIDE RESEARCH, DISCOVERY, AND DEVELOPMENT OF NEW ANTIBIOTICS.* https://www.who.int/medicines/publications/WHO-PPL-Short_Summary_25Feb-ET_NM_WHO.pdf (2017).

27. Organization, W. H. *Guidelines for the Prevention and Control of Carbapenem-Resistant Enterobacteriaceae, Acinetobacter baumannii and Pseudomonas aeruginosa in Health Care Facilities*. (2017).

28. Spellberg, B., Powers, J. H., Brass, E. P., Miller, L. G. & Edwards, J. E. Trends in Antimicrobial Drug Development: Implications for the Future. *Clin Infect Dis* 38, 1279–1286 (2004).

29. Bouhss, A., Trunkfield, A. E., Bugg, T. D. H. & Mengin-Lecreulx, D. The biosynthesis of peptidoglycan lipid-linked intermediates. *Fems Microbiol Rev* 32, 208–233 (2008).

30. Sham, L.-T. *et al.* MurJ is the flippase of lipid-linked precursors for peptidoglycan biogenesis. *Science* 345, 220–222 (2014).

31. Straume, D. *et al.* Class A PBPs have a distinct and unique role in the construction of the pneumococcal cell wall. *P Natl Acad Sci Usa* 117, 6129–6138 (2020).

32. Born, P., Breukink, E. & Vollmer, W. In Vitro Synthesis of Cross-linked Murein and Its Attachment to Sacculi by PBP1A from *Escherichia coli*. *J Biol Chem* 281, 26985–26993 (2006).

33. Typas, A., Banzhaf, M., Gross, C. A. & Vollmer, W. From the regulation of peptidoglycan synthesis to bacterial growth and morphology. *Nat Rev Microbiol* 10, 123–136 (2012).

34. Egan, A. J. F., Errington, J. & Vollmer, W. Regulation of peptidoglycan synthesis and remodelling. *Nat Rev Microbiol* 18, 446–460 (2020).

35. Gray, A. N. *et al.* Coordination of peptidoglycan synthesis and outer membrane constriction during *Escherichia coli* cell division. *Elife* 4, e07118 (2015).

36. Meeske, A. J. *et al.* SEDS proteins are a widespread family of bacterial cell wall polymerases. *Nature* 537, 634–638 (2016).

37. Typas, A. & Sourjik, V. Bacterial protein networks: properties and functions. *Nat Rev Microbiol* 13, 559–572 (2015).

38. Vollmer, W. & Bertsche, U. Murein (peptidoglycan) structure, architecture and biosynthesis in *Escherichia coli*. *Biochimica Et Biophysica Acta Bba - Biomembr* 1778, 1714–1734 (2008).

39. Bertsche, U., Breukink, E., Kast, T. & Vollmer, W. In Vitro Murein (Peptidoglycan) Synthesis by Dimers of the Bifunctional Transglycosylase-Transpeptidase PBP1B from *Escherichia coli. J Biol Chem* 280, 38096–38101 (2005).

40. Rohs, P. D. A. *et al.* A central role for PBP2 in the activation of peptidoglycan polymerization by the bacterial cell elongation machinery. *Plos Genet* 14, e1007726 (2018).

41. Cho, H. *et al.* Bacterial cell wall biogenesis is mediated by SEDS and PBP polymerase families functioning semi-autonomously. *Nat Microbiol* 1, 16172–16172 (2016).

42. Banzhaf, M. *et al.* Cooperativity of peptidoglycan synthases active in bacterial cell elongation. *Mol Microbiol* 85, 179–194 (2012).

43. Müller, P. *et al.* The Essential Cell Division Protein FtsN Interacts with the Murein (Peptidoglycan) Synthase PBP1B in *Escherichia coli. J Biol Chem* 282, 36394–36402 (2007).

44. Bertsche, U. *et al.* Interaction between two murein (peptidoglycan) synthases, PBP3 and PBP1B, in *Escherichia coli*. *Mol Microbiol* 61, 675–690 (2006).

45. Ranjit, D. K., Jorgenson, M. A. & Young, K. D. PBP1B Glycosyltransferase and Transpeptidase Activities Play Different Essential Roles during the De Novo Regeneration of Rod Morphology in E*scherichia coli. J Bacteriol* 199, (2017).

46. Mueller, E. A., Egan, A. J., Breukink, E., Vollmer, W. & Levin, P. A. Plasticity of *Escherichia coli* cell wall metabolism promotes fitness and antibiotic resistance across environmental conditions. *Elife* 8, e40754 (2019).

47. Vigouroux, A. *et al.* Class-A penicillin binding proteins do not contribute to cell shape but repair cell-wall defects. *Elife* 9, e51998 (2020).

48. Hugonnet, J.-E. *et al.* Factors essential for L,D-transpeptidase-mediated peptidoglycan cross-linking and β-lactam resistance in *Escherichia coli. Elife* 5, e19469 (2016).

49. Jorgenson, M. A. *et al.* Simultaneously inhibiting undecaprenyl phosphate production and peptidoglycan synthases promotes rapid lysis in *Escherichia coli. Mol Microbiol* 112, 233–248 (2019).

50. Auer, G. K. *et al.* Mechanical Genomics Identifies Diverse Modulators of Bacterial Cell Stiffness. *Cell Syst* 2, 402–411 (2016).

51. Kodama, T. *et al.* Synthesis and Characterization of the Spore Proteins of *Bacillus subtilis* YdhD, YkuD, and YkvP, Which Carry a Motif Conserved among Cell Wall Binding Proteins. *J Biochem* 128, 655–663 (2000).

52. Biarrotte-Sorin, S. *et al.* Crystal Structure of a Novel β-Lactam-insensitive Peptidoglycan Transpeptidase. *J Mol Biol* 359, 533–538 (2006).

53. Lavollay, M. *et al.* The Peptidoglycan of Stationary-Phase *Mycobacterium tuberculosis* Predominantly Contains Cross-Links Generated by l,d -Transpeptidation. *J Bacteriol* 190, 4360–4366 (2008).

54. Winkle, M. *et al.* DpaA detaches Braun's lipoprotein from peptidoglycan. doi:10.1101/2021.02.21.432140.

55. Cameron, T. A., Anderson-Furgeson, J., Zupan, J. R., Zik, J. J. & Zambryski, P. C. Peptidoglycan Synthesis Machinery in *Agrobacterium tumefaciens* During Unipolar Growth and Cell Division. *Mbio* 5, e01219-14 (2014).

56. Asmar, A. T. & Collet, J.-F. Lpp, the Braun lipoprotein, turns 50—major achievements and remaining issues. *Fems Microbiol Lett* 365, (2018).

57. Sandoz, K. M. *et al.* β-Barrel proteins tether the outer membrane in many Gram-negative bacteria. *Nat Microbiol* 1–8 (2020) doi:10.1038/s41564-020-00798-4.

58. Godessart, P. *et al.* β-Barrels covalently link peptidoglycan and the outer membrane in the α-proteobacterium *Brucella abortus*. *Nat Microbiol* 1–7 (2020) doi:10.1038/s41564-020-00799-3.

59. Dai, Y., Pinedo, V., Tang, A. Y., Cava, F. & Geisinger, E. A New Class of Cell Wall-Recycling l,d-Carboxypeptidase Determines β-Lactam Susceptibility and Morphogenesis in *Acinetobacter baumannii*. *Mbio* 12, e0278621 (2021).

60. Islam, N. *et al.* Peptidoglycan recycling contributes to outer membrane integrity and carbapenem tolerance in *Acinetobacter baumannii*. *Biorxiv* 2021.11.23.469614 (2021) doi:10.1101/2021.11.23.469614.

61. Simpson, B. W. *et al. Acinetobacter baumannii* Can Survive with an Outer Membrane Lacking Lipooligosaccharide Due to Structural Support from Elongasome Peptidoglycan Synthesis. *Mbio* 12, e0309921 (2021).

62. Cava, F., Pedro, M. A. de, Lam, H., Davis, B. M. & Waldor, M. K. Distinct pathways for modification of the bacterial cell wall by non-canonical D-amino acids. *Embo J* 30, 3442–3453 (2011).

63. Dramsi, S., Magnet, S., Davison, S. & Arthur, M. Covalent attachment of proteins to peptidoglycan. *Fems Microbiol Rev* 32, 307–320 (2008).

64. Magnet, S. *et al.* Identification of the l , d -Transpeptidases Responsible for Attachment of the Braun Lipoprotein to *Escherichia coli* Peptidoglycan. *J Bacteriol* 189, 3927–3931 (2007).

65. Egan, A. J. F. Bacterial outer membrane constriction: Outer membrane constriction. *Mol Microbiol* 107, 676–687 (2018).

66. Winkle, M. *et al.* DpaA Detaches Braun's Lipoprotein from Peptidoglycan. *Mbio* 12, e00836-21 (2021).

67. Magnet, S., Dubost, L., Marie, A., Arthur, M. & Gutmann, L. Identification of the L,D-transpeptidases for peptidoglycan cross-linking in *Escherichia coli*. *J Bacteriol* 190, 4782–5 (2008).

68. Baranowski, C. *et al.* Maturing *Mycobacterium smegmatis* peptidoglycan requires non-canonical crosslinks to maintain shape. *Elife* 7, e37516 (2018).

69. Le, N.-H. *et al.* Peptidoglycan editing provides immunity to *Acinetobacter baumannii* during bacterial warfare. *Sci Adv* 6, eabb5614 (2020).

70. Pagliai, F. A. *et al.* The Transcriptional Activator LdtR from '*Candidatus Liberibacter asiaticus'* Mediates Osmotic Stress Tolerance. *Plos Pathog* 10, e1004101 (2014).

71. Lam, H. *et al.* D-Amino Acids Govern Stationary Phase Cell Wall Remodeling in Bacteria. *Science* 325, 1552–1555 (2009).

72. Alvarez, L., Aliashkevich, A., Pedro, M. A. de & Cava, F. Bacterial secretion of D-arginine controls environmental microbial biodiversity. *Isme J* 12, 438–450 (2018).

73. Kang, K. N. *et al.* Septal Class A Penicillin-Binding Protein Activity and ld -Transpeptidases Mediate Selection of Colistin-Resistant Lipooligosaccharide-Deficient *Acinetobacter baumannii. Mbio* 12, (2021).

74. Toth, M., Lee, M., Stewart, N. K. & Vakulenko, S. B. Effects of Inactivation of d,d-Transpeptidases of *Acinetobacter baumannii* on Bacterial Growth and Susceptibility to β-Lactam Antibiotics. *Antimicrob Agents Ch* 66, e0172921 (2021).

75. Paradis-Bleau, C. *et al.* Lipoprotein cofactors located in the outer membrane activate bacterial cell wall polymerases. *Cell* 143, 1110–20 (2010).

76. Greene, N. G., Fumeaux, C. & Bernhardt, T. G. Conserved mechanism of cell-wall synthase regulation revealed by the identification of a new PBP activator in *Pseudomonas aeruginosa*. *P Natl Acad Sci Usa* 115, 3150–3155 (2018).

77. Lenz, J. D. *et al.* Amidase Activity of AmiC Controls Cell Separation and Stem Peptide Release and Is Enhanced by NlpD in *Neisseria gonorrhoeae*. *J Biol Chem* 291, 10916–10933 (2016).

78. Uehara, T., Dinh, T. & Bernhardt, T. G. LytM-Domain Factors Are Required for Daughter Cell Separation and Rapid Ampicillin-Induced Lysis in *Escherichia coli. J Bacteriol* 191, 5094–5107 (2009).

79. Leeuw, E. D. *et al.* Molecular characterization of *Escherichia coli* FtsE and FtsX. *Mol Microbiol* 31, 983–993 (1999).

80. Pichoff, S., Du, S. & Lutkenhaus, J. Roles of FtsEX in cell division. *Res Microbiol* 170, 374–380 (2019).

81. Satta, G. *et al.* Target for bacteriostatic and bactericidal activities of beta-lactam antibiotics against *Escherichia coli* resides in different penicillin-binding proteins. *Antimicrob Agents Ch* 39, 812–818 (1995).

82. Cross, T. *et al.* Spheroplast-Mediated Carbapenem Tolerance in Gram-Negative Pathogens. *Antimicrob Agents Ch* 63, (2019).

83. Diedrich, D. L. & Cota-Robles, E. H. Heterogeneity in Lipid Composition of the Outer Membrane and Cytoplasmic Membrane of *Pseudomonas* BAL-31. *J Bacteriol* 119, 1006–1018 (1974).

84. Raetz, C. R. H. Biochemistry of Endotoxins. *Annu Rev Biochem* 59, 129–170 (1990).

85. Raetz, C. R. H. & Whitfield, C. LIPOPOLYSACCHARIDE ENDOTOXINS. *Biochemistry-us* 71, 635–700 (2002).

86. Schneider, H. *et al.* Heterogeneity of molecular size and antigenic expression within lipooligosaccharides of individual strains of *Neisseria gonorrhoeae* and *Neisseria meningitidis*. *Infect Immun* 45, 544–549 (1984).

87. Preston, A., Mandrell, R. E., Gibson, B. W. & Apicella, M. A. The Lipooligosaccharides of Pathogenic Gram-Negative Bacteria. *Crit Rev Microbiol* 22, 139–180 (2008).

88. Bertani, B. & Ruiz, N. Function and Biogenesis of Lipopolysaccharides. *Ecosal Plus* 8, (2018).

89. Whitfield, C. & Trent, M. S. Biosynthesis and Export of Bacterial Lipopolysaccharides*. *Annu Rev Biochem* 83, 99–128 (2014).

90. Steeghs, L. *et al. Meningitis* bacterium is viable without endotoxin. *Nature* 392, 449–449 (1998).

91. Moffatt, J. H. *et al.* Colistin resistance in *Acinetobacter baumannii* is mediated by complete loss of lipopolysaccharide production. *Antimicrob Agents Ch* 54, 4971–7 (2010).

92. Peng, D., Hong, W., Choudhury, B. P., Carlson, R. W. & Gu, X.-X. *Moraxella catarrhalis* Bacterium without Endotoxin, a Potential Vaccine Candidate. *Infect Immun* 73, 7569–7577 (2005).

93. Moffatt, J. H. *et al.* Insertion sequence ISAba11 is involved in colistin resistance and loss of lipopolysaccharide in *Acinetobacter baumannii*. *Antimicrob Agents Ch* 55, 3022–4 (2011).

94. Baba, T. *et al.* Construction of *Escherichia coli* K-12 in-frame, single-gene knockout mutants: the Keio collection. *Mol Syst Biol* 2, 2006.0008-2006.0008 (2006).

95. Young, K. *et al.* The envA Permeability/Cell Division Gene of *Escherichia coli* Encodes the Second Enzyme of Lipid A Biosynthesis. *J Biol Chem* 270, 30384–30391 (1995).

96. Kalinin, D. V. & Holl, R. LpxC inhibitors: a patent review (2010-2016). *Expert Opin Ther Pat* 27, 1227–1250 (2017).

97. Caroff, M. & Karibian, D. Structure of bacterial lipopolysaccharides. *Carbohyd Res* 338, 2431–2447 (2003).

98. Zhou, Z., White, K. A., Polissi, A., Georgopoulos, C. & Raetz, C. R. H. Function of *Escherichia coli* MsbA, an Essential ABC Family Transporter, in Lipid A and Phospholipid Biosynthesis*. *J Biol Chem* 273, 12466–12475 (1998).

99. Polissi, A. & Georgopoulos, C. Mutational analysis and properties of the *msbA* gene of *Escherichia coli*, coding for an essential ABC family transporter. *Mol Microbiol* 20, 1221–1233 (1996).

100. Chng, S.-S., Gronenberg, L. S. & Kahne, D. Proteins Required for Lipopolysaccharide Assembly in *Escherichia coli* Form a Transenvelope Complex. *Biochemistry-us* 49, 4565–4567 (2010).

101. Ruiz, N., Gronenberg, L. S., Kahne, D. & Silhavy, T. J. Identification of two inner-membrane proteins required for the transport of lipopolysaccharide to the outer membrane of *Escherichia coli*. *Proc National Acad Sci* 105, 5537–5542 (2008).

102. Sperandeo, P. *et al.* Characterization of lptA and lptB, two essential genes implicated in lipopolysaccharide transport to the outer membrane of *Escherichia coli*. *J Bacteriol* 189, 244–53 (2006).

103. Wu, T. *et al.* Identification of a protein complex that assembles lipopolysaccharide in the outer membrane of *Escherichia coli. Proc National Acad Sci* 103, 11754–11759 (2006).

104. Mühlradt, P. F., Menzel, J., Golecki, J. R. & Speth, V. Outer membrane of *Salmonella*. Sites of export of newly synthesised lipopolysaccharide on the bacterial surface. *European J Biochem Febs* 35, 471–81 (1973).

105. Mühlradt, P. F., Menzel, J., Golecki, J. R. & Speth, V. Lateral Mobility and Surface Density of Lipopolysaccharide in the Outer Membrane of *Salmonella typhimurium*. *Eur J Biochem* 43, 533–539 (1974).

106. Rojas, E. R. *et al.* The outer membrane is an essential load-bearing element in Gram-negative bacteria. *Nature* 559, 617–621 (2018).

107. Clifton, L. A. *et al.* Effect of Divalent Cation Removal on the Structure of Gram-Negative Bacterial Outer Membrane Models. *Langmuir* 31, 404–412 (2015).

108. Simpson, B. W. & Trent, M. S. Pushing the envelope: LPS modifications and their consequences. *Nat Rev Microbiol* 17, 403–416 (2019).

109. Ding, P.-H., Wang, C.-Y., Darveau, R. P. & Jin, L. *Porphyromonas gingivalis* LPS stimulates the expression of LPS-binding protein in human oral keratinocytes in vitro. *Innate Immun* 19, 66–75 (2012).

110. Yamamoto, M. & Akira, S. Lipid A receptor TLR4-mediated signaling pathways. *Adv Exp Med Biol* 667, 59–68 (2010).

111. Xiao, X., Sankaranarayanan, K. & Khosla, C. Biosynthesis and structure–activity relationships of the lipid a family of glycolipids. *Curr Opin Chem Biol* 40, 127–137 (2017).

112. Javan, NG. & Sharon, W. Association of *Helicobacter pylori* infection and stomach cancer: our experience. *Int Surg J* 5, 2794–2798 (2018).

113. Telepnev, M. V. *et al.* Tetraacylated Lipopolysaccharide of *Yersinia pestis* Can Inhibit Multiple Toll-Like Receptor–Mediated Signaling Pathways in Human Dendritic Cells. *J Infect Dis* 200, 1694–1702 (2009).

114. Boll, J. M. *et al.* Reinforcing Lipid A Acylation on the Cell Surface of *Acinetobacter baumannii* Promotes Cationic Antimicrobial Peptide Resistance and Desiccation Survival. *Mbio* 6, e00478-15 (2015).

115. Li, J. *et al.* Colistin: the re-emerging antibiotic for multidrug-resistant Gram-negative bacterial infections. *Lancet Infect Dis* 6, 589–601 (2006).

116. Wagenlehner, F. *et al.* Systematic review on estimated rates of nephrotoxicity and neurotoxicity in patients treated with polymyxins. *Clin Microbiol Infec* 27, 671–686 (2021).

117. Storm, D. R., Rosenthal, K. S. & Swanson, P. E. Polymyxin and Related Peptide Antibiotics. *Annu Rev Biochem* 46, 723–763 (1977).

118. Humphrey, M. *et al.* Colistin resistance in *Escherichia coli* confers protection of the cytoplasmic but not outer membrane from the polymyxin antibiotic. *Microbiol Read Engl* 167, 001104 (2021).

119. Ledger, E. V. K., Sabnis, A. & Edwards, A. M. Polymyxin and lipopeptide antibiotics: membrane-targeting drugs of last resort. *Microbiology+* 168, (2022).

120. Sabnis, A. *et al.* Colistin kills bacteria by targeting lipopolysaccharide in the cytoplasmic membrane. *Elife* 10, e65836 (2021).

121. Velkov, T., Thompson, P. E., Nation, R. L. & Li, J. Structure--activity relationships of polymyxin antibiotics. *J Med Chem* 53, 1898–916 (2010).

122. Powers, J.-P. S. & Hancock, R. E. W. The relationship between peptide structure and antibacterial activity. *Peptides* 24, 1681–1691 (2003).

123. Sampson, T. R. *et al.* Rapid killing of *Acinetobacter baumannii* by polymyxins is mediated by a hydroxyl radical death pathway. *Antimicrob Agents Ch* 56, 5642–9 (2012).

124. Deris, Z. Z. *et al.* A secondary mode of action of polymyxins against Gram-negative bacteria involves the inhibition of NADH-quinone oxidoreductase activity. *J Antibiotics* 67, 147–151 (2014).

125. Moffatt, J. H. *et al.* Colistin resistance in *Acinetobacter baumannii* is mediated by complete loss of lipopolysaccharide production. *Antimicrob Agents Ch* 54, 4971–7 (2010).

126. Henry, R. *et al.* Colistin-Resistant, Lipopolysaccharide-Deficient *Acinetobacter baumannii* Responds to Lipopolysaccharide Loss through Increased Expression of Genes Involved in the Synthesis and Transport of Lipoproteins, Phospholipids, and Poly-β-1,6- N -Acetylglucosamine. *Antimicrob Agents Ch* 56, 59–69 (2012).

127. Park, Y. K. *et al.* Independent emergence of colistin-resistant *Acinetobacter spp*. isolates from Korea. *Diagn Micr Infec Dis* 64, 43–51 (2009).

128. Guérin, F. *et al.* Cluster-dependent colistin hetero-resistance in *Enterobacter cloacae* complex. *J Antimicrob Chemother* 71, 3058–3061 (2016).

129. Bos, M. P. & Tommassen, J. Viability of a capsule- and lipopolysaccharide-deficient mutant of *Neisseria meningitidis. Infect Immun* 73, 6194–7 (2005).

130. Sperandeo, P. *et al.* Functional analysis of the protein machinery required for transport of lipopolysaccharide to the outer membrane of *Escherichia coli*. *J Bacteriol* 190, 4460–9 (2008).

131. Martorana, A. M. *et al.* Functional Interaction between the Cytoplasmic ABC Protein LptB and the Inner Membrane LptC Protein, Components of the Lipopolysaccharide Transport Machinery in *Escherichia coli. J Bacteriol* 198, 2192–2203 (2016).

132. Boll, J. M. *et al.* A penicillin-binding protein inhibits selection of colistin-resistant, lipooligosaccharide-deficient *Acinetobacter baumannii*. *Proc National Acad Sci* 113, E6228–E6237 (2016).

133. Henry, R. *et al.* Colistin-resistant, lipopolysaccharide-deficient *Acinetobacter baumannii* responds to lipopolysaccharide loss through increased expression of genes involved in the synthesis and transport of lipoproteins, phospholipids, and poly-β-1,6-N-acetylglucosamine. *Antimicrob Agents Ch* 56, 59–69 (2011).

134. El-Halfawy, O. M. & Valvano, M. A. Antimicrobial Heteroresistance: an Emerging Field in Need of Clarity. *Clin Microbiol Rev* 28, 191–207 (2015).

135. Andersson, D. I., Nicoloff, H. & Hjort, K. Mechanisms and clinical relevance of bacterial heteroresistance. *Nat Rev Microbiol* 17, 479–496 (2019).

136. Nicoloff, H., Hjort, K., Levin, B. R. & Andersson, D. I. The high prevalence of antibiotic heteroresistance in pathogenic bacteria is mainly caused by gene amplification. *Nat Microbiol* 4, 504–514 (2019).

137. Kuper, K. M., Boles, D. M., Mohr, J. F. & Wanger, A. Antimicrobial Susceptibility Testing: A Primer for Clinicians. *Pharmacotherapy* 29, 1326–1343 (2009).

138. Reller, L. B., Weinstein, M., Jorgensen, J. H. & Ferraro, M. J. Antimicrobial susceptibility testing: a review of general principles and contemporary practices. *Clin Infect Dis Official Publ Infect Dis Soc Am* 49, 1749–55 (2009).

139. Pfeltz, R. F., Schmidt, J. L. & Wilkinson, B. J. A Microdilution Plating Method for Population Analysis of Antibiotic-Resistant *Staphylococci. Microb Drug Resist* 7, 289–295 (2001).

140. Nurjadi, D. *et al.* Phenotypic Detection of Hemin-Inducible Trimethoprim-Sulfamethoxazole Heteroresistance in *Staphylococcus aureus*. *Microbiol Spectr* 9, e01510-21 (2021).

141. Anderson, S. E., Sherman, E. X., Weiss, D. S. & Rather, P. N. Aminoglycoside Heteroresistance in *Acinetobacter baumannii* AB5075. *Msphere* 3, e00271-18 (2018).

142. Jo, J. & Ko, K. S. Tigecycline Heteroresistance and Resistance Mechanism in Clinical Isolates of *Acinetobacter baumannii. Microbiol Spectr* 9, e01010-21 (2021).

143. Hung, K.-H., Wang, M.-C., Huang, A.-H., Yan, J.-J. & Wu, J.-J. Heteroresistance to Cephalosporins and Penicillins in *Acinetobacter baumannii*. *J Clin Microbiol* 50, 721–726 (2012).

144. Pournaras, S., Ikonomidis, A., Markogiannakis, A., Maniatis, A. N. & Tsakris, A. Heteroresistance to carbapenems in *Acinetobacter baumannii*. *J Antimicrob Chemoth* 55, 1055–1056 (2005).

145. Saravolatz, S. N., Martin, H., Pawlak, J., Johnson, L. B. & Saravolatz, L. D. Ceftaroline-Heteroresistant *Staphylococcus aureus. Antimicrob Agents Ch* 58, 3133–3136 (2014).

146. Choby, J. E., Ozturk, T., Satola, S. W., Jacob, J. T. & Weiss, D. S. Widespread cefiderocol heteroresistance in carbapenem-resistant Gram-negative pathogens. *Lancet Infect Dis* 21, 597–598 (2021).

147. Howard-Anderson, J. *et al.* Prevalence of colistin heteroresistance in carbapenem-resistant *Pseudomonas aeruginosa* and association with clinical outcomes in patients: an observational study. *J Antimicrob Chemoth* 77, 793–798 (2021).

148. Wozniak, J. E. *et al.* A Nationwide Screen of Carbapenem-Resistant *Klebsiella pneumoniae* Reveals an Isolate with Enhanced Virulence and Clinically Undetected Colistin Heteroresistance. *Antimicrob Agents Ch* 63, (2019).

149. Gunn, J. S. The *Salmonella* PmrAB regulon: lipopolysaccharide modifications, antimicrobial peptide resistance and more. *Trends Microbiol* 16, 284–290 (2008).

150. Winfield, M. D. & Groisman, E. A. Phenotypic differences between *Salmonella* and *Escherichia coli* resulting from the disparate regulation of homologous genes. *P Natl Acad Sci Usa* 101, 17162–17167 (2004).

151. Prost, L. R. *et al.* Activation of the Bacterial Sensor Kinase PhoQ by Acidic pH. *Mol Cell* 26, 165–174 (2007).

152. Véscovi, E. G., Soncini, F. C. & Groisman, E. A. Mg2+ as an Extracellular Signal: Environmental Regulation of Salmonella Virulence. *Cell* 84, 165–174 (1996).

153. Bader, M. W. *et al.* Recognition of Antimicrobial Peptides by a Bacterial Sensor Kinase. *Cell* 122, 461–472 (2005).

154. Zwir, I. *et al.* Dissecting the PhoP regulatory network of *Escherichia coli* and *Salmonella enterica*. *P Natl Acad Sci Usa* 102, 2862–2867 (2005).

155. Wösten, M. M. S. M., Kox, L. F. F., Chamnongpol, S., Soncini, F. C. & Groisman, E. A. A Signal Transduction System that Responds to Extracellular Iron. *Cell* 103, 113–125 (2000).

156. Kox, L. F. F., Wösten, M. M. S. M. & Groisman, E. A. A small protein that mediates the activation of a two-component system by another two-component system. *Embo J* 19, 1861–1872 (2000).

157. Tamayo, R. *et al.* Identification of cptA, a PmrA-regulated locus required for phosphoethanolamine modification of the *Salmonella enterica* serovar typhimurium lipopolysaccharide core. *J Bacteriol* 187, 3391–9 (2005).

158. Roland, K. L., Martin, L. E., Esther, C. R. & Spitznagel, J. K. Spontaneous *pmrA* mutants of *Salmonella typhimurium* LT2 define a new two-component regulatory system with a possible role in virulence. *J Bacteriol* 175, 4154–4164 (1993).

159. Guo, L. *et al.* Regulation of Lipid A Modifications *by Salmonella typhimurium* Virulence Genes phoP-phoQ. *Science* 276, 250–253 (1997).

160. Zhou, Z. *et al.* Lipid A Modifications in Polymyxin-resistant *Salmonella typhimurium* PMRA-DEPENDENT 4-AMINO-4-DEOXY-l-ARABINOSE, AND PHOSPHOETHANOLAMINE INCORPORATION*. *J Biol Chem* 276, 43111–43121 (2001).

161. Gunn, J. S. & Miller, S. I. PhoP-PhoQ activates transcription of *pmrAB,* encoding a two-component regulatory system involved in *Salmonella typhimurium* antimicrobial peptide resistance. *J Bacteriol* 178, 6857–6864 (1996).

162. Sun, S., Negrea, A., Rhen, M. & Andersson, D. I. Genetic analysis of colistin resistance in *Salmonella enterica* serovar Typhimurium. *Antimicrob Agents Ch* 53, 2298–305 (2009).

163. Cannatelli, A. *et al.* MgrB Inactivation Is a Common Mechanism of Colistin Resistance in KPC-Producing *Klebsiella pneumoniae* of Clinical Origin. *Antimicrob Agents Ch* 58, 5696–5703 (2014).

164. Sandegren, L. & Andersson, D. I. Bacterial gene amplification: implications for the evolution of antibiotic resistance. *Nat Rev Microbiol* 7, 578–588 (2009).

165. Hjort, K., Nicoloff, H. & Andersson, D. I. Unstable tandem gene amplification generates heteroresistance (variation in resistance within a population) to colistin in *Salmonella enterica*. *Mol Microbiol* 102, 274–289 (2016).

166. Kang, K. N. *et al.* Colistin heteroresistance in *Enterobacter cloacae* is regulated by PhoPQ-dependent 4-amino-4-deoxy-l-arabinose addition to lipid A. *Mol Microbiol* 111, 1604–1616 (2019).

167. Needham, B. D. *et al.* Modulating the innate immune response by combinatorial engineering of endotoxin. *Proc National Acad Sci* 110, 1464–1469 (2013).

168. Raetz, C. R. H., Reynolds, C. M., Trent, M. S. & Bishop, R. E. Lipid A Modification Systems in Gram-Negative Bacteria. *Annu Rev Biochem* 76, 295–329 (2007).

169. Gunn, J. S. & Richards, S. M. Recognition and Integration of Multiple Environmental Signals by the Bacterial Sensor Kinase PhoQ. *Cell Host Microbe* 1, 163–165 (2007).

170. Herrera, C. M., Hankins, J. V. & Trent, M. S. Activation of PmrA inhibits LpxT-dependent phosphorylation of lipid A promoting resistance to antimicrobial peptides. *Mol Microbiol* 76, 1444–1460 (2010).

171. Perez, J. C. & Groisman, E. A. Acid pH activation of the PmrA/PmrB two-component regulatory system of *Salmonella enterica*. *Mol Microbiol* 63, 283–293 (2007).

172. Trent, M. S., Ribeiro, A. A., Lin, S., Cotter, R. J. & Raetz, C. R. An inner membrane enzyme in *Salmonella* and *Escherichia coli* that transfers 4-amino-4-deoxy-L-arabinose to lipid A: induction on polymyxin-resistant mutants and role of a novel lipid-linked donor. *J Biological Chem* 276, 43122–31 (2001).

173. Miller, S. I., Kukral, A. M. & Mekalanos, J. J. A two-component regulatory system (*phoP phoQ*) controls Salmonella typhimurium virulence. *P Natl Acad Sci Usa* 86, 5054–8 (1989).

174. Kawasaki, K., Ernst, R. K. & Miller, S. I. Inhibition of *Salmonella enterica* Serovar Typhimurium Lipopolysaccharide Deacylation by Aminoarabinose Membrane Modification. *J Bacteriol* 187, 2448–2457 (2005).

175. Mitrophanov, A. Y., Jewett, M. W., Hadley, T. J. & Groisman, E. A. Evolution and Dynamics of Regulatory Architectures Controlling Polymyxin B Resistance in Enteric Bacteria. *Plos Genet* 4, e1000233 (2008).

176. Winfield, M. D., Latifi, T. & Groisman, E. A. Transcriptional Regulation of the 4-Amino-4-deoxy-L-arabinose Biosynthetic Genes in *Yersinia pestis*. *J Biol Chem* 280, 14765–14772 (2005).

177. Rubin, E. J., Herrera, C. M., Crofts, A. A. & Trent, M. S. PmrD Is Required for Modifications to *Escherichia coli* Endotoxin That Promote Antimicrobial Resistance. *Antimicrob Agents Ch* 59, 2051–2061 (2015).

178. Soncini, F. C. & Groisman, E. A. Two-component regulatory systems can interact to process multiple environmental signals. *J Bacteriol* 178, 6796–801 (1996).

179. Kato, A. & Groisman, E. A. Connecting two-component regulatory systems by a protein that protects a response regulator from dephosphorylation by its cognate sensor. *Gene Dev* 18, 2302–2313 (2004).

180. Luo, S.-C. *et al.* Structural Basis of a Physical Blockage Mechanism for the Interaction of Response Regulator PmrA with Connector Protein PmrD from *Klebsiella pneumoniae*. *J Biol Chem* 288, 25551–25561 (2013).

181. Morand, P. C. *et al.* Specific Distribution within the *Enterobacter cloacae* Complex of Strains Isolated from Infected Orthopedic Implants. *J Clin Microbiol* 47, 2489–2495 (2009).

182. Sanders, W. E. & Sanders, C. C. *Enterobacter spp.*: pathogens poised to flourish at the turn of the century. *Clin Microbiol Rev* 10, 220–241 (1997).

183. John, J. F., Sharbaugh, R. J. & Bannister, E. R. *Enterobacter cloacae*: bacteremia, epidemiology, and antibiotic resistance. *Rev Infect Dis* 4, 13–28 (1982).

184. Guérin, F. *et al.* Cluster-dependent colistin hetero-resistance in *Enterobacter cloacae* complex. *J Antimicrob Chemoth* 71, 3058–3061 (2016).

185. Mezzatesta, M. L., Gona, F. & Stefani, S. *Enterobacter cloacae* complex: clinical impact and emerging antibiotic resistance. *Future Microbiol* 7, 887–902 (2012).

186. Carlet, J. & Mainardi, J. -L. Antibacterial agents: back to the future? Can we live with only colistin, co-trimoxazole and fosfomycin? *Clin Microbiol Infec* 18, 1–3 (2012).

187. Nation, R. L. & Li, J. Colistin in the 21st century. *Curr Opin Infect Dis* 22, 535–543 (2009).

188. Band, V. I. *et al.* Antibiotic failure mediated by a resistant subpopulation in *Enterobacter cloacae*. *Nat Microbiol* 1, 16053 (2016).

189. Reis, A. O., Luz, D. A. M., Tognim, M. C. B., Sader, H. S. & Gales, A. C. Polymyxin-Resistant *Acinetobacter spp*. Isolates: What is Next? *Emerg Infect Dis* 9, 1025–1027 (2003).

190. Park, B. S. *et al.* The structural basis of lipopolysaccharide recognition by the TLR4–MD-2 complex. *Nature* 458, 1191–1195 (2009).

191. Kawai, T. & Akira, S. Pathogen recognition with Toll-like receptors. *Curr Opin Immunol* 17, 338–344 (2005).

192. Soncini, F. C., Véscovi, E. G. & Groisman, E. A. Transcriptional autoregulation of the *Salmonella typhimurium phoPQ* operon. *J Bacteriol* 177, 4364–4371 (1995).

193. Ren, Y. *et al.* Complete Genome Sequence of *Enterobacter cloacae* subsp. cloacae Type Strain ATCC 13047. *J Bacteriol* 192, 2463–2464 (2010).

194. Lee, H., Hsu, F.-F., Turk, J. & Groisman, E. A. The PmrA-regulated *pmrC* gene mediates phosphoethanolamine modification of lipid A and polymyxin resistance in *Salmonella enterica*. *J Bacteriol* 186, 4124–33 (2004).

195. Jayol, A., Nordmann, P., Brink, A. & Poirel, L. Heteroresistance to colistin in *Klebsiella pneumonia*e associated with alterations in the PhoPQ regulatory system. *Antimicrob Agents Ch* 59, 2780–4 (2015).

196. Merode, A. E. J. van, Mei, H. C. van der, Busscher, H. J. & Krom, B. P. Influence of culture heterogeneity in cell surface charge on adhesion and biofilm formation by *Enterococcus faecalis*. *J Bacteriol* 188, 2421–6 (2006).

197. Guérin, F., Isnard, C., Cattoir, V. & Giard, J. C. Complex Regulation Pathways of AmpC-Mediated β-Lactam Resistance in *Enterobacter cloacae* Complex. *Antimicrob Agents Ch* 59, 7753–61 (2015).

198. Hankins, J. V. *et al.* Elucidation of a novel *Vibrio cholerae* lipid A secondary hydroxy-acyltransferase and its role in innate immune recognition. *Mol Microbiol* 81, 1313–1329 (2011).

199. Zhou, Z., Lin, S., Cotter, R. J. & Raetz, C. R. Lipid A modifications characteristic of *Salmonella typhimurium* are induced by NH4VO3 in *Escherichia coli* K12. Detection of 4-amino-4-deoxy-L-arabinose, phosphoethanolamine and palmitate. *J Biological Chem* 274, 18503–14 (1999).

200. Klein, D. R., Holden, D. D. & Brodbelt, J. S. Shotgun Analysis of Rough-Type Lipopolysaccharides Using Ultraviolet Photodissociation Mass Spectrometry. *Anal Chem* 88, 1044–1051 (2016).

201. Boll, J. M. & Hendrixson, D. R. A Regulatory Checkpoint during Flagellar Biogenesis in *Campylobacter jejuni* Initiates Signal Transduction To Activate Transcription of Flagellar Genes. *Mbio* 4, e00432-13 (2013).

202. Boll, J. M. & Hendrixson, D. R. A specificity determinant for phosphorylation in a response regulator prevents in vivo cross-talk and modification by acetyl phosphate. *Proc National Acad Sci* 108, 20160–20165 (2011).

203. Davies, B. W., Bogard, R. W., Young, T. S. & Mekalanos, J. J. Coordinated Regulation of Accessory Genetic Elements Produces Cyclic Di-Nucleotides for *V. cholerae* Virulence. *Cell* 149, 358–370 (2012).

204. Höltje, J. V. Growth of the stress-bearing and shape-maintaining murein sacculus of *Escherichia coli*. *Microbiol Mol Biology Rev Mmbr* 62, 181–203 (1998).

205. Koch, A. L. Biophysics of bacterial walls viewed as stress-bearing fabric. *Microbiol Rev* 52, 337–353 (1988).

206. Braun, M. & Silhavy, T. J. Imp/OstA is required for cell envelope biogenesis in *Escherichia coli*: Imp/OstA and envelope biogenesis. *Mol Microbiol* 45, 1289–1302 (2002).

207. Vaara, M. Polymyxins and their novel derivatives. *Curr Opin Microbiol* 13, 574–581 (2010).

208. Cai, Y., Chai, D., Wang, R., Liang, B. & Bai, N. Colistin resistance of *Acinetobacter baumannii*: clinical reports, mechanisms and antimicrobial strategies. *J Antimicrob Chemoth* 67, 1607–1615 (2012).

209. Harris, T. L. *et al.* Small Molecule Downregulation of PmrAB Reverses Lipid A Modification and Breaks Colistin Resistance. *Acs Chem Biol* 9, 122–127 (2014).

210. Arroyo, L. A. *et al.* The *pmrCAB* operon mediates polymyxin resistance in *Acinetobacter baumannii* ATCC 17978 and clinical isolates through phosphoethanolamine modification of lipid A. *Antimicrob Agents Ch* 55, 3743–51 (2011).

211. Du, S. & Lutkenhaus, J. Assembly and activation of the Escherichia coli divisome. *Mol Microbiol* 105, 177–187 (2017).

212. Vollmer, W., Blanot, D. & Pedro, M. A. D. Peptidoglycan structure and architecture. *Fems Microbiol Rev* 32, 149–167 (2008).

213. Caveney, N. A. *et al.* Structural insight into YcbB-mediated beta-lactam resistance in *Escherichia coli. Nat Commun* 10, 1849 (2019).

214. Kuru, E. *et al.* In Situ Probing of Newly Synthesized Peptidoglycan in Live Bacteria with Fluorescent D-Amino Acids . *Angewandte Chemie Int Ed* 51, 12519–12523 (2012).

215. Kuru, E. *et al.* Fluorescent D-amino-acids reveal bi-cellular cell wall modifications important for *Bdellovibrio bacteriovorus* predation. *Nat Microbiol* 2, 1648–1657 (2017).

216. Kuru, E. *et al.* Mechanisms of Incorporation for D-Amino Acid Probes That Target Peptidoglycan Biosynthesis. *Acs Chem Biol* 14, 2745–2756 (2019).

217. Mainardi, J.-L. *et al.* Unexpected Inhibition of Peptidoglycan LD-Transpeptidase from *Enterococcus faecium* by the β-Lactam Imipenem*. *J Biol Chem* 282, 30414–30422 (2007).

218. Yourassowsky, E., Linden, M. P. V. D., Lismont, M. J. & Crokaert, F. Growth Curve Patterns of *Escherichia coli, Serratia marcescens*, and *Proteus vulgaris* Submitted to Different Tigemonam Concentrations. *J Chemotherapy* 1, 49–53 (2016).

219. Buijs, J., Dofferhoff, A. S. M., Mouton, J. W., Wagenvoort, J. H. T. & Meer, J. W. M. V. D. Concentration-dependency of β-lactam-induced filament formation in Gram-negative bacteria. *Clin Microbiol Infec* 14, 344–349 (2008).

220. Nagy, E., Losick, R. & Kahne, D. Robust Suppression of Lipopolysaccharide Deficiency in *Acinetobacter baumannii* by Growth in Minimal Medium. *J Bacteriol* 201, (2019).

221. Egan, A. J. F. *et al.* Induced conformational changes activate the peptidoglycan synthase PBP1B. *Mol Microbiol* 110, 335–356 (2018).

222. Yakhnina, A. A. & Bernhardt, T. G. The Tol-Pal system is required for peptidoglycan-cleaving enzymes to complete bacterial cell division. *P Natl Acad Sci Usa* 117, 6777–6783 (2020).

223. Pazos, M. *et al.* Z-ring membrane anchors associate with cell wall synthases to initiate bacterial cell division. *Nat Commun* 9, 5090 (2018).

224. Haeusser, D. P. & Margolin, W. Splitsville: structural and functional insights into the dynamic bacterial Z ring. *Nat Rev Microbiol* 14, 305–319 (2016).

225. Aarsman, M. E. G. *et al.* Maturation of the *Escherichia coli* divisome occurs in two steps. *Mol Microbiol* 55, 1631–1645 (2005).

226. Typas, A. *et al.* Regulation of peptidoglycan synthesis by outer membrane proteins. *Cell* 143, 1097–1109 (2010).

227. Egan, A. J. F. *et al.* Outer-membrane lipoprotein LpoB spans the periplasm to stimulate the peptidoglycan synthase PBP1B. *Proc National Acad Sci* 111, 8197–8202 (2014).

228. Egan, A. J. F., Biboy, J., Veer, I. van't, Breukink, E. & Vollmer, W. Activities and regulation of peptidoglycan synthases. *Philosophical Transactions Royal Soc B Biological Sci* 370, 20150031 (2015).

229. Banzhaf, M. *et al.* Outer membrane lipoprotein NlpI scaffolds peptidoglycan hydrolases within multi-enzyme complexes in Escherichia coli. *Embo J* 39, e102246 (2020).

230. Hernández-Rocamora, V. M. *et al.* Coupling of polymerase and carrier lipid phosphatase prevents product inhibition in peptidoglycan synthesis. *Cell Surf* 2, 1–13 (2018).

231. Peters, K. *et al.* Copper inhibits peptidoglycan LD-transpeptidases suppressing β-lactam resistance due to bypass of penicillin-binding proteins. *Proc National Acad Sci* 115, 201809285 (2018).

232. Stover, C. K. *et al.* New use of BCG for recombinant vaccines. *Nature* 351, 456–460 (1991).

233. Tucker, A. T. *et al.* Defining Gene-Phenotype Relationships in *Acinetobacter baumannii* through One-Step Chromosomal Gene Inactivation. *Mbio* 5, e01313-14 (2014).

234. Glauner, B., Höltje, J. V. & Schwarz, U. The composition of the murein of *Escherichia coli.* *J Biol Chem* 263, 10088–10095 (1988).

235. Schindelin, J. *et al.* Fiji: an open-source platform for biological-image analysis. *Nat Methods* 9, 676–682 (2012).

236. Ducret, A., Quardokus, E. M. & Brun, Y. V. MicrobeJ, a tool for high throughput bacterial cell detection and quantitative analysis. *Nat Microbiol* 1, 16077 (2016).

237. Kazi, M. I. *et al.* Discovery and characterization of New Delhi metallo-β-lactamase-1 inhibitor peptides that potentiate meropenem-dependent killing of carbapenemase-producing *Enterobacteriaceae*. *J Antimicrob Chemoth* 75, 2843–2851 (2020).

238. Kazi, M. I., Schargel, R. D. & Boll, J. M. Generating Transposon Insertion Libraries in Gram-Negative Bacteria for High-Throughput Sequencing. *J Vis Exp* (2020) doi:10.3791/61612.

239. Begg, K. J. *et al.* The balance between different peptidoglycan precursors determines whether *Escherichia coli* cells will elongate or divide. *J Bacteriol* 172, 6697–703 (1990).

240. Lleo, M. M., Canepari, P. & Satta, G. Bacterial cell shape regulation: testing of additional predictions unique to the two-competing-sites model for peptidoglycan assembly and isolation of conditional rod-shaped mutants from some wild-type cocci. *J Bacteriol* 172, 3758–3771 (1990).

241. Navarro, P. P. *et al.* Cell wall synthesis and remodeling dynamics determine bacterial division site architecture and cell shape. *Biorxiv* 2021.10.02.462887 (2021) doi:10.1101/2021.10.02.462887.

242. Liu, X., Biboy, J., Consoli, E., Vollmer, W. & Blaauwen, T. den. MreC and MreD balance the interaction between the elongasome proteins PBP2 and RodA. *Plos Genet* 16, e1009276 (2020).

243. Leclercq, S. *et al.* Interplay between Penicillin-binding proteins and SEDS proteins promotes bacterial cell wall synthesis. *Sci Rep-uk* 7, 43306 (2017).

244. Liu, B., Persons, L., Lee, L. & Boer, P. A. J. Roles for both FtsA and the FtsBLQ subcomplex in FtsN-stimulated cell constriction in *Escherichia coli*. *Mol Microbiol* 95, 945–970 (2015).

245. Boes, A., Olatunji, S., Breukink, E. & Terrak, M. Regulation of the Peptidoglycan Polymerase Activity of PBP1b by Antagonist Actions of the Core Divisome Proteins FtsBLQ and FtsN. *Mbio* 10, e01912-18 (2019).

246. Satta, G., Canepari, P., Botta, G. & Fontana, R. Control of cell septation by lateral wall extension in a pH-conditional morphology mutant of *Klebsiella pneumoniae*. *J Bacteriol* 142, 43–51 (1980).

247. Georgopapadakou, N. H., Smith, S. A. & Sykes, R. B. Mode of action of azthreonam. *Antimicrob Agents Ch* 21, 950–956 (1982).

248. Potluri, L. *et al.* Septal and lateral wall localization of PBP5, the major D,D-carboxypeptidase of *Escherichia coli*, requires substrate recognition and membrane attachment. *Mol Microbiol* 77, 300–23 (2010).

249. Leimanis, S. *et al.* PBP5 Complementation of a PBP3 Deficiency in *Enterococcus hirae*. *J Bacteriol* 188, 6298–6307 (2006).

250. Korsak, D., Vollmer, W. & Markiewicz, Z. *Listeria monocytogenes* EGD lacking penicillin-binding protein 5 (PBP5) produces a thicker cell wall. *Fems Microbiol Lett* 251, 281–288 (2005).

251. Pisabarro, A. G., Prats, R., Váquez, D. & Rodríguez-Tébar, A. Activity of penicillin-binding protein 3 from *Escherichia coli. J Bacteriol* 168, 199–206 (1986).

252. Botta, G. A. & Park, J. T. Evidence for involvement of penicillin-binding protein 3 in murein synthesis during septation but not during cell elongation. *J Bacteriol* 145, 333–340 (1981).

253. Singh, S. K., Parveen, S., SaiSree, L. & Reddy, M. Regulated proteolysis of a cross-link-specific peptidoglycan hydrolase contributes to bacterial morphogenesis. *P Natl Acad Sci Usa* 112, 10956–61 (2015).

254. Ohara, M., Wu, H. C., Sankaran, K. & Rick, P. D. Identification and Characterization of a New Lipoprotein, NlpI, in *Escherichia coli* K-12. *J Bacteriol* 181, 4318–4325 (1999).

255. Auer, G. K. & Weibel, D. B. Bacterial Cell Mechanics. *Biochemistry-us* 56, 3710–3724 (2017).

256. Wang, C. *et al.* Isolation, Characterization, and Pharmaceutical Applications of an Exopolysaccharide from *Aerococcus Uriaeequi*. *Mar Drugs* 16, 337 (2018).

257. Park, J. T. & Uehara, T. How Bacteria Consume Their Own Exoskeletons (Turnover and Recycling of Cell Wall Peptidoglycan)†. *Microbiol Mol Biol R* 72, 211–227 (2008).

258. Band, V. I. & Weiss, D. S. Heteroresistance: A cause of unexplained antibiotic treatment failure? *Plos Pathog* 15, e1007726 (2019).

259. Mohamed, Y. F., Abou-Shleib, H. M., Khalil, A. M., El-Guink, N. M. & El-Nakeeb, M. A. Membrane permeabilization of colistin toward pan-drug resistant Gram-negative isolates. *Braz J Microbiol* 47, 381–388 (2016).

260. Lester, W. Rifampin: A Semisynthetic Derivative of Rifamycin-A Prototype for the Future. *Annu Rev Microbiol* 26, 85–102 (1972).

261. Mosaei, H. & Zenkin, N. Inhibition of RNA Polymerase by Rifampicin and Rifamycin-Like Molecules. *Ecosal Plus* 9, (2020).

262. Ramirez, D. *et al.* Dioctanoyl Ultrashort Tetrabasic β-Peptides Sensitize Multidrug-Resistant Gram-Negative Bacteria to Novobiocin and Rifampicin. *Front Microbiol* 12, 803309 (2021).

263. Jammal, J., Zaknoon, F., Kaneti, G., Goldberg, K. & Mor, A. Sensitization of Gram-negative bacteria to rifampin and OAK combinations. *Sci Rep-uk* 5, 9216 (2015).

264. Park, H. J. *et al.* Colistin monotherapy versus colistin/rifampicin combination therapy in pneumonia caused by colistin-resistant *Acinetobacter baumannii*: A randomised controlled trial. *J Glob Antimicrob Re* 17, 66–71 (2019).

265. Hong, D. J. *et al.* In vitro antimicrobial synergy of colistin with rifampicin and carbapenems against colistin-resistant *Acinetobacter baumannii* clinical isolates. *Diagn Micr Infec Dis* 86, 184–189 (2016).

266. Nastro, M. *et al.* Activity of the colistin-rifampicin combination against colistin-resistant, carbapenemase-producing Gram-negative bacteria. *J Chemother Florence Italy* 26, 211–6 (2013).